UDK
62:502/504

ISSN 1849-4714 (Tisak)
ISSN 1849-5079 (Online)

INŽENJERSTVO OKOLIŠA

ENVIRONMENTAL ENGINEERING

Scientific and professional journal in the area of environmental engineering

GEOTEHNIČKI FAKULTET, SVEUČILIŠTE U ZAGREBU

FACULTY OF GEOTECHNICAL ENGINEERING, UNIVERSITY OF ZAGREB

VOLUME 8
NUMBER 1-2
DECEMBER 2021

ENVIRONMENTAL ENGINEERING - INŽENJERSTVO OKOLIŠA

Scientific and professional journal in the area of environmental engineering

The Journal publishes scientific and technical papers and other articles in the interdisciplinary area of environmental engineering. The scientific topics covered by the Journal include geo-engineering, water resources management, technical aspects of environmental protection and similar areas. Contributions include original scientific papers, preliminary comunnications, short notes, review papers or technical papers.

Short journal name: EnvEng-IO

Journal is published biannually.

All papers published in journal have been peer-reviewed.

The full text of all articles is available for free at the journal web site:
http://www.gfv.unizg.hr/hr/journalio.html

ISSN 1849-4714 (Print)
ISSN 1849-5079 (Online)
UDK 62:502/504

The journal "ENVIRONMENTAL ENGINEERING - INŽENJERSTVO OKOLIŠA" is active journal with updated content in the portal of the Croatian scientific and professional journals "Hrčak".

The logo is visible in the journal footer: https://hrcak.srce.hr/io

Journal is indexed and included in:

CASSI - Chemical Abstracts Service Source Index

Printed by: TISKARA ZELINA d.d., K.Krizmanić 1, HR-10380 Sveti Ivan Zelina, Hrvatska

Edition: 200 copies

University of Zagreb
FACULTY OF GEOTECHNICAL ENGINEERING

STUDIJ INŽENJERSTVA OKOLIŠA

IMPRESSUM

Publisher:
FACULTY OF GEOTECHNICAL ENGINEERING, UNIVERSITY OF ZAGREB
Hallerova aleja 7, HR - 42000 Varaždin
Tel.: + 385 (0)42 408 900
Fax: + 385 (0)42 313 587
E - mail: ured.dekana@gfv.unizg.hr
URL: http://www.gfv.unizg.hr

Editorial address:
FACULTY OF GEOTECHNICAL ENGINEERING, UNIVERSITY OF ZAGREB
Hallerova aleja 7, HR - 42000 Varaždin
Tel.: + 385 (0)42 408 911
Fax: + 385 (0)42 313 387
E - mail: casopis@gfv.unizg.hr
URL: https://environmentalengineering-journal.com/ ; https://hrcak.srce.hr/io

EDITORIAL TEAM

Editor-in-chief opening remarks

Dear readers,

This year, as well as previous was challenging from different aspects. The COVID pandemic marked activities in all areas of our lives, including our scientific activity. However, despite that I have the privilege and great honor to introduce you to the new number of the journal Environmental Engineering-Inženjerstvo okoliša published by the Faculty of Geotechnical Engineering, University of Zagreb, Croatia. With the publication of this issue, the continuity of publishing, which began eight years ago, continues which we are extremely proud of.

The new editorial board continues the tradition of presenting a wide range of scientific and expert activities of environmental engineering through selected papers and trying to provide solutions to problems arising from the coexistence of people and the Earth.
Therefore, this number resulted with ten papers, including six original scientific papers and four professional papers, with co-authors from 12 different institutions from Croatia and abroad.

The step forward happened in October 2020, when the journal signed a license agreement with EBSCO Publishing, Inc. to enter the EBSCO scientific database. The journal will be promoted by the EBSCO Discovery Service (EDS) and in the Central & Eastern European Academic Source (CEEAS), including current Volume.

I would use this opportunity to express my sincere gratitude to the dean prof. Hrvoje Meaški for supporting the journal.

At the end, I would like to give my gratitude to all hard-working team members and to our sponsors.
I hope you will enjoy it.
With best regards,

Assoc. Prof. Dr. Aleksandra Anić Vučinić
Editor-in-chief
Department for environmental engineering
Faculty of Geotechnical Engineering
University of Zagreb
Croatia

C O N T E N T

INDOOR AIR QUALITY IN A HIGH SCHOOL CLASSROOM IN RIJEKA, CROATIA (SICK CLASSROOMS CAUSED BY RISING CO_2 LEVELS)

Tatjana Ivošević [1*], Patricija Nikolaus [2], Tatjana Pranjić-Petrović [3], Ivica Orlić [4]
[1] *Education and Teacher Training Agency, Trpimirova 6, 51000 Rijeka, Croatia*
University of Rijeka Faculty of Maritime Studies, Studentska ulica 2, 51000 Rijeka, Croatia
[2] *Andrija Mohorovičić Grammar School, Frana Kurelca 1, 51000 Rijeka, Croatia*
[3] *The Civil Engineering and Technical School, Podhumskih žrtava 4, 51000 Rijeka, Croatia*
[4] *Independent researcher, Rijeka, Croatia*
*E-mail of corresponding author: ivosevic@pfri.hr; tatjana.ivosevic@azoo.hr

Abstract: *School's indoor air quality (IAQ) is very important as it can affect student's learning abilities and lead to health issues. Therefore, indoor air quality, and in particular the CO_2 concentration, was monitored on a daily basis from mid-November till the end of December 2017, by using several low-cost instruments. The measuring was performed in the physics classroom of a grammar school in Rijeka, Croatia. Detailed CO_2 generation rates, air exchange rates, and ventilation rates are calculated and reported in this work, from the experimentally obtained data. Very high concentrations of over 4.000 ppm were recorded, indicating that ventilation rates are far below 5 Ls^{-1} per person, which is the lowest recommended value of ventilation rate according to the European standard EN 13779. The experimentally obtained data are compared with the theoretical models and a strong correlation are achieved. This is one of the first comprehensive studies of this kind in Croatia; therefore, we hope that it will stimulate interest between health workers, scientists, and school management to implement indoor air quality monitoring practices and perhaps introduce automated ventilation systems in classrooms for the benefit of students' health and their learning abilities.*
Keywords: *indoor air quality, CO_2 concentrations, ventilation rate, EN13779, classroom.*

Received: 07.09.2020. / Accepted: 28.08.2020.
Published online: 01.12.2021.

Original scientific paper
https://doi.org/10.37023/ee.8.1-2.1

1. INTRODUCTION

Indoor air quality in schools has been a public concern for a number of years, as adverse effects of poor air quality have far-reaching effects on children's and students' health. It is estimated that in European countries, primary to high school students receive an average of 7.475 hours (approximately 4.5 hours a day) of instruction in formal classroom settings during the 9 years of compulsory education (OECD 2014). The school's indoor air quality (IAQ) is, therefore, very important, as it can affect students' learning abilities and lead to serious health issues.

The concentration of CO_2 is often used as an indicator of IAQ, especially in high-occupancy spaces such as schools. One of the main reasons is that in recent years, inexpensive and reasonably accurate instruments for measuring CO_2 concentration have become available. On the other hand, CO_2 is an inert gas, and its key emission sources (building occupants, students) are evenly distributed within the classrooms. Typical concentrations of CO_2 in the exhaled air are 4–5%. This is approximately a hundred times higher than the background CO_2 concentration, therefore the classroom concentration will strongly depend on the number of students, their activity, and time spent in the classroom. Factors that will influence a reduction of CO_2 concentration are ventilation rate and size of the classroom. Therefore, without adequate ventilation to remove and dilute CO_2 generated by students, its concentration can quickly increase to very high levels. These may be especially critical for young children, as they inhale higher volumes of air in relation to their body weight and respiratory tract surface area than adults, and their tissues and organs are still actively growing (Selgrade et al. 2008; Ginsberg et al. 2007). This can lead to child–adult differences in delivered doses of the polluted and toxic air. Although CO_2 is not considered to pose serious health risks, it has been demonstrated that elevated concentration levels can have significant impact on students' health and performance, such as lower attention and drowsiness (Mendell & Heath 2005; Bakó-Biró et al. 2011).

From a regulatory point of view, the European regulation EN 13779 provides minimum ventilation rates (VR) values in classrooms as a function of required indoor air quality. According to this regulation, VR has to be at least 20, 12.8, 8, and 5 Ls^{-1} per person (for non-smoking rooms) when high, medium, moderate, and low air quality targets have to be reached, respectively (CEN 2006).

The American Society of Heating, Refrigeration and Air Conditioning Engineers (ASHARE) recommends that indoor CO_2 concentrations be maintained at or below 1.000 ppm in schools (ASHRAE 2013). Furthermore, the

recommended limit averaged over one school shift should be lower than 1.500 ppm (DfES, 2018; Bakó-Biró et al. 2011). The ASHRAE also recommends minimum VRs of 5 Ls^{-1} per person for students of up to 9 years of age (ASHRAE 2013; Goldwin & Batterman 2007).

The conclusion is that adequate ventilation rates need to be guaranteed in order to maintain satisfactory air quality in classrooms. Indoor CO_2 concentrations above 1.000 ppm are generally regarded as indicative of VR, which is unacceptable with respect to air pollution and body odours.

In recent years, the WHO Regional Office for Europe in collaboration with local agencies, initiated a pilot project to measure indoor air quality in several primary schools in Croatia, as well as in other Eastern European countries. Their results are summarised in the Report (WHO 2015), which includes school surveys conducted from 2012 until early 2014 in five European countries: Albania, Croatia, Latvia, Estonia, and Lithuania. According to that report, the highest reported CO_2 concentration measured in primary school classrooms in Croatia was 2.500 ppm.

In another study, measurements of CO_2 concentrations were carried out in two Croatian primary schools during the five working days (March 2014). Daily average values of CO_2 in these two schools were 1.630 ppm for urban, and 2.370 ppm for rural school. (Tasić et al. 2015).

All these studies, along with our results, suggest that alarmingly high CO_2 concentrations and poor IAQ are very common in many schools, especially during the heating season. The situation is critical and requires urgent addressing by school management and responsible government agencies.

2. METHODS

2.1. Sampling site description & measurement period

All measurements were performed in the Andrija Mohorovičić Grammar School (AMGS) in Rijeka in the period between 24 Nov. and 22 Dec. 2017. The school is in the city centre, and it is surrounded by streets with moderate traffic intensity (**Figure 1**).

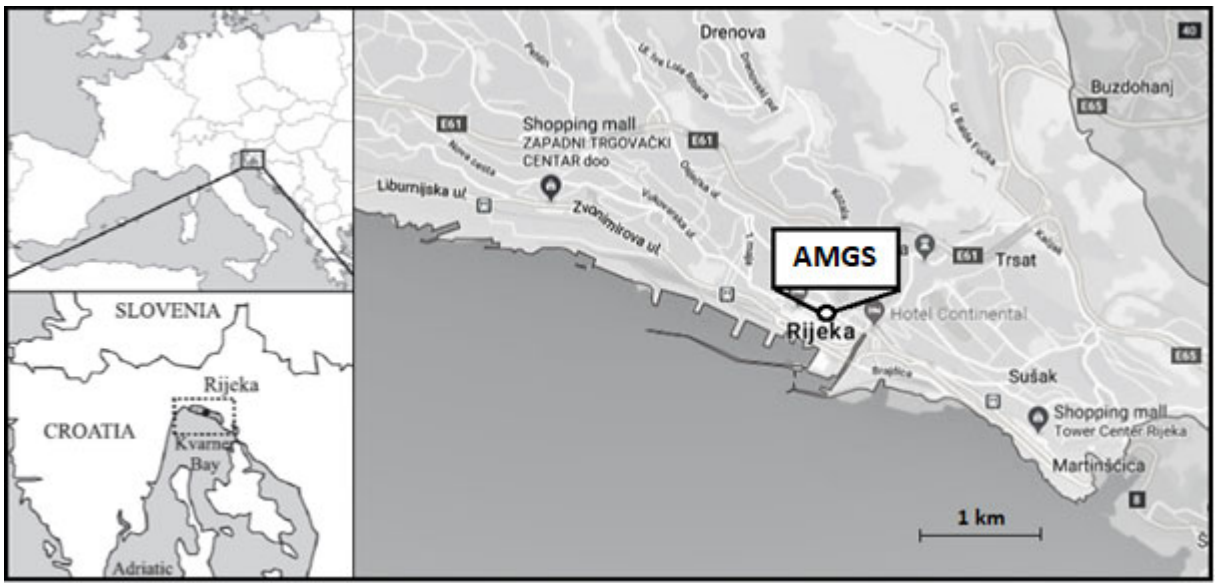

Figure 1. *The location of Andrija Mohorovičić Grammar School (AMGS) in the City of Rijeka, Croatia)*

This is a contemporary building built in 1897, with very solid walls and without an automated ventilation system. The only ventilation was provided in a traditional manner, by occasionally opening windows and doors, and during the winter period, mainly through small imperfections in windows and doors. However, some 15 years ago, the traditional wooden windows were replaced with new ones that allow very little air infiltration. In this way the energy conservation rating of the building was significantly improved. On the other hand, the airtightness of the new windows greatly reduced the ventilation rate of the building. For that reason, our study took place during the winter season, when windows are opened rarely, to reduce fuel consumption used for the central heating system (hot water filled radiators).

All our measurements took place in a specialized physics classroom which has typical school furniture and hardwood floors. This classroom was typically used by 15–18-year-old students (gymnasium grades 1–4). Physical dimensions of the classroom and the number of students is given in **Table 1**.

Table 1. Characteristics of the classroom and the number of students (A – floor area, h – height, N – number of students in the classroom)

SCHOOL	A/m^2	h /m	Vair /m^3	WINDOWS	Open wind. area / m^2	N
AMGS	62.3	4.1	259	3	4.62	22-26

2.2. Instrumentation and measurement

The following three different low-cost instruments were used to measure CO_2 concentration in this work:
1. DT-802 Detector (DT) manufactured by CEM (Shenzhen Everbest Machinery Industry Co.),
2. Green Eye CO_2 meter and data logger (GE) by Tech Grow Co. and
3. CO_2 + CO + RH/T Portable Meter and data logger (CM07) by CO_2Meter Inc.

All the dedicated instruments and loggers for measuring CO_2 concentration are in the range suitable for monitoring air quality in schools or offices, and their characteristics are given in **Table 2**.

Table 2. Characteristics of the instruments (Range ± accuracy)

INSTRUMENTS	CO_2 / ppm	t / °C	RH / %	CO / ppm
DT	(1–9.999) ± 75	(-5–50) ± 1	(0.1–90) ± 5	
GE	(1–10.000) ± 40	(-10–60) ± 0.6	(20–99) ± 5	
CM07	(1–9.999) ± 30	(-10–60) ± 0.9	(20–99) ± 3	(1–1.000) ± 10

All instruments use the non-dispersive infrared CO_2 detection method (NDIR). They were positioned in the classroom at a height of 1.5 m.

3. RESULTS AND DISCUSSION

3.1. Intercomparison of all instruments

To check the validity of our three instruments, simultaneous measurements were performed in the same classroom, with a wide range of CO_2 concentrations (2.200–3.200 ppm).

As evident from **Figure 2,** results from all three instruments are in agreement with each other, as variations from mean values are typically from 5 to 10 ppm, which is less than the instrumental errors specified by the manufacturers. Average values of CO_2 concentrations obtained by these three instruments were used throughout this work.

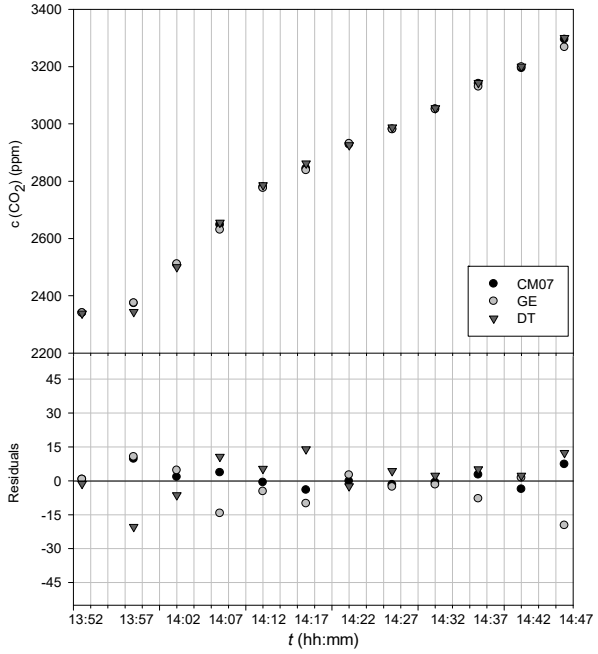

Figure 2. *The CO_2 concentrations measured by our three instruments (accuracy for CO_2; CM07 ± 30 ppm ± 5 % of reading (0-5000 ppm); GE ± 50 ppm; DT ± 8 % (2000 - 9999)) in a wide range of CO_2 concentrations. The lower graph shows residuals from the mean values (in ppm)*

3.2. Outdoor concentrations of CO_2

Outdoor concentrations of CO_2 were measured in the morning and the afternoon hours before the class. The obtained concentrations were found to be within the characteristic range for urban areas i.e. between 410 and 500 ppm (Turnjanin et al. 2014; Bréon et al. 2015).

As evident from **Figure 3**, concentrations obtained in the morning hours were lower, averaging 446 ppm. Afternoon concentrations were somewhat higher, ranging from 435 to 490 ppm. This was expected, due to emissions caused by road traffic, as well as domestic heating (Bréon et al. 2015). As outdoor CO_2 concentrations for year 2017 were not found in the Croatian public reports (Report 2017), the obtained values were compared to the available monthly data from the nearest stations in Hungary (for Nov. and Dec. 2017, 420,56 and 422.35 ppm, respectively) and Germany (for Nov. and Dec. 2017, 411.01 and 412.68 ppm, respectively). These background values were lower than the values measured in Rijeka, as the two stations were located in relatively unpolluted areas: one in the village of Hegyhatsal (station H, Hungary), and the other in the Alpine Region of Hohenpeissenberg (station HPB, Germany) (NOAA 2019).

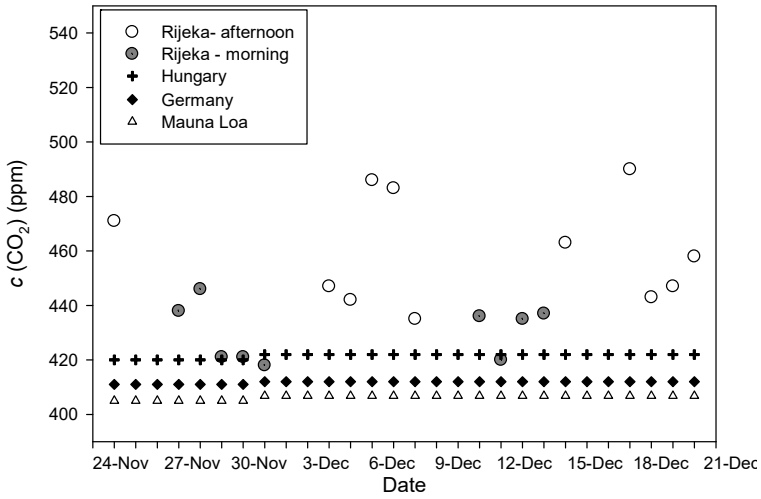

Figure 3. *Outdoor CO_2 concentrations in Rijeka during the morning (grey dots) and the afternoon hours (white dots) from the 24th Nov. to the 22nd Dec. 2017, and CO_2 monthly average concentrations obtained from stations in Hungary, Germany and Mauna Loa*

3.3. Measurement of indoor CO_2 concentrations and temperature

The air quality in the AMGS physics classroom was monitored in the winter period, when the outdoor temperatures were relatively low, ranging from 3 to 12°C. Throughout the sampling campaign, all classrooms were heated with oil-powered central heating radiators. To preserve fuel and to keep temperatures in the classrooms at more comfortable levels, it was common that teachers and student's open windows to ventilate classrooms only occasionally. Therefore, the air quality in classrooms was often poor and temperatures were much higher than recommended. This was one of the major reasons why we embarked on this project, with the aim to objectively assess the air quality in classrooms.

To maintain controlled experimental conditions during the four-week study, it was ensured that the classroom windows were closed the entire teaching period (four to five classes). The classroom was ventilated only during the breaks, when doors were opened for 5 to 10 minutes. However, it must be noted that not opening windows for long periods of time during cold winter days is very common in our schools. Both students and teachers often complain of poor air quality. At the same time, they want to enjoy comfortable room temperatures, and are, therefore, hesitant to open windows. (In our survey, most of the students wrote: "Poor air quality and closed windows in classrooms aren't uncommon in our schools. Teachers usually don't open windows during the class, and only a few will open them during short breaks.").

As expected, the build-up of CO_2 concentrations in the classroom was high, and at the end of the teaching period sometimes exceeding 4.000 ppm. Typical increases of CO_2 concentrations in the physics classroom for one week (Mon. to Fri., afternoon session) are shown in **Figure 4**.

The initial concentration of CO_2 in the classroom was different each day, and it depended on whether the classroom was used by another teacher prior to our measurements. As evident from **Table 3**, the initial concentrations in the morning sessions varied from 437 to 1.373 ppm and from 887 to 1.704 ppm in the afternoon sessions. This is not surprising, as CO_2 concentrations converged to nearly the outdoor levels overnight, while the breaks between morning and afternoon shifts were not long enough to allow for full replacement of air in the classroom. The results of all twenty measurements are shown in **Table 3**.

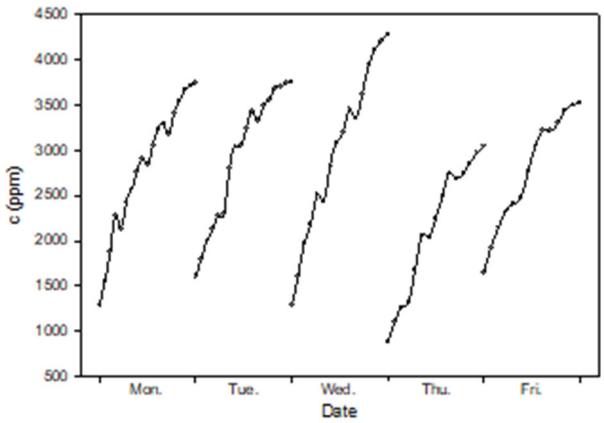

Figure 4. *A typical increase in CO_2 concentrations (in ppm) in the physics classroom during one week of measurements. From the moment when students entered the classroom in the afternoon (at 2 pm), the CO_2 concentration levels increased and reached the peak by the end of the afternoon shift. Occasional sharp drops in the CO_2 concentration were caused by open doors during short breaks.*

Table 3. The results of all the measurements. Data are sorted in ascending order, by the product of the number of physics classes (d*t* in hours), and the average number of students (N) throughout the measurement session. The initial, maximum, and average CO_2 concentrations are given for all days, together with the outdoor and indoor average temperatures (from Nov. 24 to Dec. 22). (M – morning schedule, A – afternoon schedule).

Day	Date	M/A	dt (h)	N	Ndt (h)	c (CO_2) (ppm)			t (°C)		
						d*c*	Initial	Max	Avg.	Outdoor	Indoor avg.
Thu.	30 Nov.	M	1.5	24	36	1305	1559	2864	2071	8	23.5
Thu.	21 Dec.	A	1.5	25	38	1750	1213	2963	2533	4	21.4
Fri.	24 Nov.	A	2.25	20	45	1967	1092	3059	2326	12	23
Fri.	8 Dec.	A	2.25	23	52	1883	1647	3530	2544	11	23.1
Fri.	1 Dec.	M	2.25	24	54	2384	505	2889	2153	8	23.5
Fri.	22 Dec.	A	2.25	24	54	2044	1592	3636	2079	10	23.5
Tue.	19 Dec.	A	2.25	26	59	1660	1704	3364	2630	3	23.8
Thu.	7 Dec.	A	2.25	26	59	2161	887	3048	3161	9	21.7
Thu.	14 Dec.	M	2.25	26	59	2426	437	2863	2955	9	23.3
Mon.	27 Nov.	M	3	23	69	2005	1343	3348	1951	6	23.9
Tue.	5 Dec.	A	3	24	72	2153	1605	3758	2829	6	23.5
Tue.	28 Nov.	M	3	25	75	2918	554	3472	2966	6	25.1
Tue.	12 Dec.	M	3	25	75	1775	1737	3512	2914	12	23.1
Mon.	4 Dec.	A	3	26	78	2455	1295	3750	2450	5	21.5
Mon.	18 Dec.	A	3	26	78	2402	1533	3935	2177	6	22.9
Wed.	29 Nov.	M	3.75	24	90	2530	1028	3558	2984	8	26.3
Wed.	20 Dec.	A	3.75	25	94	2551	1618	4169	2664	5	24.4
Wed.	6 Dec.	A	3.75	26	98	2994	1291	4285	3162	6	24.1
Mon.	11 Dec.	M	3.75	26	98	2781	1586	4367	1691	12	21
Wed.	13 Dec.	M	4.5	25	113	2572	872	3444	2716	7	23.6

Data are sorted in ascending order by the product of average number of students (N) and the number of continuous physics classes (d*t* in hours), with the aim to assess the influence of the product N·d*t* on the overall increase of the CO_2 concentration (d*c*). Due to an obviously low ventilation rate (VR), it is striking to notice that for the entire campaign, the CO_2 concentration built up to a total of over 3.000 ppm, and in several instances even over 4.000 ppm. The column "Avg" contains the average CO_2 concentrations during the entire teaching period. The average values ranged from 1.691 to 3.162 ppm. These concentrations are considerably above the ASHRAE recommended average limit values of 1,500 ppm over one school shift (DfES 2018; Bakó-Biró et al. 2011; ASHRAE 2013). The European standards for Indoor Air Quality are even more restrictive. According to the EN 15251 standard (CEN 2007), indoor air quality is classified into four categories based on the difference between outdoor and indoor CO_2 concentrations (**Table 4**).

Our results show that the IAQ for the entire sampling period was most of the time in the category IV, indicating a very poor IAQ, and a substandard ventilation rate. At the same time, because of a low ventilation rate, the classroom temperature increased to much higher levels than recommended. According to the European standard

EN 15251, an optimal temperature for classrooms is between 21 and 23°C. Our measurements show that in 15 out of 20 days, temperatures were higher than recommended, on several occasions reaching a maximum of 28°C!

Table 4. Four categories of indoor air quality according to the EN 15251. For simplicity, it is assumed that the outdoor CO_2 concentration is constant and equal to 400 ppm.

CATEGORY	c (ppm)
I	400 < c < 750
II	750 < c < 900
III	900 < c < 1200
IV	c > 1200

3.4. Theoretical model

Classrooms, such as the one used for measurements presented in this work, are ideal sites for measuring ventilation rates and for testing a simplified theoretical model of CO_2 concentration build-up, as given by **Equation 1**. This equation describes changes in CO_2 concentrations, at rates determined by the number of occupants in a known volume, and the ventilation rate of a confined classroom space. With the assumption that (nearly) ideal conditions are maintained (well mixed air, and no sudden, disruptive CO_2 sources or drains, e.g., opening doors or windows, increased number of occupants or their activity level), **Equation 1** expresses the mass balance of CO_2 entering and leaving the volume at any instant, *t* (Batterman 2017):

$$V\frac{dc(t)}{dt} = Qc_{out} - Q \cdot c(t) + S \qquad (1)$$

This equation describes the rate of CO_2 concentration increase, dc(t)/dt, within the volume of a classroom (V in m^3). Q is the air flow in/out of a classroom (in m^3h^{-1}), which can be used to estimate Ventilation Rate (VR) and/or Air Exchange Rate (AER), c_{out} is outdoor CO_2 concentration, c(t) is indoor CO_2 concentration and S is indoor source of CO_2 concentrations. The indoor source of CO_2 is a function of the number of students in the room, N and the CO_2 generation rate per person, G_p (in $Lmin^{-1}$ per person):

$$S = N \cdot G_p \qquad (2)$$

Air exchange rate, AER (in h^{-1}), is defined as:

$$AER = \frac{Q}{V} \qquad (3)$$

By substituting **Equation 2** for *S* and **Equation 3** for AER into **Equation** 1, the final expression for CO_2 concentration change for the ideal case is obtained:

$$\frac{dc(t)}{dt} = AER \cdot \left(c_{out} - c(t)\right) + \frac{NG_p}{V} \qquad (4)$$

In this equation the first term describes the CO_2 drain rate, and the second term is the CO_2 source. The equation written in this form is suitable for experimentally determining two unknown variables, AER and G_p.

3.5. Air Exchange and Ventilation rates, AER and VR

To estimate an air exchange rate, we use a special case of **Equation 4**, i.e., when S = 0, meaning that there are no occupants in the classroom (N = 0). The **Equation 4** transforms to a simplified form **Equation 5** which can now be used to calculate the AER from the experimental data.

$$\frac{dc}{dt} = AER \cdot \left(c_{out} - c(t)\right) \qquad (5)$$

This is a so-called decay, or step-down method (Sherman 1990; Smith 1988). The measurement period started in the evening hours (after the last class session) and ended in the morning when the indoor and outdoor concentrations of CO_2 were almost equal. Throughout the measurement, windows and doors were kept closed to make sure that the leakage rate was the same as during the class periods.

The CO_2 concentrations experimentally obtained during this measurement demonstrate a typical exponential decrease of CO_2 concentration and are shown in **Figure 5**.

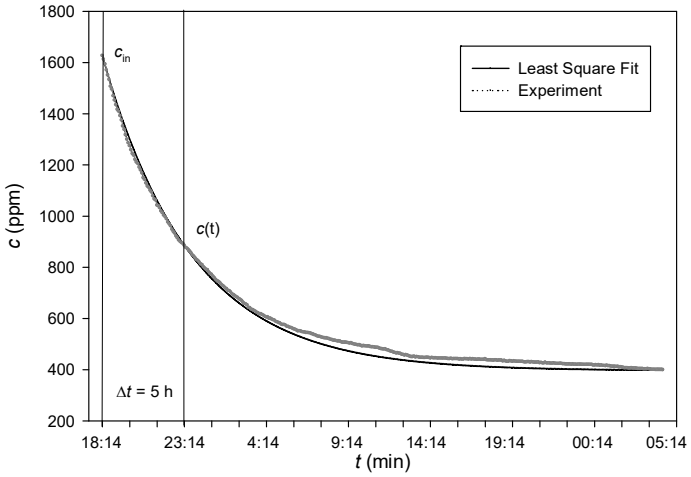

Figure 5. *The CO2 concentrations measured during the night (unoccupied) in the classroom with the closed windows and doors shows a typical, exponential decrease. The smooth line represents the least square fit of the exponential function [Eq. (5)] to the experimental values*

In this case, integration of **Equation 5** will give the following formula for determination of the indoor CO_2 concentration:

$$c(t) = c_{out} + (c_i - c_{out})e^{-AER \cdot t} \qquad (6)$$

where c_i is the initial concentration in ppm. After rearranging, **Equation 6** gives the expression for calculating the AER from the CO_2 decay function:

$$AER = \frac{1}{\Delta t} \ln\left(\frac{c(t) - c_{out}}{c_i - c_{out}}\right) \qquad (7)$$

where c_{out} is approximated with 400 ppm.

The least square fit of the experimental data with this exponential function gave the air exchange rate of 0.18 h^{-1}, for unoccupied classroom with closed windows and doors. Fitting results are shown in Figure 6. The obtained value was much lower than the lowest recommended value of 4 h^{-1} for classrooms by the EN 15251 (CEN 2007).

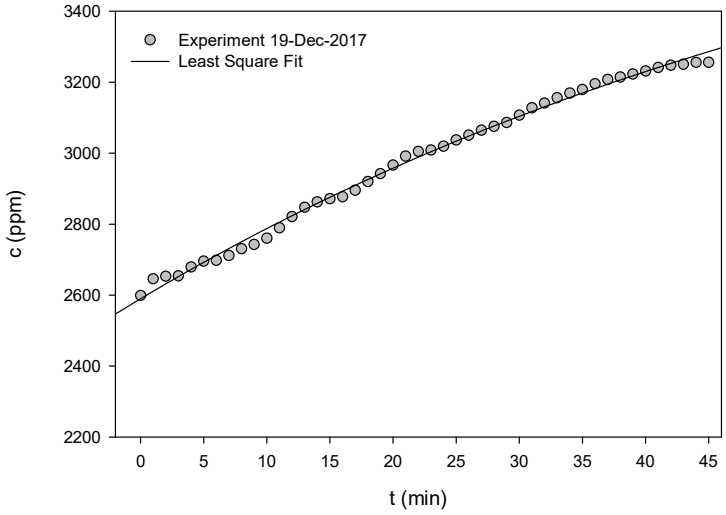

Figure 6. *A comparison between the experimental and best fitted values of CO_2 concentrations by 20 students in closed windows classroom for 19 Dec. 2017*

3.6. Estimation of the CO_2 generation rate

Once the air exchange rate is obtained with closed windows, the least square fit of the experimental data with Eq. (4) gives us a CO_2 generation rate, Gp, which is now the only unknown parameter in **Equation 4**.

For that purpose, CO_2 concentrations were monitored during a 45-minute class, with 20 students occupying the classroom. The measured CO_2 concentrations increased from 2.598 to 3.256 ppm during the class. This concentration increase was a result of the initial concentration, the concentration build-up by 20 students, and the small, but still measurable leak of CO_2 through the gaps in doors and windows.

Experimental data and the obtained fit are shown in **Figure 7**. The obtained fitted value of G_p for this period was 0.31 $Lmin^{-1}$. The obtained value is in the expected range of CO_2 generation for 15 to 18-year-old students in sedentary physical activity level, which is typically between 0.319 and 0.343 $Lmin^{-1}$ (Batterman 2014; Haverinen-Shaughnessy et al. 2011).

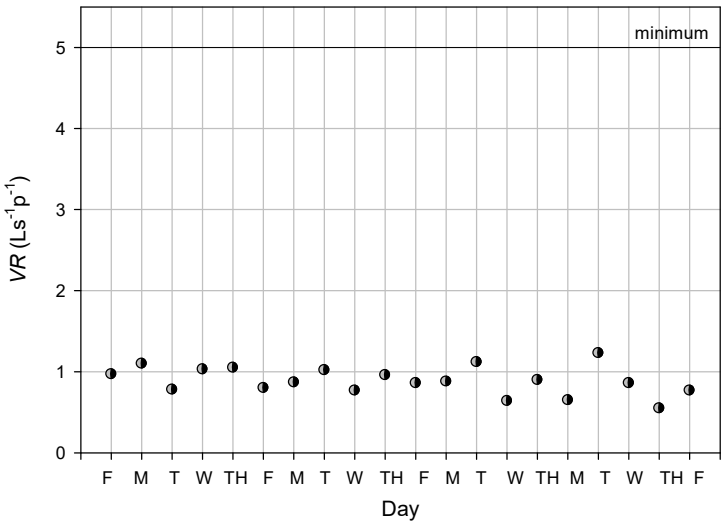

Figure 7. *The calculated ventilation rates for all days were considerably below the ASHARE and EN13779 minimum recommended value*

Air exchange rates in an occupied classroom were defined by means of **Equation 4**. This expression was used to calculate the AER for all days. From the obtained AER, a more commonly used ventilation rate (VR) in $Ls^{-1}p^{-1}$ was calculated with the following expression:

$$VR = \frac{AER \cdot V_{air}}{N} \qquad (8)$$

where V is the volume of air in classroom (**Table 1**) and N is the average number of students (**Table 3**).

The obtained VRs for all days are presented in **Figure 7** (in occupied classroom). As evident from **Figure 7**, ventilation rates varied from 0.56 to 1.23 Ls^{-1} per person. These values are far below the minimum recommended limit value of 5 $Ls^{-1}p^{-1}$ (ASHRAE 2013; CEN 2006).

3.7. Simulation of the entire session

To check the validity of the experimentally obtained CO_2 generation rate G_p and ventilation rate for the closed windows classroom, the data obtained for a typical working day (11 Dec. 2017) during five consecutive physics classes and four breaks (5 to 15 minutes) were used. The experimentally obtained data were compared with the theoretical model for calculating the CO_2 concentration, c(t), as given by **Equation 9**, which was obtained by integrating **Equation 4** into the entire teaching period:

$$c(t) = \frac{N \cdot G_p}{V_{air}} \cdot t + c_{out} + (c_i - c_{out})e^{-AER \cdot t} \qquad (9)$$

By applying the experimentally obtained Gp (0.31 $Lmin^{-1}$) and AER (0.003 min^{-1}) with the exact number of occupants for each class (27, 24, 26, 25 and 25 respectively), to the above equation, a very strong simulation of the experimentally obtained data was achieved (**Figure 8**).

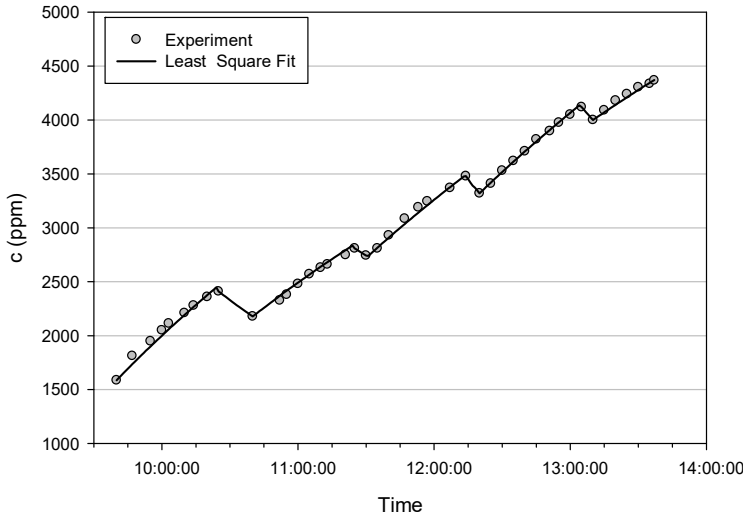

Figure 8. *A comparison between the experimental data obtained on 11 Dec. 2017 and theoretically calculated CO_2 concentrations in closed windows classroom during 5 consecutive physics classes*

During the 5- and 15-minute breaks, when the classroom was empty, **Equation 5** was used to calculate the decay of CO_2 concentrations (the decrease was typically 5 % to 10 %, depending on the length of the break). As evident from **Figure 8**, correlation between the experimentally obtained CO_2 concentrations and simulated values was nearly perfect with R^2 of 0.98. This confirms the validity of the theoretical model used, the experimentally obtained values of CO_2 generation rates, G_p, as well as the ventilation rates for the physics classroom used in this work during the entire teaching session.

4. CONCLUSION

The results of this study show limited ventilation of classrooms during lectures, during the heating season. Very high concentrations of CO_2, of over 4.000 ppm, were measured on several occasions. This is a result of a limited ventilation of classrooms during the heating season, as traditionally, the only ventilation in most of our schools is provided by opening windows. As outdoor temperatures are low during the winter, school's management, teachers, and students are hesitant to open windows and ventilate rooms. Closed windows, over a prolonged period of time, result in a poor ventilation rate, and consequently, in alarmingly high CO_2 concentrations.

Indoor air quality, and in particular the CO_2 concentration, was monitored in the physics classroom on a daily basis from mid-November till the end of December 2017, by using several low-cost instruments. The measuring took place in a grammar school in Rijeka, Croatia.

Detailed CO_2 generation rates, air exchange rates, and ventilation rates were calculated and reported in this work, from the experimentally obtained data. The experimentally obtained data were compared with the theoretical model and a strong correlation was achieved. Ventilation rates were found to be in the range between 0.6 and 1.2 Ls^{-1} per person, which is far below the lowest recommended value of ventilation rate according to the EU regulation of 5 Ls^{-1} per person (EN 15251).

Poor IAQ can have significant impact on students' health and performance. These data may be useful in assessing health effects of student's exposure, in understanding the underlying mechanisms, and in implementing preventive policies in terms of occupied classroom standards. The simplest solutions for reduction of CO_2 concentrations in an occupied classroom are changing the behaviour of teachers, such as having them open the windows at every break between classes, or installing low-cost instruments with an alarm that activates when CO_2 concentrations are above 1.500 ppm. The best technological interventions are an installation of automated ventilation systems in classrooms, which would automatically inject fresh air into the room when CO_2 concentration exceeds 1.000 ppm.

This is the first report of this kind in Croatia; therefore, we hope that many studies by health workers and researchers will follow. Also, we hope that schools' management will introduce the appropriate IAQ monitoring practices and install automated ventilation systems in classrooms for the benefit of student's health and an improvement of their learning abilities.

Acknowledgments*:* The authors thank the school principal Henry Ponte and the students of Andrija Mohorovičić Grammar School in Rijeka.

5. REFERENCES

ASHRAE (2013) Standard 62.1-Ventilation for Acceptable Indoor Air Quality. Atlanta, GA, American Society of Heating, Refrigeration, and Air-Conditioning Engineers, Inc. http://www.myiaire.com/product-docs/ultraDRY/ASHRAE62.1.pdf

Bakó-Biró Zs, Clements-Croome DJ, Kochhar N, Awbi HB and Williams MJ (2011) Ventilation rates in schools and pupils' performance. Build. Environ. 48:215–223. doi:10.1016/j.buildenv.2011.08.018

Batterman S (2017) Review and Extension of CO_2-Based Methods to Determine Ventilation Rates with Application to School Classrooms. Int. J. Environ. Res. Public Health. 14(2):145–167. doi:10.3390/ijerph14020145

Bréon FM, Broquet G, Puygrenier V, Chevallier F, Xueref-Remy I, Ramonet M, Dieudonné E, Lopez M, Schmidt M, Perrussel O and Ciais P (2015) An attempt at estimating Paris area CO_2 emissions from atmospheric concentration measurements, Atmos. Chem. Phys. 15(4):1707–1724. doi:10.5194/acp-15-1707-2015

CEN (2006) European Committee for Standardisation, EN 13779–Ventilation for non-residential buildings–Performance requirements for ventilation and room conditioning systems, European Committee for Standardisation, Brussels, Belgium.
http://www.cres.gr/greenbuilding/PDF/prend/set4/WI_25_Pre-FV_version_prEN_13779_Ventilation_for_non-resitential_buildings.pdf

CEN (2007) European Committee for Standardisation, EN 25151:2007. Indoor environmental input parameters for design and assessment of energy performance of buildings addressing indoor air quality, thermal environment, lighting and acoustics. http://www.cres.gr/greenbuilding/PDF/prend/set4/WI_31_Pre-FV_version_prEN_15251_Indoor_Environment.pdf

DfES (2018) Building Bulletin 101 Guidelines on ventilation thermal comfort and indoor air quality in schools. Department for Education and Skills, London, U.K. Accessed August 28, 2019. https://www.gov.uk/government/publications/building-bulletin-101-ventilation-for-school-buildings

Ginsberg G, Asgharian B, Kimbell JS and Ultman JS (2007) Modelling Approaches for Estimating the Dosimtry of Inhaled Toxicants in Children. J. Toxicol. Environ. Health A. 71:165–195. doi: 10.1080/15287390701597889

Goldwin C and Batterman S (2007) Indoor air quality in Michigan schools. Indoor Air J. 17(2):109–121. doi:10.1111/j.1600-0668.2006.00459.x

Haverinen-Shaughnessy U, Moschandreas DJ and Shaughnessy RJ (2011) Association between substandard classroom ventilation rates and students' academic achievement. Indoor Air J. 21:121–131. doi:10.1111/j.1600-0668.2010.00686.x

Mendell MJ and Heath GA (2005) Do Indoor Pollutants and Thermal Conditions in Schools Influence Student Performance? A Critical Review of the Literature. Indoor Air J. 15:27–52. doi:10.1111/j.1600-0668.2004.00320.x

NOAA (2019) Mauna Loa CO_2 monthly mean data from 1958 to 2019. National Oceanic and Atmospheric Administration, Earth System Research Laboratory. Accessed August 28, 2019.
https://www.esrl.noaa.gov/gmd/ccgg/trends/data.html

OECD (2014) Indicator D1: How much time do students spend in the classroom?, in Education at a Glance 2014: OECD Indicators. OECD Publishing. http://www.oecd.org/education/EAG2014-Indicator%20D1%20(eng).pdf

Report on the inventory of greenhouses gases in the Republic of Croatia for period 1980-2015 (2017) Hrvatska agencija za okoliš i prirodu. Accessed August 28, 2019.
http://www.haop.hr/sites/default/files/uploads/dokumenti/012_klima/dostava_podataka/Izvjesca/HRV_NIR_2017.pdf

Selgrade MK, Plopper CG, Gilmour MI, Conolly RB and Foos BS (2008) Assessing the health effects and risks associated with children's inhalation exposures asthma and allergy. J. Toxicol. Environ. Health A 71:196–207. doi:10.1080/15287390701597897

Sherman MH (1990) Tracer-Gas Techniques for Measuring Ventilation in a Single Zone. Build. And Environ. 25(4):365–374. doi:10.3390/ijerph14020145

Smith PN (1988) Determination of Ventilation Rates in Occupied Buildings from Metabolic CO_2 Concentrations and Production Rates. Build. and Environ. 23(2):95–102.
https://www.aivc.org/sites/default/files/airbase_3353.pdf

Tasić V, Živković M, Lazović I, Brdarić D, Capak K, Barišin A, Jovašević-Stojanović M (2015) Measurement of gas pollutants in the Serbian and Croatian schools. The 47th International October Conference on Mining and Metallurgy Bor, Serbia, 439–444. https://www.bib.irb.hr/893976

Turnjanin V, Vučićević B, Jovanović M, Mirkov N, Lazović I (2014) Indoor CO_2 measurements in Serbian schools and ventilation rate calculation. Energy 77:290–296. doi:10.1016/j.energy.2014.10.028

WHO (2015) School environment: policies and current status. WHO Regional Office for Europe.
http://www.euro.who.int/__data/assets/pdf_file/0009/276624/School-environment-Policies-current-status-en.pdf?ua=1

MICROBIOLOGICAL QUALITY OF WELL WATER FROM KOPRIVNICA-KRIŽEVCI COUNTY IN 2018

Sanja Furmeg [1]*, Lana Feher Turković [2], Ana Mojsović Ćuić [2], Vesna Jaki Tkalec [1], Maja Kiš [1]
[1] *Croatian Veterinary Institute, Veterinary Department Križevci, Ivana Zakmardija Dijankovečkog 10, 48260 Križevci, Croatia*
[2]*University of Applied Health Sciences, Mlinarska cesta 38, 10000 Zagreb, Croatia*
*E-mail of corresponding author: sanja.furmeg@gmail.com

Abstract: *In this study, microbiological quality of drinking water deriving from the private wells from Koprivnica-Križevci County was investigated. A total of 287 samples from different locations were collected during 2018 and analysed for the following microbiological parameters: total coliforms, Escherichia coli, Enterococcus spp., Clostridium perfringens, Pseudomonas aeruginosa, and the number of aerobic heterotrophic bacteria at 36 °C and 22 °C. The results showed that 24 % of the analysed water samples were of unsatisfactory microbiological quality, with high incidence of faecal contamination. Well water is still the main source of drinking water for many residents of this County, especially in its rural parts, so continuous monitoring and disinfection of drinking water deriving from private wells is of exceptional importance for the public health.*
Keywords: *drinking water, water microbiology, private wells, health safety.*

Received: 11.11.2019. / Accepted: 20.02.2020.
Published online: 01.12.2021.

Original scientific paper
https://doi.org/10.37023/ee.8.1-2.2

1. INTRODUCTION

According to data of Croatian Institute of Public Health (2018), more than 87 % of Croatian population uses public water supply system and drinks tap water, which is regularly controlled and conforms to health safety standards. It means that more than 13 % households in Croatia rely on private wells as their only source of drinking water. Health safety of well water intended for human consumption depends upon several factors. These primarily include quality and purity of raw water, technology of purification and application of disinfecting procedures. Sanitary-technical and hygienic conditions of the water supply objects also have great importance in maintaining drinking water quality. Monitoring of drinking water deriving from public water supply systems is carried out on a national level, while monitoring of well water or local water supply systems is performed only upon an owner's personal request. Drinking water has to possess good sensory features (no colour, taste and odour), without the presence of substances in concentrations which could detrimentally influence the human organism as well as without agents causing diseases (pathogens) which could be transferred through drinking water (Vukić Lušić et al. 2017). In order to prevent hydric infections, it is of outmost importance to have a constant control of drinking water safety, which is also prescribed by the Law on the Water Intended for Human Consumption (Official Gazette 56/13, 64/15, 104/17, 115/18).

Routine microbiological analysis of drinking water plays an essential role in measures to protect public health. In general terms, the greatest microbial risks are associated with consumption of water that is contaminated with human or animal faeces. Wastewater discharges and inadequate drainage from nearby facilities (septic tanks, stables) are the major source of faecal microorganisms, including pathogens (Cabral 2010). Water-related infections are transferred and spread through the water on the limited area within a relatively short period of time, and may occur as endemic, pandemic or individually. It is not only bacteria, viruses and parasites that may be transferred by water, but also their toxins which may be present in the water even when the microorganisms are no longer there (Marjanović & Tofant 2008).

Health safety control of drinking water in Croatia is conducted pursuant to the Croatian water quality regulations (Official Gazette 125/17). In Koprivnica-Križevci County there is a developed public water supply system, with its tendency for expansion. However, private wells and local water supply systems are still the only source of drinking water for the residents in the rural parts of the County. Private wells are also used as source of drinking water for farm animals (Denžić Lugomer et al. 2019).

Since microbiological contamination of drinking water may present a great risk for human health, but also for the health of animals, the goal of this research was to establish the microbiological status of water from the private wells from Koprivnica-Križevci County.

2. MATERIALS AND METHODS

Well water samples from different locations in Koprivnica-Križevci County were submitted to the Laboratory of Food and Feed Microbiology, Veterinary Department Križevci for microbiological analysis. Most of the samples were collected by qualified laboratory employees, in clean, sterile glass bottles and transported in cooling boxes to the laboratory within six hours from the sampling, guided by the rules of good laboratory practice. Immediately after arriving to the laboratory, the samples were subjected to microbiological analysis. Some of the samples were delivered by owners, who were prior given a sterile bottle for sampling and detail instructions about the proper sampling methods for well water samples. A total of 287 well water samples were collected during 2018. Conducted microbiological analysis included following parameters: total coliforms, *Escherichia coli*, *Enterococcus* spp., *Clostridium perfringens*, *Pseudomonas aeruginosa* and the number of aerobic heterotrophs at 36 °C and 22 °C.

For confirming and determining the total number of coliform bacteria and *E. coli* in water samples, the membrane filtration method was used, according to the standard procedure EN ISO 9308-1:2014/A1:2017. In case of *E. coli* and total coliforms, the solid selective agar CCA (Chromocult® Coliform Agar, Merck, Germany) was used and incubated at 36 ± 2 °C for 21 ± 3 hours. The typical colonies of *E. coli* are dark blue to violet, indole positive and oxidase negative. The total coliform bacteria on CCA range from pink to red colonies and were confirmed as oxidase negative and no indole production (**Figure 1A**).

For confirming and determining the number of *Enterococcus* spp. by membrane filtration method, prescribed by the standard procedure EN ISO 7899 -2:2000, Slanetz and Bartley agar (Merck, Germany) was used and incubation temperature at 37 ± 0.5 °C for 44 ± 4 hours (**Figure 1B**).

For enumeration of vegetative cells and spores of *C. perfringens*, the method of membrane filtration was used, according to the standard procedure EN ISO 14189:2016. The volume of 100 ml of water sample was filtrated through the membrane filter (pore size 0.20 µm). TSC agar (Tryptone Sulfite Cycloserine Agar, Biokar, France) was used and incubated in anaerobic conditions at 44 °C for 24 hours.

Detection of *P. aeruginosa* was conducted pursuant to the standard procedure EN ISO 16266:2008, using the membrane filtration method. Pseudomonas Agar (Merck, Germany) was incubated at 36 ± 2 °C during 44 ± 4 hours. This is a selective medium containing cetrimide. Typical colonies produce pigment pyocyanin giving the blue-green colour. Typical *P. aeruginosa* colonies are oxidase positive, fluorescent under the UV light (360 ± 20 nm) and they can produce ammonia from the acetamide (**Figure 1C**).

For determining the number of aerobic heterotrophic bacterial colonies (heterotrophic plate count), a procedure was used according to the norm EN ISO 6222:2000. The number of microorganism colonies was established in 1 ml of water sample, by using pouring plate method with Yeast Extract Agar (Merck, Germany). The plates were incubated at 22 ± 1 °C for 68 hours and at 36 °C during 44 ± 4 hours (**Figure 1D**).

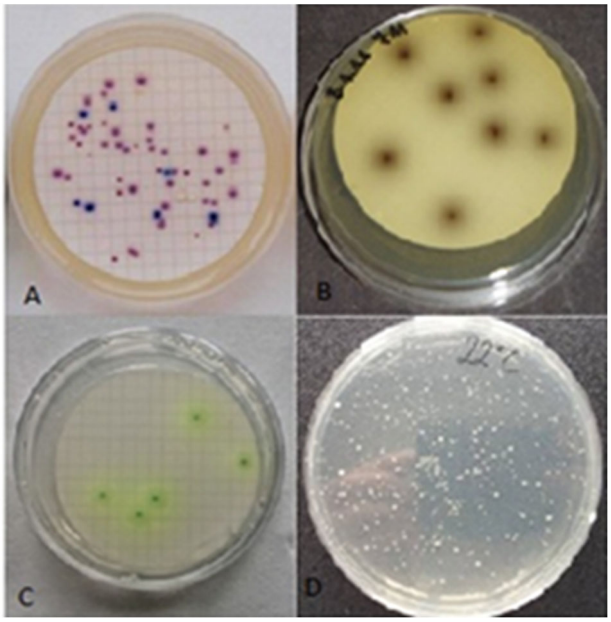

Figure 1. *Representative groups of bacteria isolated from well water: A) Escherichia coli and coliform bacteria on the CCA agar; B) Enterococcus spp. on the BAA agar; C) Pseudomonas aeruginosa on a selective Pseudomonas agar; D) Number of colonies of aerobic heterotrophic bacteria on the YEA agar (source: Veterinary Department Križevci)*

3. RESULTS AND DISCUSSION

Water for human consumption must meet the standards defined by the Ordinance on conformity parameters, analytical methods, monitoring and drinking water safety plans, and keeping register of legal entities which provide public water supply (Official Gazette 125/17). Maximum Permissible Concentrations (MPC) set by this Ordinance for the number of colonies at 22 °C are up to 100 CFU/ml; for the number of colonies at 36 °C up to 20 CFU/ml, whereas for *E. coli*, total coliforms, *Enterococcus* spp., *C. perfringens* and *P. aeruginosa*, defined MPC are 0 CFU/100 ml.

Considering that, among 287 analysed well water samples, 76.0 % (218 samples) were compliant to Ordinance (Official Gazette 125/17). The percentages of unsatisfactory samples per individually analysed microbiological parameter, are shown in **Table 1**. The microbiological quality of well waters significantly differs from one well to another according to indicators of faecal contamination. Results of total coliform bacteria determination showed that the number of colonies ranges from 0 CFU/100 mL up to 206 CFU/100 ml. The results of this study showed that 67 samples were unsatisfactory due to determined presence of coliforms. Presence of *E. coli* bacteria, as well as the presence of *Enterococcus* spp. in water is the most common indicator of faecal pollution. *E. coli* is a part of the normal intestinal microflora of humans and animals, therefore is widely distributed in the environment, mainly by different human activities. Water contaminated with *E. coli* and intestinal enterococci presents a high potential risk for the human health. **Figure 2** shows the concentration of *E. coli* in 287 analysed well water samples. The number of colonies varies from 1 CFU/100 ml up to 150 CFU/100 ml. Results of *Enterococcus* spp. determination showed that the number of colonies ranges from 0/100 ml to 127/100 ml (**Figure 3**). Results of this study showed that the *E. coli* is present in 59 samples (20.6 %), which indicate poor microbiological quality of the examined water samples. The number of *Enterococcus* spp. colonies in the analysed samples varies from 2/100 ml up to 127/100 ml. According to the Croatian water quality regulations (Official Gazette 125/17), 56 samples (19.5 %) were unsatisfactory due to this parameter (**Figure 4**).

Table 1. Unsatisfactory well water samples pursuant to the Maximum Permissible Concentrations set out by the Croatian water quality regulations per individually analysed microbiological parameter

ANALYSED PARAMETER	NUMBER OF UNSATISFACTORY SAMPLES (Out of total 287 water samples)	%
Total coliforms	67	23.34
Escherichia coli	59	20.56
Enterococcus spp.	56	19.51
Clostridium perfringens	1	0.35
Pseudomonas aeruginosa	11	3.83
Heterotrophic plate count at 22°C	64	22.30
Heterotrophic plate count at 36°C	68	23.69

Sulphite-reducing clostridia, namely *C. perfringens*, are spore-forming Gram-positive, non-motile, anaerobic, sulphite-reducing rods. *C. perfringens* is present in higher numbers in the faeces of some animals (such as dogs) and less often of many other warm-blooded animals and humans. Because of ability to produce endospores, it is exceptionally resistant to unfavourable conditions in water environments, including UV irradiation, temperature and pH extremes and disinfection processes, such as chlorination (Cabral 2010). The presence of *C. perfrigens* in water indicates contamination with faeces or wastewaters for a longer period of time (Denžić Lugomer et al. 2017). In this study, the presence of this anaerobic bacterium was established only in one sample, with concentration of 13 CFU/100 ml.

Presence of opportunistic pathogen *P. aeruginosa* indicate inadequate maintenance of the water supply system and it is very important that drinking water is without it. Bacteria of this genus are capable of growing in environments with small amounts of nutrients. It is highly resilient, changes odour, colour and taste of water and is responsible for the occurrence of the biofilm in water distribution system. Despite of the widespread distribution of *P. aeruginosa* in the different environments such as soil, water and sewage, water contamination with this bacterium is considered to occur in low proportion, regards to other water contaminants (Vukić Lušić et al. 2017). In this study, *P. aeruginosa* was detected in only 3.83 % of the analysed samples (**Figure 4D**).

Denžić Lugomer et al. (2019) investigated the water quality on farms in northwest Croatia and determined the presence of *P. aeruginosa* in 5.8 % of analysed samples. All the unsatisfactory samples in that study came from water wells, while all samples from water distribution system were satisfactory. In a study by Vukić Lušić et al. (2017), *P. aeruginosa* was detected in only 0.3 % analysed samples from water distribution system in Primorje-Gorski kotar County during 2014.-2016.

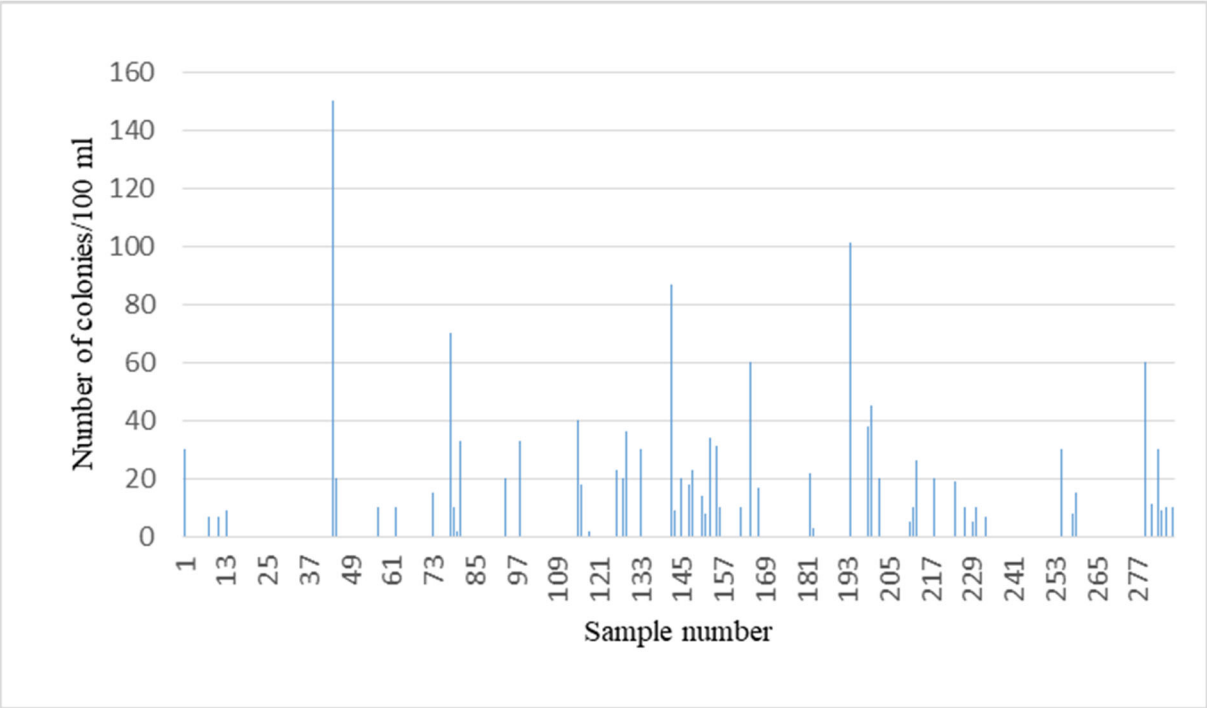

Figure 2. *Variation of E. coli (CFU/100 ml) in analysed well water samples*

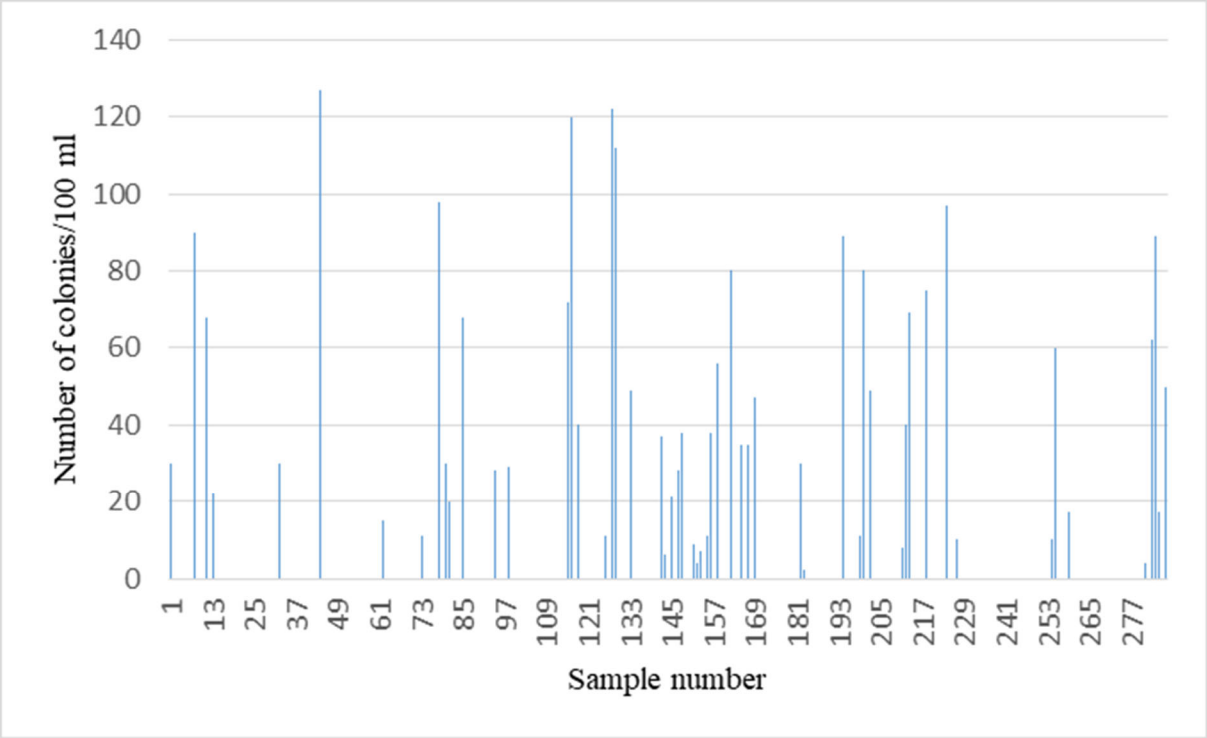

Figure 3. *Variations of Enterococcus spp. (CFU/100 ml) in analysed well water samples*

Similar research was also conducted in the neighbour area of the Bjelovar-Bilogora County, which included analyses of water sampled at the milk collection centres during the period from 2011.-2016. Analysed water was

used for human consumption, for the purposes of the households and as drinking water for cattle. The results have shown that out of the total of 147 examined water samples, 68 samples were microbiologically unsatisfactory, i.e. 46.3 %. The number of samples which did not correspond to the prescribed MPC values was 56 samples for intestine enterococci (38.1 %), 41 samples to total coliforms (27.9 %), 32 samples to *E. coli* (21.8 %). *C. perfringens* was determined in 11 samples (7.5 %), whereas *P. aeruginosa* was found in 3 samples (2 %). In the mentioned research, the number of unsatisfactory samples was decreasing during the years, which indicates the fact that more care was dedicated to well water quality control in milk collection centres (Denžić Lugomer et al. 2016). By further comparing the results obtained in this work to similar examinations conducted on the territory of the Republic of Croatia, it may be concluded that the number of unsatisfactory samples in previous years in various areas of Croatia was much higher (Smilović et al. 2011). Still, monitoring of drinking water from private wells is not conducted regularly, nor in the way the public water supply systems are being controlled. This may partly be explained by a relatively small number of samples analysed in some of the mentioned studies (Senta & Marijanović Rajčić 2007). In some areas of Croatia connection to the public water supply system still isn't provided. Likewise, awareness of the Croatian citizens when it comes to health safety of the drinking water could be considered as insufficient. The water pollution most commonly occurs by the penetration of organic matter from septic tanks, improperly built or deteriorated sewage systems, cattle barns and farms with improper disposal of farmyard manure (Denžić Lugomer et al. 2016).

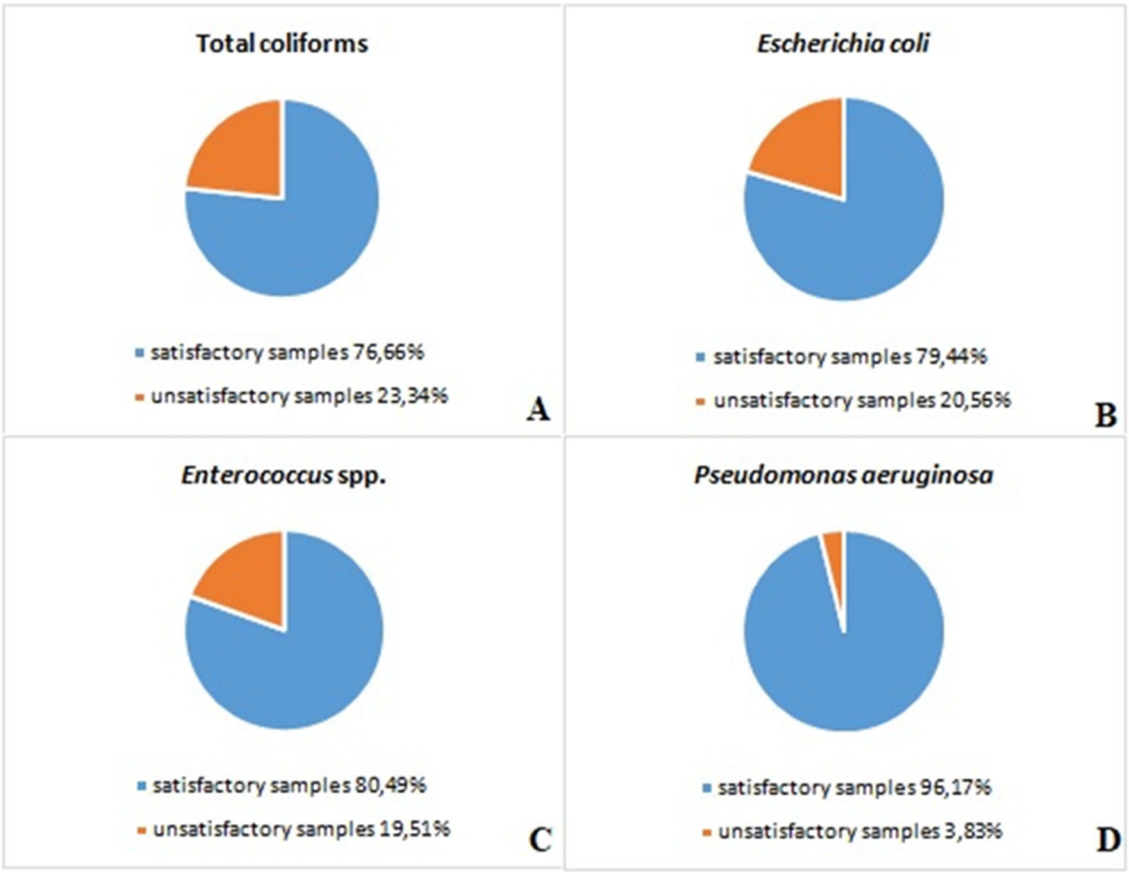

Figure 4. *The proportion of satisfactory and unsatisfactory analysed water samples from private wells for the parameter of: A) total coliforms; B) Escherichia coli; C) Enterococcus spp.; D) Pseudomonas aeruginosa*

The evaluation of drinking water health safety in the Međimurje County during the period 2004.- 2008., showed that 83.0 % of water samples from individual water supply objects (wells or water pipes) were unsatisfactory in terms of health safety. The percentage of chemical and microbiological contamination in water samples was 45.5 % and 32.5 % respectively. At the same time, 98.3 % of drinking water samples from the public water supply system were confirmed as satisfactory (Smilović et al. 2011).

In the microbiological examination of the well water samples from the Zagreb surroundings, 61.8 % of analysed well water samples had a poor microbiological quality. Out of the total of 34 examined water samples, 24 contained coliform bacteria and in two samples enterococci were determined (Senta & Marijanović Rajčić 2007).

Due to the still high proportion of unsatisfactory samples, both from this study, but also from the previously mentioned studies, it may be concluded that, in addition to regular control of water performed by the institutions

in charge of public health, it is necessary to particularly engage in the education of the Croatian citizens on the importance of drinking water safety, as well as on the proper procedures for wells disinfection.

4. CONCLUSION

The microbiological analysis of well water samples was conducted according to the standardised methods, pursuant to the current statutory regulations and existing water quality regulations in Croatia. This study showed that 24 % of analysed samples were unsatisfactory according to the above-mentioned regulations. The most unsatisfactory samples pursuant to the Maximum Permissible Concentrations were total coliforms, *E. coli* and *Enterococcus* spp. Since in this study only samples of drinking water deriving from private wells were investigated, it is necessary to point out the need for continuous microbiological monitoring of well water, particularly in the places where it is used as the only source of drinking water for human and animal consumption. The quality of water from the private wells could vary, therefore it is important to determine the main sources of contamination and adequate measures to protect the wells from external pollution. The population of the Koprivnica-Križevci County, as well as the other consumers of drinking water deriving from private wells, needs to be educated on the importance of disinfection and should be provided with guidelines about appropriate disinfection procedures. Regular microbiological analysis before and after the disinfection would be very useful to establish the efficiency of the procedure.

5. REFERENCES

Cabral JPS (2010) Water Microbiology. Bacterial Pathogens and Water. International Journal of Environmental Research and Public Health, 7 10):3657-3703

Croatian Institute of Public Health (2018) Drinking water safety in Croatia (https://www.hzjz.hr/en/division-of-environmental-health/drinking-water-safety-in-croatia)

Croatian water quality regulation (2017) Ordinance on conformity parameters, analytical methods, monitoring and drinking water safety plans, and keeping register of legal entities which provide public water supply. NN. 125/17

Denžić Lugomer M, Jaki Tkalec V, Kiš M, Pavliček D, Furmeg S, Sokolović J (2017) Water quality on cattle farms in the northwest Croatia. Croatian Journal of Food Technology, Biotechnology and Nutrition 12(3-4):126-130

Denžić Lugomer M, Jaki Tkalec V, Pavliček D, Kiš M, Sokolović J, Majnarić D (2016) Analiza pitke vode na sabiralištima mlijeka Bjelovarsko-bilogorske županije. Croatian Journal of Food Technology, Biotechnology and Nutrition 11(3-4):176-181

Denžić Lugomer M, Pavliček D, Kiš M, Jaki Tkalec V, Furmeg S, Sokolović S, Majnarić D (2019) Water quality on farms in northwest Croatia. Veterinarska stanica 50(2):115-124

EN ISO 14189:2016 - Water quality - Enumeration of Clostridium perfringens - Method using membrane filtration (ISO 14189:2013; EN ISO 14189:2016)

EN ISO 16266:2008 - Water quality - Detection and enumeration of Pseudomonas aeruginosa - Method by membrane filtration (ISO 16266:2006; EN ISO 16266:2008)

EN ISO 6222:2000 - Water quality - Enumeration of culturable micro-organisms - Colony count by inoculation in a nutrient agar culture medium (ISO 6222:1999; EN ISO 6222:1999)

EN ISO 7899-2:2000 - Water quality - Detection and enumeration of intestinal enterococci - Part 2: Membrane filtration method

EN ISO 9308 – 1:2014/A1:2017 – Water quality - Enumeration of Escherichia coli and coliform bacteria - Part 1: Membrane filtration method for waters with low bacterial background flora (ISO 9308-1:2014/Amd 1:2016; EN ISO 9308-1:2014/A1:2017)

Marjanović S, Tofant A (2008) Kvaliteta vode za napajanje goveda – čimbenik dobrobiti. Meso X:127-131

Official Gazette: Law on the Water Intended for Human Consumption. 56/13, 64/15, 104/17, 125/17, 115/18

Senta A, Marijanović Rajčić M (2007) Zdravstvena ispravnost pitke vode iz privatnih zdenaca u Zagrebu. Liječnički vjesnik 129:39-43

Smilović V, Vrbanec Megla L, Tarandek Strnad S (2011) Zdravstvena ispravnost vode za piće u javnim i individualnim vodoopskrbnim objektima u Međimurskoj županiji. Hrvatski časopis za javno zdravstvo 7(28): 1845-3082

Vukić Lušić D, Đandara A, Piškur V, Linšak Ž, Bilajac L, Lušić D (2017) Zdravstvena ispravnost vode za piće u Gorskom kotaru u petogodišnjem razdoblju od 2011. do 2015. Medicina Fluminensis 53:216-224

Vukić Lušić D, Herceg Z, Cenov A, Glad M, Lušić D (2017) Prisutnost *P. aeruginosa* u distribucijskim sustavima vode za piće u Primorsko-goranskoj županiji. Knjiga sažetaka 1. simpozij sanitarnog inžinjerstva s međunarodnim učešćem, Maestro, Daniel (ur.), Ljubljana: Inštitut za sanitarno inženirstvo, Ljubljana, Slovenia, 42-4

DEPENDENCE OF CONCENTRATION OF RADON ON ENVIRONMENTAL PARAMETERS – MULTIPLE LINEAR REGRESSION MODEL

Anita Ptiček Siročić [1*], Sanja Kovač [1], Davor Stanko [1], Iva Pejak [1]
[1] *University of Zagreb, Faculty of Geotechnical Engineering, Hallerova aleja 7, HR42000, Varaždin, Croatia*
*E-mail of corresponding author: anitaps@gfv.unizg.hr

Abstract: *Radon (^{222}Ra) is a colourless and odourless natural radioactive element in gaseous state. The concentration of radon in the air is usually low, but it can be very high inside of a living space, because of its possibility to penetrate from a foundation soil over a basement into a building itself. People are daily exposed to a certain concentration of radon that is found in soil, water, air and food. This paper shows a correlation analysis of environmental parameters by using the model of multiple regressions. It defines certain statistical relations between environmental parameters such as temperature, humidity, and atmospheric pressure with measured values of radon concentrations. Measurements were carried out at several locations in various residential buildings in north-western Croatia. The results indicated that individual environmental parameters and radon concentration at individual locations were connected. For example, at one location the concentration of radon was decreasing if atmospheric pressure was increasing. Measurements at another location indicated that the concentration of radon was increasing if air humidity was increasing. Due to large number of different parameters affecting the concentration of radon in residential buildings, a satisfactory statistical model to predict the concentration of radon with environmental parameters is not easy to achieve since it was observed variability of radon concentrations with environmental parameters within different local sites. It is necessary to consider a longer period to determine with certainty a mathematical model that would give the most accurate prediction of radon concentration dependence on environmental parameters which can affect human health and quality of life.*
Keywords: *radon, temperature, humidity, regression model*

Received: 06.11.2020. / Accepted: 05.02.2021.
Published online: 01.12.2021.

Original scientific paper
https://doi.org/10.37023/ee.8.1-2.3

1. INTRODUCTION

Radon (222Rn) is a natural noble radioactive gas, whose main source is soil. Radon is formed as a progeny in the radioactive series of uranium, which is found in the Earth's crust. On its way to the atmosphere, radon mixes with the air that people inhale and take into the body (James 1988). The main consequence of the presence of high concentrations of radon in the environment is the development of deadly lung cancer (by inhalation) and gastric cancer (by ingesting water). Radon concentrations change significantly over time, and thus throughout the year. For a more reliable estimate of the radiation dose of radon and its short-lived offspring in the environment, it is necessary to perform measurements for at least one year. The measurement is performed using specially developed nuclear trace detectors that are exposed in the environment where people live every day (Zeeb et al. 2009). In accordance with (Council Directive 2013/59 Euroatom) on the basic safety standards for protection against the dangers arising from exposure to ionizing radiation for EU Member States, it has been established that the reference level of radon for indoor and workplace should not exceed 300 Bq/m^3. This reference level has also been transposed into Croatian legislation by the Ordinance on radiation limits, the recommended dose limit and the assessment of personal radiation (Official Gazette 38/18). According to research conducted in residential areas of the Republic of Croatia, the concentration of radon varies from county to county (Radolić et al. 2006; Mostečak et al. 2018). For example, Istria, Karlovac or Lika-Senj counties are the counties with the highest measured radon concentration in the range of 101-200 Bq/m^3, while in Baranja, Požega - Slavonia County radon concentrations are lower and amount to 51-100 Bq/m^3 (Radolić et al. 2006).

Correlation between the hourly indoor radon variations with environmental parameters indicated that indoor radon concentrations may be affected by both indoor-to-outdoor temperature, humidity and pressure differences (Steck 2009; Xie et al. 2015). The aim of this study was to investigate the relationship between environmental parameters and temperature, humidity and atmospheric pressure with the concentration of radon in the air indoors at several locations in north-western Croatia.

2. EXPERIMENTAL PART

Radon concentrations were measured at 8 locations in the Varaždin and Koprivnica-Križevci counties (north-western Croatia) in the period between 2018 and 2020 within 7 to 14 days measurements, **Figure 1.** Radon concentration measurements were performed with an Airthings Corentium Pro measuring instrument (https://www.airthings.com/pro). Corentium Pro contains four radon chambers that work in parallel to obtain the most accurate and accurate results. The principle of operation is as follows: the device causes indoor air through a passive diffusion chamber and accurately calculates the radon level using alpha spectrometry. Radon is identified by silicon photodiodes for measuring energy and counting α particles derived from the decaying chain of radon. The measuring instrument is calibrated for reference instruments in accredited laboratories and is AARST-NRPP certified (certified by the American Association of Radon Technologists and Scientists). In addition to four radon chambers, the instrument also has sensors for measuring temperature, pressure and humidity.

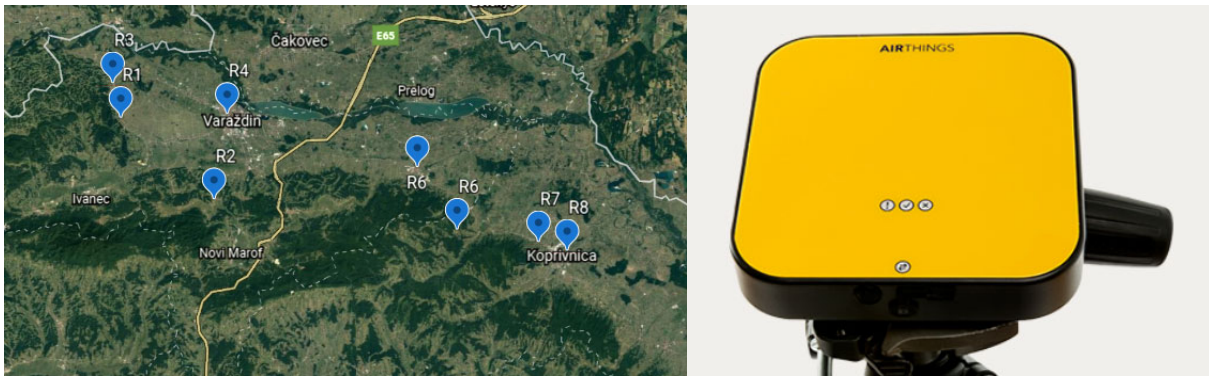

a) **b)**

Figure 1. *a) Map of measurement location b) Airthings Corentium Pro measuring instrument*

3. RESULTS AND DISSCUSSION

The values of radon concentration, temperature, humidity and atmospheric pressure were measured at the different locations (**Figure 1**). **Tables 1-4** show the values of individual measured parameters. **Table 1** shows the minimum; maximum and average values of radon concentration and it can be seen that the radon concentration is lower on the ground floor and on the first floor compared to the basement. The values of radon concentration obtained at location 7. show a deviation from other measurements and it is possible to assume that the basement rooms of this location have good ventilation and the concentration of radon is significantly lower than on the ground floor.

Table 1. Radon concentration values (min., max. and average)

Location	c_{MIN} [Bq/m^3]	c_{MAX} [Bq/m^3]	c_{av} [Bq/m^3]
LOCATION 1 – basement	9.00	123.00	46.20
LOCATION 1 – ground floor	9.00	72.00	21.70
LOCATION 2 – basement	2.17	207.00	70.00
LOCATION 3 – ground floor	1.85	232.00	56.00
LOCATION 4 – 1st floor	0.54	154.00	52.20
LOCATION 5 – 1st floor	2.95	363.00	132.00
LOCATION 6 – basement	2.49	220.00	83.00
LOCATION 7 – basement	1.35	68.00	16.00
LOCATION 7 – ground floor	0.89	112.00	36.00
LOCATION 8 – basement	1.45	262.00	87.00
LOCATION 8 – 1st floor	0.80	112.00	36.00

Table 2 shows the temperature values for individual locations. The results show that the temperature values in the basement and ground floor are approximately the same at most locations, if the average measured temperatures are observed, except at location 8, where there is a significant difference in the average measured values. It is to be assumed that deviations are present due to measurements during the winter months when the heating of the rooms in which people stay is increased (Ptiček Siročić et al. 2020).

Table 3 shows the results of the minimum, maximum and average values of humidity parameters. The measured values of the environmental humidity parameter range from 39 to 75 %, depending on the location

and the period of the year. If we compare the values from **Tables 1-3,** the radon concentration is higher if the humidity is lower, but only in the case of measurements in the basement and ground floor.

Table 2. Temperature values (min., max. and average)

Location	T_{MIN} [°C]	T_{MAX} [°C]	T_{av} [°C]
LOCATION 1 – basement	21.0	24.6	22.5
LOCATION 1 – ground floor	21.0	23.6	22.8
LOCATION 2 – basement	21.4	24.4	23.6
LOCATION 3 – ground floor	13.1	26.8	23.6
LOCATION 4 – 1st floor	24.9	30.6	27.3
LOCATION 5 – 1st floor	17.4	26.2	20.4
LOCATION 6 – basement	14.6	19.4	16.1
LOCATION 7 – basement	15.0	19.4	16.9
LOCATION 7 – ground floor	19.8	30.2	25.1
LOCATION 8 – basement	15.2	19.2	16.8
LOCATION 8 – 1st floor	14.2	19.2	16.8

Table 3. Values of the environmental humidity parameter (min., max. and average)

Location	H_{MIN} [%]	H_{MAX} [%]	H_{av} [%]
LOCATION 1 – basement	39.9	52.2	44.3
LOCATION 1 – ground floor	55.8	62.1	59.4
LOCATION 2 – basement	32.0	47.0	39.0
LOCATION 3 – ground floor	44.0	86.9	53.0
LOCATION 4 – 1st floor	46.0	61.9	53.8
LOCATION 5 – 1st floor	41.0	62.0	54.0
LOCATION 6 – basement	50.0	96.0	75.0
LOCATION 7 – basement	43.0	60.0	52.0
LOCATION 7 – ground floor	33.0	52.0	41.0
LOCATION 8 – basement	48.0	67.0	62.0
LOCATION 8 – 1st floor	43.0	64.0	55.0

Table 4 shows the minimum, maximum and average values of atmospheric pressure. Atmospheric pressure values generally depend on altitude, and the higher it is, the lower the pressure. The values of the measured atmospheric pressure at individual locations range from 98 to 102 kPa. The results show that the radon concentration is higher at the locations where the lowest value of atmospheric pressure was measured (**Tables 1 and 4**). Namely, at location 5, the average measured radon concentration was 132 Bq/m^3 and the average atmospheric pressure was 99.96 kPa.

4. ESTABLISHMENT OF A MULTIPLE LINEAR REGRESSION MODEL

Based on the measured values of radon concentration and the environmental parameters (temperature, humidity, atmospheric pressure), the statistical correlation between the above indicators was determined. In other words, an attempt was made to determine whether there was a relationship between radon concentration and environmental parameters (Steck 2009; Xie et al. 2015). Using a univariate linear regression technique, a correlation (dependence) between the radon concentration and the environmental parameter was established. The technique of determining the correlation coefficient between two quantities, i.e. between the radon concentration and each individual environmental parameter was used (Roselund et al. 2008).

Table 4. Atmospheric pressure values (min., max. and average)

Location	p_{MIN} [kPa]	p_{MAX} [kPa]	p_{av} [kPa]
LOCATION 1 – basement	98.57	100.51	99.21
LOCATION 1 – ground floor	98.61	99.41	99.08
LOCATION 2 – basement	98.44	101.06	99.69
LOCATION 3 – ground floor	98.34	100.60	99.53
LOCATION 4 – 1st floor	97.46	99.74	98.73
LOCATION 5 – 1st floor	98.00	101.23	99.96
LOCATION 6 – basement	98.37	100.14	99.16
LOCATION 7 – basement	96.83	100.66	98.90
LOCATION 7 – ground floor	100.50	102.09	101.36
LOCATION 8 – basement	99.54	101.32	100.48
LOCATION 8 – 1st floor	99.69	101.80	100.67

Figures 2 and 3 show the scatter plots for radon concentration and individual environmental parameters (humidity and pressure) and the regression direction is plotted with the indicated calculated Pearson correlation coefficient. **Figure 2** shows the scatter plot for the ratio of radon concentration to humidity parameter at location 6 - basement, with a calculated decreasing Pearson correlation coefficient of -0.12 and a plotted regression direction that is decreasing. In cases of connection between radon concentration and humidity parameters, the obtained correlation coefficients are negative, and a negative correlation was observed between the radon concentration and the environmental humidity parameter. The ratio of radon concentration and pressure for location 3, ground floor is shown in **Figure 3**, with a scattering diagram with the calculated corresponding correlation coefficient and plotted ascending regression direction. Pearson's correlation coefficient is positive and amounts to 0.23, and the correlation between radon concentration and pressure is positive. From the above relations it can be concluded that there is a proportional relationship between air pressure and radon concentration, i.e., the higher the air pressure, the higher the radon concentration. **Table 5** shows the values of all correlation coefficients between radon concentration and environmental parameters (temperature, humidity, and atmospheric pressure) at individual locations.

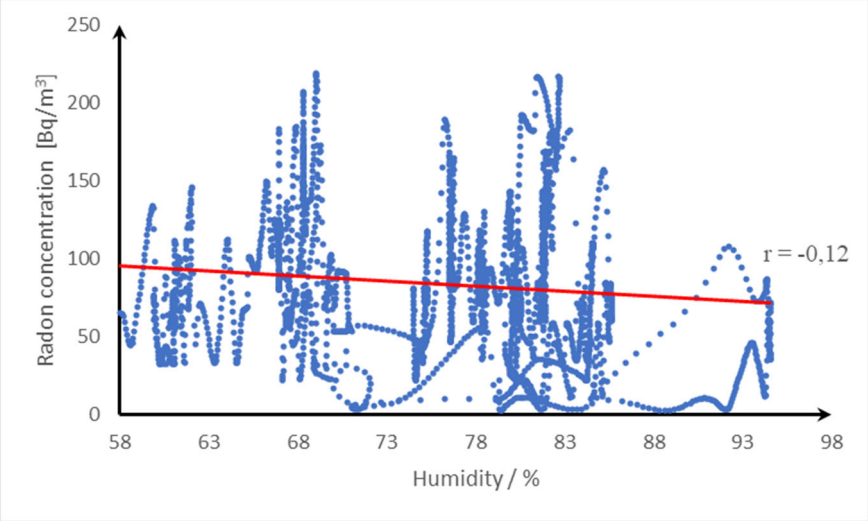

Figure 2. *Humidity - radon concentration scattering diagram, location 6 - basement*

Since all calculated correlation coefficients at absolute value are less than 0.5, these results indicate that a weak correlation was found in all interrelationships between radon concentration and environmental parameters. In this situation, it is advisable for each radon concentration to take those environmental parameters for which $|r| \geq 0.25$, i.e. which have a significant impact on them. For this reason, these indicators were taken as independent variables in multiple regression analysis (Roselund et al. 2008).

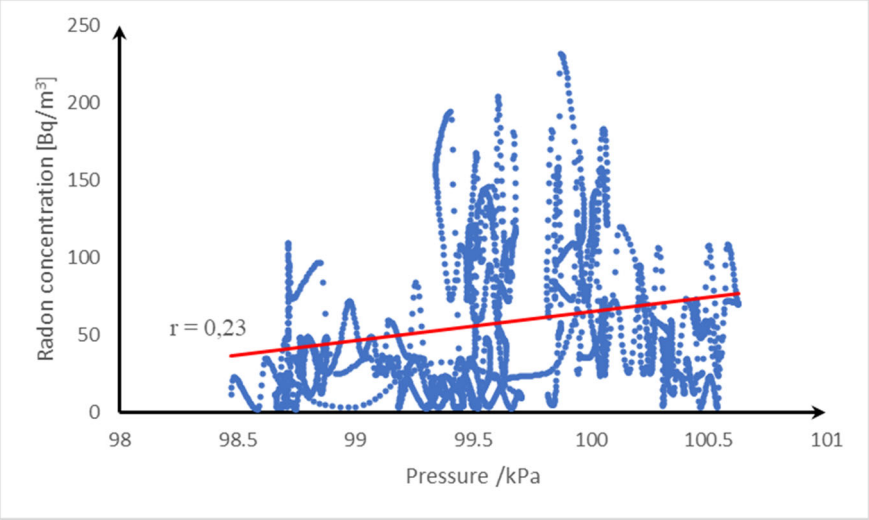

Figure 3. *Pressure scattering diagram - radon concentration, location 3 – ground floor*

Table 5. Correlation coefficients of radon concentration and environmental parameters

Location	Temperature [°C]	Humidity [%]	Pressure [kPa]
LOCATION 1 – basement	0.23	-0.17	0.11
LOCATION 1 – ground floor	0.13	-0.05	0.23
LOCATION 2 – basement	**-0.32**	0.16	**-0.30**
LOCATION 3 – ground floor	**0.33**	**-0.35**	0.23
LOCATION 4 – 1st floor	0.03	0.05	**-0.34**
LOCATION 5 – 1st floor	-0.17	**0.43**	-0.03
LOCATION 6 – basement	-0.08	-0.12	**-0.26**
LOCATION 7 – basement	0.11	0.23	0.11
LOCATION 7 – ground floor	-0.17	**0.28**	-0.20
LOCATION 8 – basement	0.19	0.21	**-0.37**
LOCATION 8 – 1st floor	-0.08	**0.38**	**-0.27**

At location 1, there is no significant influence of environmental parameters on the radon concentration, more precisely, the correlation coefficients in absolute value are less than 0.25. At location 2, temperature (r = -0.32) and atmospheric pressure (r = -0.30) have a significant influence on the radon concentration. Significant influence of temperature (r = 0.33) and humidity (r = -0.35) on radon concentration was obtained by correlation analysis at location 3. Correlation analysis also determined a significant influence of atmospheric pressure on radon concentration at location 4, where is r = -0.34. A significant influence of the environmental parameter of air humidity on the radon concentration at location 5 was calculated (r = 0.43), while the influence of pressure on the radon concentration at the same location was extremely low (r = 0.03), in contrast to the recorded influence of pressure at location 6. (r = -0.26). It is interesting to note that for the basement at location 7 there is no significant influence of environmental parameters on the radon concentration, but on the ground floor the influence of humidity was recorded (r = 0.28). At location 8, a significant influence of atmospheric pressure was recorded in the basement (r = -0.37) and on the first floor (r = -0.27). Also, on the first floor, the influence of humidity (r = 0.38) on the radon concentration is visible.

In general, an attempt was made to formulate a model of multiple linear regression of shapes according to the equation:

$$y = a_1x_1 + a_2x_2 + \cdots + a_nx_n \quad (1)$$

where y is the radon concentration, x_1, …, x_n are independent variables (environmental parameters that have a significant impact on radon concentration) and a_1,…, a_n are …. (Roselund et al. 2008).

For the application of the multiple linear regression model, 3 locations were considered, namely: a) location 2, b) location 3 and c) location 8, because at those specified locations two absolute values of the correlation coefficients are greater than 0.25. In other words, the influence of certain environmental parameters on radon concentration is statistically significant at these locations. In addition to the equations of the multiple regression model, scatter plots are also shown.

a) For location 2, the following multiple regression model was obtained, equation (2):

$$y = 1221{,}78 - 8{,}62 * T - 9{,}53 * p \quad (2)$$

where *T* is the value of the ambient temperature parameter and *p* is the value of the ambient pressure environmental parameter. It can be seen from the obtained model that the value of radon concentration (*y*) is inversely proportional to the values of the ambient temperature and pressure parameters. In other words, the higher the value of temperature and pressure, the lower the concentration of radon in the air. This conclusion is confirmed by the negative signs in front of the environmental parameters of temperature and pressure. Furthermore, the obtained results are confirmed by the descending directions (**Figures 4 and 5**), which confirm the inverse proportionality of radon concentration and temperature, i.e. radon concentration and pressure.

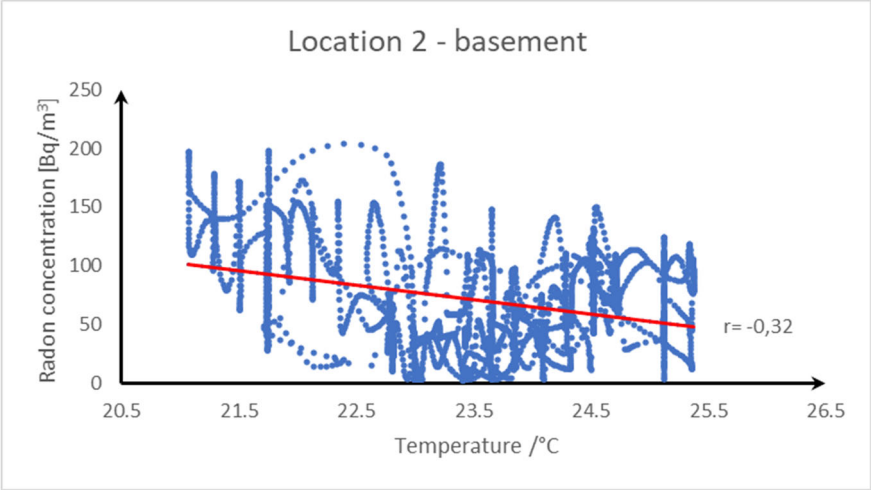

Figure 4. *Scattering diagram with plotted regression direction between radon concentration and temperature*

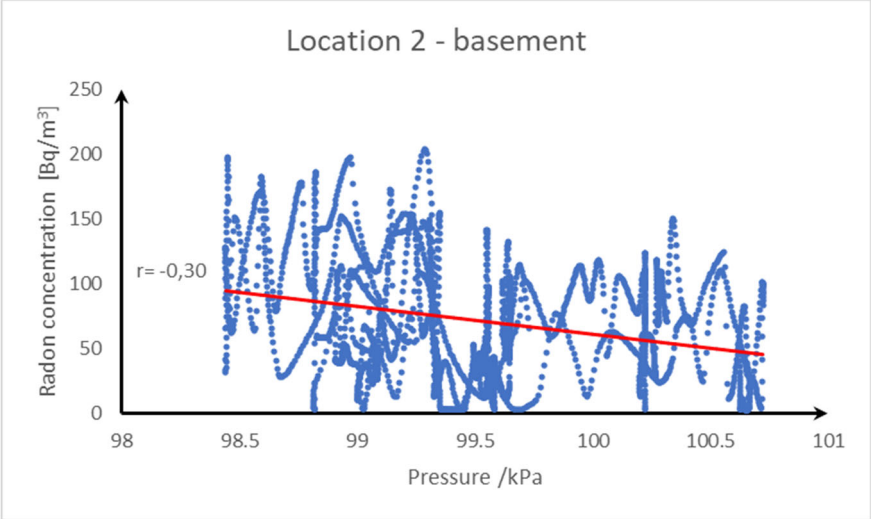

Figure 5. *Scattering diagram with plotted regression direction between radon concentration and pressure*

b) For measurement at location 3, the following multiple regression model was obtained, equation (3):

$$y = 63{,}11 + 1{,}85 * T - 0{,}93 * H \quad (3)$$

where *T* is the value of the ambient temperature parameter and *H* is the value of the ambient humidity parameter. It can be seen from this model that the value of radon concentration (*y*) is proportional to the value of the environmental temperature parameter and inversely proportional to the value of the environmental humidity parameter. This indicates that with increasing temperature, the concentration of radon in the air increases. Conversely, the higher the humidity parameter value, the lower the radon concentration in the air. This is confirmed by the results in **Figures 6 and 7** where one ascending direction and one descending direction are visible. In the single model, a positive correlation was obtained in relation to radon concentrations and temperature, while in relation to radon concentration and humidity, the correlation was negative, which is confirmed by the negative sign in front of the *H* parameter.

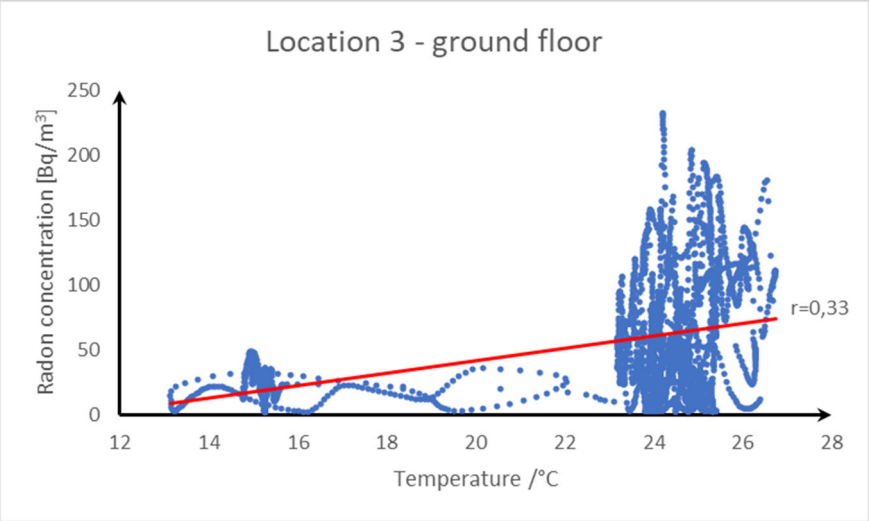

Figure 6. *Scattering diagram with plotted regression direction between radon concentration and temperature*

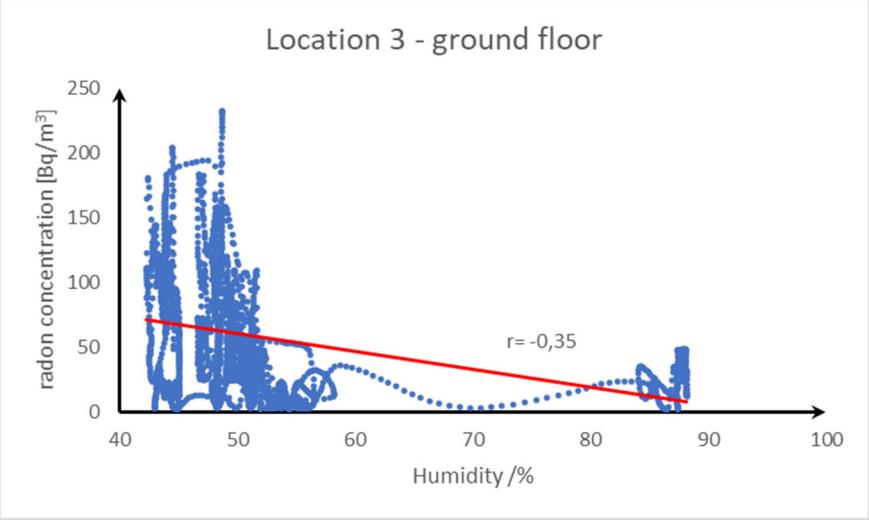

Figure 7. *Scattering diagram with plotted regression direction between radon concentration and humidity*

c) For the measurement at location 8, the following multiple regression model was obtained, equation (4):

$$y = 297{,}38 + 2{,}27 * H - 3{,}79 * p \quad (4)$$

where *H* is the value of the ambient humidity parameter and p is the value of the atmospheric pressure environmental parameter. It can be seen from this model that the value of the radon concentration (*y*) is proportional to the humidity value, i.e., the radon concentration increases with increasing humidity. However, the concentration of radon is inversely proportional to the value of atmospheric pressure, and as the atmospheric pressure increases, the concentration of radon in the air decreases. Observing the single regression model (**Figure 8 and Figure 9),** the correlation coefficient is positive, and this is confirmed by the positive sign in front of the humidity parameter value. However, in **Figure 9** the correlation coefficient is negative which confirms the negative sign in front of the atmospheric pressure parameter.

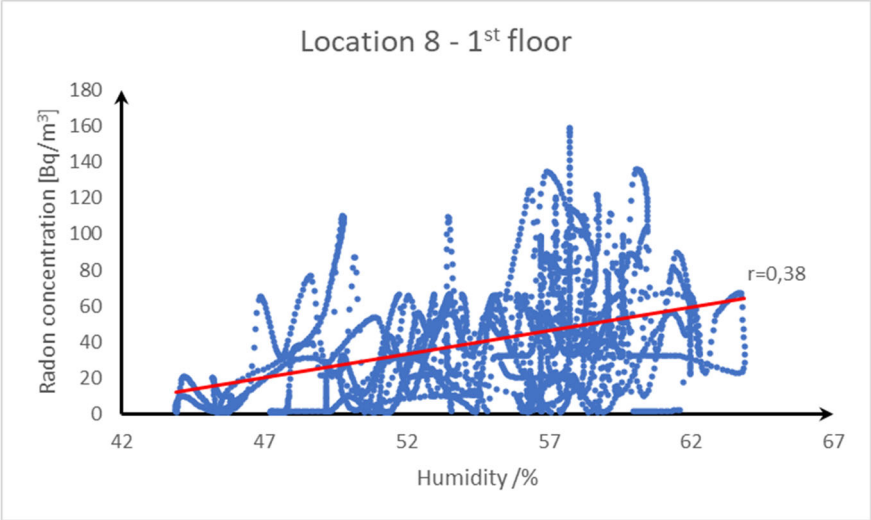

Figure 8. *Scattering diagram with plotted regression direction between radon concentration and humidity*

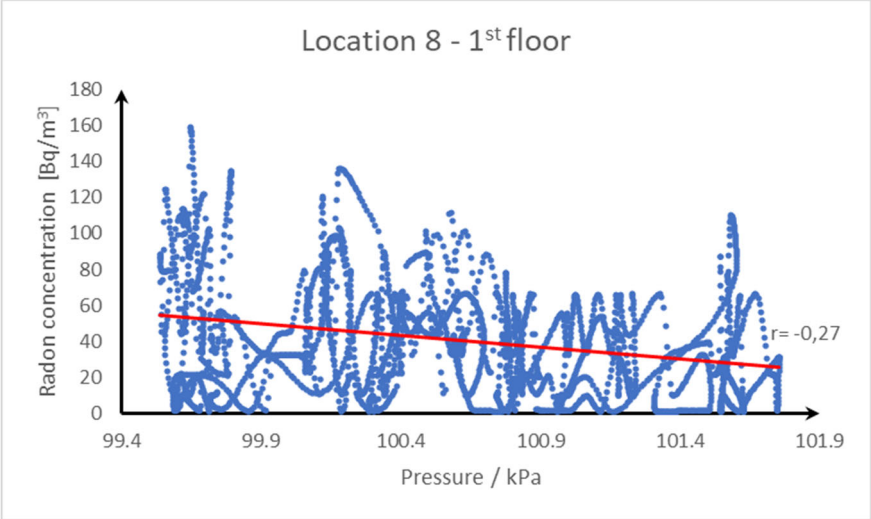

Figure 9. *Scattering diagram with plotted regression direction between radon concentration and pressure*

The obtained models can be used for the purpose of predicting radon concentrations at individual locations, which means that from the given equations for given values of input (independent) variables, it is possible to calculate or predict the radon concentration at an individual location (Roselund et al. 2008). At location 2, if we take the average values of the parameter T = 23,6 °C and the parameter p = 99,69 kPa, the radon concentration will be 68,30 Bq/m^3, as can be seen from equation 5 where the parameter values are included in equation (2):

$$\begin{gathered} y = 1221{,}78 - 8{,}62 * T - 9{,}53 * p \\ y = 1221{,}78 - 8{,}62 * 23{,}6 - 9{,}53 * 99{,}69 \\ y = 1221{,}78 - 203{,}43 - 950{,}05 = 68{,}3\ \mathrm{Bq/m^3} \end{gathered} \tag{5}$$

The average value of the measured radon concentration at location 2 is 70 Bq/m^3. Likewise, the radon concentration for location 3 can be calculated using equation (3). If we consider the average value of T= 23,6 ° C, and the average value of H (humidity) 53 %, we get the value of radon concentration which is 57,48 Bq/m^3, and the procedure of obtaining radon concentration can be seen in equation (6):

$$\begin{gathered} y = 63{,}11 + 1{,}85 * T - 0{,}93 * H \\ y = 63{,}11 + 1{,}85 * 23{,}6 - 0{,}93 * 53 \\ y = 63{,}11 + 43{,}66 - 49{,}29 = 57{,}48\ \mathrm{Bq/m^3} \end{gathered} \tag{6}$$

The average value of the measured radon concentration at location 2 is 56 Bq/m^3. If at location 8 on the 1st floor the average humidity parameter is 55 % and the average atmospheric pressure is 100.67 kPa. The equation (4) of the multiple models is considered. The result is a radon concentration value of 40,69 Bq/m^3, equation (7):

$$\begin{gathered} y = 297{,}38 + 2{,}27 * H - 3{,}79 * p \\ y = 297{,}38 + 2{,}27 * 55 - 3{,}79 * 100{,}67 \\ y = 297{,}38 + 124{,}85 - 381{,}54 = 40{,}69\ \mathrm{Bq/m^3} \end{gathered} \tag{7}$$

The average value of the measured radon concentration of radon at location 8 is 36 Bq/m^3. If calculated results of the concentration of the Radon are compared with the measured values, it is obvious that there is very small difference between them. This observation led to the conclusion that mathematical models of predicting the value of the concentration of Radon are accurate and can be used in practice.

5. CONCLUSION

Radon as a radioactive element contributes the most to natural radiation on Earth. In the open air, radon concentrations are low and harmless to human health, while indoors they can be elevated and as such dangerous to human health. In the Republic of Croatia, i.e., in Varaždin and Koprivnica-Križevci counties, at measuring locations, most households are not exposed to too high values of radon concentration. Since most radon comes from ground soil, the highest radon concentrations were measured in basements. By applying multiple regression analysis and establishing a mathematical model, it is possible to determine the statistical relationship between individual environmental parameters and radon concentration. The univariate model between the radon concentration and each environmental parameter and the obtained correlation coefficient also help to establish a multiple linear regression. For example, if the calculated correlation coefficient for certain parameters in a univariate model is the correlation coefficient is negative, the multiple regression model will show the inverse proportionality of the radon concentration to the value of a certain environmental parameter. The results indicate different relationships between radon concentration and temperature, humidity and atmospheric pressure at individual measurement sites. At all locations where the correlation coefficient between radon concentration and atmospheric pressure in absolute value is greater than 0.25, there is a negative correlation between these two quantities, i.e., the radon concentration decreases with increasing atmospheric pressure.

The main issue of obtaining a mathematical model capable of predicting radon concentration dependence on the environmental parameters for all locations and especially for certain region is hard to achieve as it was observed to be a local site function. However, given the change in climatic conditions at measuring sites, it is necessary to consider a longer period to determine with certainty a mathematical model that would give the most accurate prediction of radon concentration dependence on the environmental parameters which can affect human health and quality of life at these sites.

6. REFERENCES

Council Directive 2013/59/EURATOM
https://eur-lex.europa.eu/LexUriServ/LexUriServ.do?uri=OJ:L:2014:013:0001:0073:EN:PDF
https://www.airthings.com/pro
James A (1988) Radon and its decay products in indoor air: An Overview. John Wiley & Sons, New York
Mostečak A, Perković D, Kapor F, Veinović Ž (2018) Radon mapping in Croatia and its relation to geology. MGPB, 33:1-11
Ordinance on dose limits, dose constraints and assessment of individual doses (Official Gazette 38/18)
Ptiček Siročić A, Stanko D, Sakač N, Dogančić D, Trojko T (2020) Short-Term Measurement of Indoor Radon Concentration in Northern Croatia. Appl Sci 10(7),2341: 1-13
Radolic V, Vukovic B, Stanic D, Katic M, Faj Z, Lukacevic I, Planinic J, Suveljak B, Faj D, Lukic M (2006) National survey of indoor radon levels in Croatia. J Radioanal Nucl Ch, 269:87-90
Rosenlund M, Forastiere F, Stafoggia M, Porta D, Perucci M, Ranzi A, Nussio F, Perucci C.A (2008) Comparison of regression models with land-use and emissions data to predict the spatial distribution of traffic-related air pollution in Rome. J Expo Sci Env Epid,18:92–199
Steck D.J (2009) Annual average indoor radon variations over two decades. Health Phys, 96:37-47
Xie D, Liao M, Kearfott K.J (2015) Influence of environmental factors on indoor radon concentration levels in the basement and ground floor of a building – A case study. Radiat Meas, 82:52-58
Zeeb H, Shannoun F (2009) WHO handbook on indoor radon: a public health perspective, WHO Press, Geneva

INFLUENCE OF LEACHATES ON GEOTEHNICAL AND GEOCHEMICAL PROPERTIES OF TERMITE MOUND SOILS

Adebola Adekunle [1*], Fidelis Nkeshita[1], Adetayo Akinsanya[1]
[1] *Department of Civil Engineering, Federal University of Agriculture, Abeokuta, Nigeria*
* E-mail of corresponding author: adebolamay@gmail.com

Abstract This study investigated the influence of leachate prepared from Telfairia occidentalis on the geotechnical and geochemical properties of termite mound soil obtained from the premises of the federal university of agriculture, Abeokuta, south-western Nigeria. The termite mound soil samples were collected from three different locations and each sample collected was contaminated by mixing with leachates in percentage increments of 0% 10%, 15% and 20% of dry weight of the air-dried soil. The soil samples were subjected to Atterberg limits and hydraulic conductivity tests for geotechnical observation and X-ray fluorescence tests for geochemical tests. The range of values for the geotechnical analyses were obtained as; plastic limit (9.1% – 14.2%), liquid limit (28.6 % – 61%), plasticity index ((18.2% – 49.5%) and hydraulic conductivity (1.85 – 4.1 x 10^{-8}) cm/sec) with a resultant reduction in the plastic limit, liquid limit and plasticity index values but an increase in the hydraulic conductivity of the samples as the leachate concentration increased. The results from X-ray fluorescence analyses after 20% leachate contamination showed that the major elemental chemical composition for the three samples were comprised of SiO_2 (56.25 – 56.5%), Al_2O_3 (28.42 – 28.50%), Fe_2O_3 (4.46 – 6.5%), TiO_2 (1.08 – 1.23%), CaO (1.45 – 1.60%), P_2O_5 (0 – 0.04%), K_2O (0.9 – 6.1%) and MnO (0.02 – 4.7%). There was a marginal alteration of the indices with the values inferring the presence of a minimum composition of feldspar and a major composition of quartz-rich minerals and thus lending more credence to the presence of silicates as shown from the X-ray fluorescence results. It also infers that the termite mounds are predominantly made from sand materials. The termite soil samples obtained from the aforementioned locations may not be suitable for engineering works unless stabilization procedure is adopted.
Keywords Geotechnical, Geochemistry, Termite mound, Leachates

Received: 20.10.2020. / Accepted: 09.07.2021.
Published online: 01.12.2021.

Original scientific paper
https://doi.org/10.37023/ee.8.1-2.4

1. INTRODUCTION

Termites are social insects in which a vast majority of its species rely on soil for feeding. Termite mounds are formed when a ground nest enlarges above the initial concealing surface. These mounds form when Termites cement the soil particles with the aid of secretions from saliva and excrement. These hills appear to persevere against harsh weather conditions over a long period of time (Eggleton, 2000; Ramesh et al., 2016). These termite activities ensure that the mound produced differ in physical and chemical properties from adjacent soils with a clay content of up to 20% than that of the adjacent soil, indicating a preference by the termites for smaller clay particles for construction. The mounds produced has cohesive properties and mechanical strength and has a lot of applications for use such as in improving soil stability and lawn tennis clay courts. (Muddaraju, H.C. and Sunita, 2019; Felix et al., 2000; Samuel et al., 2016).

Leachates are liquid substances containing solid particles usually formed from the degradation of organic wastes and when water seeps down through solid wastes undergoing decomposition. If this process is not carefully controlled, it can cause surface and groundwater contamination (Nta and Odiong, 2017; Aderemi et al., 2011). It is therefore necessary that landfill sites where leachates may be formed are properly lined with materials that can prevent pollutants from percolating into groundwater. The presence of Leachates in soil can alter the chemical and mechanical properties of that soil. In a study carried out by Nayak et al. (2010), the Atterberg's limit, Proctor test and permeability values were altered for a 0.5M NaCl modified soil with percentage increments of 0, 20, etc. Another study showed that there was an alteration in the mechanical properties of a leachate contaminated soil in terms of liquid limit, specific gravity and direct shear strength when compared to the uncontaminated soils (Sunil et al., 2006). This study focused on the influence of percentage proportions of an artificially prepared leachate on the mechanical behaviour of termite hill soil samples under varying temperatures.

2. MATERIALS AND METHODS

2.1. Preparation of Samples

Samples of termite mound were collected from three different locations within the campus of the Federal University of Agriculture, Abeokuta, and South-western Nigeria for the experimental study and was prepared in accordance with BS 1371 -1:1990. The coordinates for the sites are Latitude 7.23°N Longitudes 3.43°E, 7.23°N, 3.44°E and 7.23°N, 3.43°E. The bulk samples were transported in polythene bags to the laboratory. Leachate samples were prepared in the laboratory by subjecting a collection of the vegetable plant Telfairia occidentalis to decomposition for up to six weeks under anaerobic conditions in a sealed container.

The termite mound samples were air dried for a few days according to the procedure adopted by Harun et al. (2013). The soil samples were subsequently crushed manually and then allowed to pass through a 4.75 mm sieve. The air-dried samples were then mixed with the prepared artificial leachates in percentage increments of 0% 10%, 15% and 20% of dry weight of the air-dried soil. The mixtures were stored in airtight containers in order to cure for two weeks thereby achieving certain biochemical properties that would be similar to that under real in-situ conditions. After the period for curing, the mixed samples were transferred to an incubator, with temperature set to 40°C, the samples were left at this temperature for a period of 8 hours each day for 30 days to simulate biochemical conditions.

2.2 Experimental Procedures

After the duration of this temperature treatment, the mixed samples were subjected to geotechnical tests including specific gravity test, Atterberg limit tests, compaction test and hydraulic conductivity test.
Specific gravity test carried out according to B.S. 1377:1990, part 2:8; For the Atterberg limit test, it was carried out according to B.S. 1377:1990, part 2:4, 2:5. The liquid limit test was carried out by placing a portion of the contaminated termite mound soil paste on the Casagrande apparatus with a groove of about 2 mm wide cut made down its centre to separate it into two halves in the paste and subsequently subjected to shallow drop of the cup. The number of such blows cause the two soil halves to come together over a distance of 13 mm and soil sample is taken for the determination of the moisture content of the soil. Moisture content was plotted against the number of blows and a straight line was drawn to pass through each of the plotted points. The plastic limit was determined by preparing a stiff paste of the contaminated sample on a glass plate which was subsequently rolled out manually using a back-and-forth movement to produce a uniform thread about 3 mm diameter without crumbling. The plasticity index was determined as the numerical difference between the liquid limit and the plastic limit.

Compaction test was carried out on the leachate contaminated termite mound soil according to B.S. 1377:1990, part 4:4 by adopting the Proctor standard compaction test. This involved the soil samples being compacted in three layers with each layer subjected to blows from a 4.5 kg hammer which administered the blows over the surface of the sample placed in a cylindrical metal mould of about 105 mm in diameter and approximately 115.5 mm in height.

The head permeability test was adopted for this study according to B.S. 1377:1990, part 5:5 in which uncontaminated and contaminated soil samples to study the hydraulic conductivity compacted to standard Proctor maximum dry density in the permeability mould (Sunil et al, 2006). Filter paper was used to prevent clogging of the perforated discs by the fine soil particles by being placed on each face of the soil sample. Nuts were fastened and the permeameter assembled properly after placing its top and bottom plates. The permeameter was linked to a standpipe which was filled with distilled water when the 0% contaminated sample was tested and leachate when the 20% contaminated sample was tested. The soil was saturated by allowing distilled water/leachate to flow continuously through the sample from the standpipe.

X-ray fluorescence (XRF) analyses were carried out on the series of mixed samples after the temperature treatment in order to investigate the mineralogical components of the soil samples before contamination (at 0%) and after contamination (at 20%).

3. RESULTS AND DISCUSSION

3.1 Atterberg Limits

Figures 1 – 3 shows the variations of plastic limit, liquid limit and plasticity indices respectively with percentage increase in leachate contamination. The range of values for plastic limit for the samples varied from 9.1% – 14.2% for the range of leachates exposure. There was a general reduction in plastic limit of the samples within the range of 0% to 20% leachate concentration with all three samples with a marginal increase/decrease in values at the 10% and 15% leachate concentrations. It is worthy to note that sample 1 had the lowest plastic limit values all through the percentage leachate contamination phases. The low values of plastic limit exhibited by the termite mound samples at 0% contamination indicate a low percentage of clay fines contained within the mound collected in which it is predominantly made up of fine to medium grain sands.

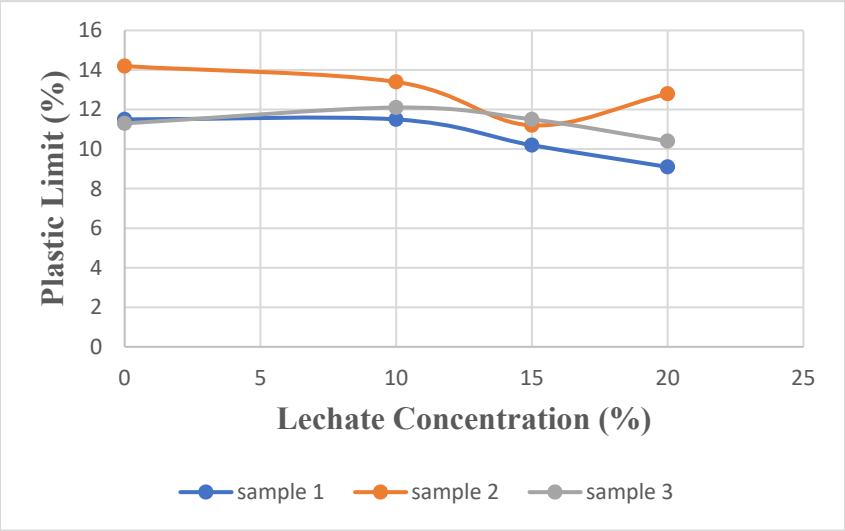

Figure 1. *Plastic limit of termite mound-leachate concentration*

The liquid limit results for the three contaminated samples ranged from 28.6% – 61%. The liquid limit showed a decreasing trend as the percentage concentration of leachates increased. The same trend could be observed for the plasticity index (18.2% – 49.5%) which resulted from the marginal differences in the values of the plastic limits of the samples. These types of trends were also observed in the study carried out by Harun et al. (2013) while observing the influence of leachates on sandy clay soil and in Sunil et al. (2006) while observing the strength and chemical characteristics on leachates on lateritic soils. The clay content of the samples as well as the chemical constituents of the leachates may have played an influential role on the behaviour of the samples. According to Das in (1994), clay minerals exhibit electrochemical properties thereby possessing charged particles and a subsequent affinity for attracting opposite charges of water molecules which are naturally dipolar. Leachates are liquid based and contains different categories of contaminants including dissolved organic components such as alcohols, inorganic compounds such as cations e.g. iron and anions e.g. chlorides and heavy metals (Christensen et al., 1994). As the percentage leachate concentration increased, the water content reduces and this result in the reduction of its ability to react with the clay particles. There would thus be a reduction in the liquid limit and plasticity index values.

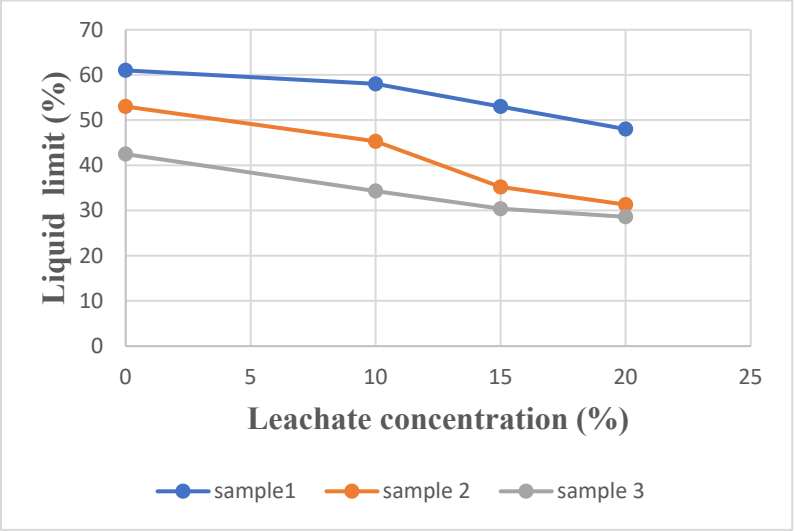

Figure 2. *Liquid limit of termite mound-leachate concentration*

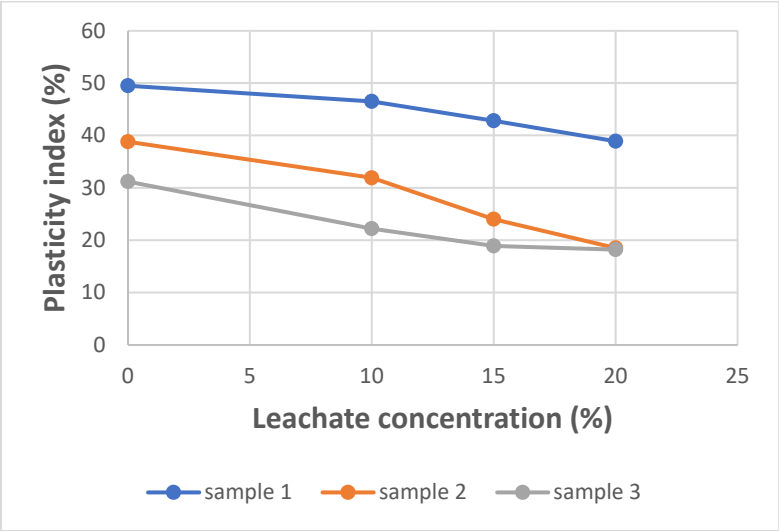

Figure 3. Plasticity index of termite mound-leachate concentration

3.2 Hydraulic Conductivity

There was an increase in the value of permeability of the termite mound samples as the percentage leachate contamination increased after heat treatment as can be seen from **Figure 4** with a range of $1.85 – 4.1 \cdot 10^{-8}$ cm/sec. Sample 2 showed a spike in the permeability values after the 10% leachate contamination. This can be attributed to the chemical reactions that may have taken place between the leachate and mineral content of clay in the samples as well as the heat treatment probably showing its aftereffects. In a study conducted by Sunil et al. (2008) on soil-leachate reaction, there was a similar trend of an increase in permeability resulting from increase in leachate concentration. The cementing agents from the activities of termites may have helped to bind fine particles to create aggregates. These aggregates may be destroyed when particles are exposed to acidic or basic conditions. The mineral contents from clay that are contained in the termite mound may also be dissolved by the action of acidic/basic agents (Uppot and Stephenson, 1989; Sunil et al., 2006 and Sridharan, 1981). The leachate may have dissolved the clay mineral contents and thus increased the effective pore space leading to an increase in hydraulic conductivity. The results also show that that there were lower values of Plastic limit and Liquid Limit as the permeability increases except in the case of the PL of sample which showed an inverse trend. It is possible that the biochemical processes that may have occurred due to the activities of termites in addition to its reaction with the leachate, may have influenced this trend. Leachates contain organic components, and this may also account for the geotechnical properties exhibited by the samples. It is in agreement with the study conducted by Alimohammadi-Jelodar and Karimpour-Fard (2018) in which it reported that Permeability can be influenced by the physical and chemical properties of the permeating fluid and the soil including the organic compositions and clay minerals. It further reported that clay of higher Liquid Limit and Plastic Limit showed lower values of permeability as against the passage of all the organic fluids that were used in the study even though the rate of decrease varied from fluid to fluid and that on increasing soil plasticity, there was corresponding reduction of permeability.

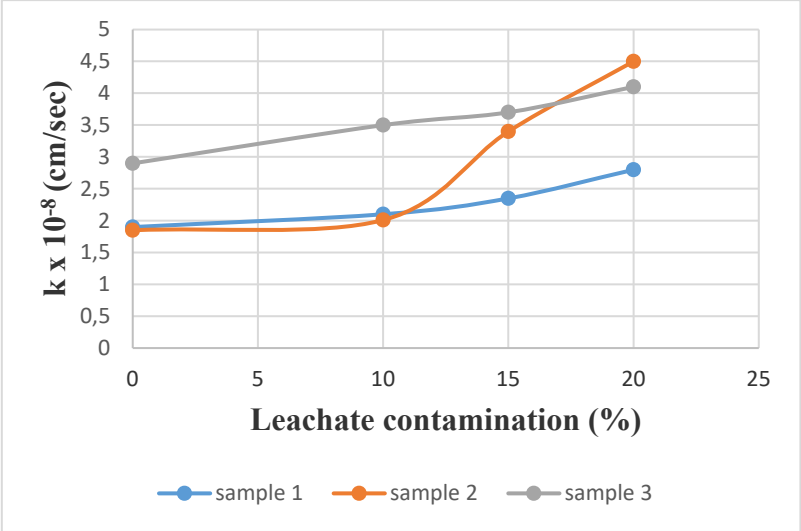

Figure 4*: Hydraulic conductivity of termite mound-leachate concentration*

3.3 Elemental Geochemistry and Geochemical Indices

The XRF results for the three termite mound samples after heat treatment and for values before (0%) and after (20%) leachate contamination is shown in **Table 1** below. A cursory look at these results shows that there were marginal alterations from the original values of the elements after contamination. This could be attributed to chemical reactions that may have taken place between the soil samples and leachates. The predominant elements are Al2O3 and Fe2O3. The use of certain geochemical indices such as K2O/Al2O3, K2O/CaO and Al2O3/TiO2 have been previously reported in literature (Momah and Okieimen, 2020).

Table 1: XRF result of the major Elemental Composition of termite mound soils

		Sample 1		Sample 2		Sample 3	
S/N	Element	0%	20%	0%	20%	0%	20%
1	AI_2O_3	55.39	56.5	56.26	56.3	54.82	56.4
2	Fe_2O_3	30.06	28.42	29.22	28.52	31.23	22.5
3	TiO_2	4.46	4.46	4.95	5.65	4.98	6.5
4	CaO	1.33	1.23	1.25	1.25	1.23	1.08
5	P_2O_5	1.65	1.45	1.55	1.5	1.61	1.6
6	K_2O	-	0.05	0.04	0.05	0.04	0.02
7	MnO	0.89	6.01	0.98	0.96	0.85	0.9

In a study conducted by Cox et al., (1995), the authors used the ratio of the indices K_2O/Al_2O_3 to establish the dominance of feldspar in relation to other minerals contained in mudstone with indications showing that values greater than 0.5 as predominantly composed of alkali K-feldspar and values below 0.4 inferring to a minimum composition of feldspar in the original mudstone. The ratio of the indices K_2O/Al_2O_3 obtained for the leachate contaminated soil samples were all below 0.4 with a range of (0.02 – 0.26) thus inferring a minimum composition of feldspar. These results are like what was obtained in a study conducted by Momah and Okieimen (2020) on termite mound in Ika area in Delta State, South-south region of Nigeria.

The values of this index that was obtained for the leachate contaminated termite mound soil were in the range of (1.97 – 2.1) thus inferring that the samples were quartz rich with a high-ratio of sandstones with minimum composition of clay minerals. These results when compared to what was obtained in the study by Momah and Okieimen (2020) were similar even though this study obtained higher index values.

4. CONCLUSION

The study was carried out to determine the influence of leachates on certain geotechnical and chemical properties of termite mound soil contaminated with a synthetic leachate made from the plant, *Telfairia occidentalis*. The leachate contamination was shown to have altered the Atterberg limits, hydraulic conductivity as well as the geochemical attributes of the soil mixture.

The result of the study indicates that there was reduction in the plastic limit, liquid limit, and plasticity index values as the concentration of leachates increased. The hydraulic conductivity of the samples was also shown to have increased as the leachate concentration increased.

The geochemical indices resulting from the XRF results show that there was a marginal alteration of the indices showing the presence of a minimum composition of feldspar and a major composition of quartz-rich minerals lending more credence to the presence of silicates as shown from the X-ray fluorescence results. It also infers that the termite mounds are predominantly made from sand materials.

The implication is that when these soils from termite mounds are modified by leachates of organic origin, it may lead to serious geotechnical challenges such as erosion, ground subsidence, seepage in landfills, etc. Thus, the soil sample obtained from this source may not be suitable for engineering works unless stabilization procedure is adopted.

5. REFERENCES

Aderemi AO, Oriaku AV, Adewumi GA, Otitoloju AA. Assessment of groundwater contamination by leachate near a municipal solid waste landfill. Afr. J. Environ. Sci. Technol. 2011; 5:933-940.

Alimohammadi-jelodar, S, Karimpour-fard, M. Permeability of two clayey soils exposed to petroleum products and Organic Solvents Civil Engineering Infrastructures Journal, svez. 51(1), pp. 131-146, 2018.

British Standard Institution, Methods of test for soils for civil engineering purposes, BS 1377 (1990).

British Standard Institution 1377, Methods of Test for Soil for Civil Engineering Purposes-Part 2: Classification Tests, BS1377, London, ISBN: 0580178676, pp. 68, 1990.

Christensen, T. H., Kjeldsen, P., Albrechtsen, H. J., Heron, G., Nielsen, P. H., Bjerg, P. L. and Holm, P. E. Crit. Rev. Environ.Sci. Technol. 24, 119-202 (1994).

Cox R, Lower DR, Cullers RL (1995). Influence of sediment recycling and basement evolution of mudrock chemistry in the Southeastern United States Geochimica et Cosmochimica Acta 59:2919-2940

Das, B. M. Principle of Geotechnical Engineering, 3rd edition, PWS Publishing Company, 436 pp., 1994.

Eggleton, P. (2000). Global patterns of termite diversity. In T. Abe, D.E. Bignell & M. Higashi (Eds.), Termites: evolution, sociality, symbioses and ecology (pp. 25−51). Dordrecht: Kluwer Academic Publishing.

Felix F.U., Alu O. C, .and Sulaiman, J. (2000). "Mound soil as construction material". J. Mater. Civ. Eng., 2000, ASCE 12(3): 205-211.

Harun, S. N., Ali Rahman, Z., Rahim, S. A., Lihan, T. and Idris, W. M. R. "Effects of Leachate on Geotechnical Characteristics of Sandy Clay Soil". AIP Conference Proceedings 1571, 530 (2013)

Momah, M and Okieimen, F. E. "Minerology, geochemical composition and geotechnical properties of termite mound soil". Journal of Ecology and The Natural Environment. Vol. 12(1), pp. 1-8, January-March 2020.

Muddaraju, H.C. and Sunita, 2019. "Study on Geotechnical Properties of Red Termite Mound Soil". International Journal of Scientific & Engineering Research Volume 10, Issue 12, December-2010.

Nayak, S, Sunil, B, Shirhari, S and Sivapullaiah, P. Geotechnical and Geological Engineering 28 (6), 899-906 (2010).

Nta SA, Odiong IC. Impact of municipal solid waste landfill leachate on soil properties in the dumpsite (A case study of Eket Local Government Area of Akwa Ibom State, Nigeria). Int. J. Sci. Eng. Sci. 2017; 1:5-7.

Ramesh K. Kandasami, Renee M. Borges, Tejas G. Murthy, "Effect of biocementation on the strength and stability of termite mounds", The International Journal of Engineering and Science, vol. 3, no. EG2, pp.99–113, 2016.

Samuel Assam, Fidelis Okafor and UmohUmoh. (2016). "Potentials of Processed Termite as a Stabilizing Agent in Clay Soil". IOSR Journal of Mechanical and Civil Engineering (IOSR-JMCE) e-ISSN: 2278-1684, p-ISSN: 2320-334X, Volume 13, Issue 4 Ver. I (Jul. - Aug. 2016), PP 40-50 Nigeria.

Sridharan, A., Nagaraj, T.S., Sivapullaiah, P.V. 1981. Heaving of soil due to acid contamination. Proc. of International Conference on Soil Mechanics Foundation Engineering, vol. 2, 383–386. Stockholm.

Sunil, B. M. S., Shrihari and Nayak, S. (2006) Effect of pH on the geotechnical properties of laterite Journal of Engineering Geology 106:20-25.

Sunil, B. M. S., Shrihari and Nayak, S. (2008) Soil-Leachate Interaction and Their Effects on Hydraulic Conductivity and Compaction Characteristics. The 12th International Conference of International Association for Computer Methods and Advances in Geomechanics, 1-6 October.

Uppot, J.O., Stephenson, R.W. 1989. Permeability of clays under organic permeants. Journal of Geotechnical Engineering, 115(1):115–131.

TREATMENT OF WASTEWATER FROM SEPARATORS FOR RAINFALL RUNOFF USING ELECTROCHEMICAL OXIDATION PROCESSES

Morana Drušković [1*], Dražen Vouk [2], Mario Šiljeg [3], Krešimir Maldini [4],
[1] *Dok-Ing Energo d.o.o., Slavonska avenija 22G, 10000 Zagreb, Croatia*
[2] *University of Zagreb, Faculty of Civil Engineering, Water Research Department, Kačićeva 26, 10000 Zagreb, Croatia*
[3] *Ministry of Economy and Sustainable Development, Radnička cesta 80, 10000 Zagreb, Croatia*
[4] *Hrvatske vode, Main Water Management Laboratory, City Street Vukovara 220, 10000 Zagreb, Croatia*
*E-mail of corresponding author: morana.druskovic@gmail.com

Abstract: *In recent years, industry has increased and with it the amount of oily wastewater, which are considered hazardous waste because they contain various types of heavy metals and oils that endanger the environment and human health. In the last twenty years, there has been increased research on new technologies to treat wastewater as efficiently and environmentally friendly as possible. A recent approach to wastewater treatment is the application of electrochemical processes such as the electro-Fenton process, which belongs to the group of electrochemical advanced oxidation processes and electrocoagulation. The aim of this work was to remove organic contaminants and heavy metals from wastewater originating from oil and grease separators that clean stormwater runoff from traffic areas. The use of stainless steel, iron and aluminum electrodes results in electrooxidation, electroreduction and electrocoagulation. At a current of 15 A the treatment efficiency was 50% for COD and 73% for mineral oil. At a current of 110 A the treatment efficiency was 96% for COD and 90% for mineral oil.*
Keywords: *electrochemical advanced oxidation processes, electrocoagulation, rainfall runoff, separators, mineral oil, COD, heavy metals*

Received: 21.09.2020. / Accepted: 10.11.2021.
Published online: 01.12.2021.

Original scientific paper
https://doi.org/10.37023/ee.8.1-2.5

1. INTRODUCTION

Wastewater is water that has changed its original composition through the introduction of pollutants whose presence causes a change in the physical, biological, chemical, or bacteriological properties of the water, and therefore it cannot be used in agriculture or for other purposes (Jurac, 2009). Oily wastewater is defined as a combination of wastewater and oil in some ratio and is usually the product of oil refining, pet-rochemicals refining, metallurgical industries, and marine products. Oil and grease should be removed from wastewater before reuse or discharge to the environment to reduce adverse impacts on human health, groundwater, soil, air, and the environment. Oil includes light and heavy hydrocarbons, oil, tar, grease, wax, soap and more. The oil in wastewater can be of mineral, animal, or plant origin. In terms of their physical properties, they are classified into 4 categories - free oils, dispersed oils, emulsified oils and dissolved oils. Oil-containing water is mostly in emulsified form. This form differs from the dispersed solution mainly in the stability of the form. This improved stability is influenced by substances - emulsifiers - located at the oil-water interface (Coca-Prados et al., 2011).

An important activity in sustainable water management is wastewater treatment. The wastewater is treated so that it can be reused or discharged into water bodies or soil. There are many known and devel-oped technologies that aim to achieve a certain quality of treated water. The most used treatment technol-ogies are chemical coagulation, flotation, and electrocoagulation. In addition, some hybrid processes have been developed - processes that consist of a combination of two or more treatment processes (Coca-Parados et al., 2011).

2. ELECTROCHEMICAL ADVANCED OXIDATION PROCESSES

Electrochemical advanced oxidation processes (EAOP) belong to the group of advanced oxidation processes (AOP) most used in wastewater treatment with high concentrations of organic pollutants. One of the most used EAOPs is the electro-Fenton process (EF), which is a combination of Fenton reagent chemistry and electro-chemistry (Brillas 2014; Grymonpre et al. 2004). Indirect anodic oxidation or electro-Fenton process results in the

oxidation of organics using chlorine, hypochlorite, hydrogen peroxide, and ozone, which are electrochemically generated and reactive. The EF process is described in detail by the following reactions (Oturan N. and Oturan M.A., 2018).

Anode:

$$2Cl^- \rightarrow Cl_2 + 2e^- \quad (1)$$

$$6HOCl + 3H_2O \rightarrow 2ClO_3^- + 4Cl^- + 1.5O_2 + 6e^- \quad (2)$$

$$2H_2O \rightarrow O_2 + 4H+ + 4e^- \quad (3)$$

Summary reaction:

$$Cl_2 + H_2O \rightarrow HOCl + H^+ + Cl^- \quad (4)$$

$$HOCl \rightarrow H^+ + OCl^- \quad (5)$$

Cathode:

$$2H_2O + 2e^- \rightarrow 2OH^- + H_2 \quad (6)$$

$$OCl^- + H_2O + 2e^- \rightarrow Cl^- + 2OH^- \quad (7)$$

Indirect anodic oxidation of organic components using iron electrodes leads to the formation of hydroxyl radicals in the EF reaction consisting of electrochemically generated Fe^{2+} and hydrogen peroxide (H2O2) according to the reaction (Orescanin et al., 2012).

$$Fe^{2+} + H_2O_2 \rightarrow Fe^{3+} + \bullet OH + OH^- \quad (8)$$

Electrocatalytic regeneration of Fe^{2+} ions to Fe^{3+} ions allows Fe^{3+} ions to be reused as a catalyst, thus avoiding the formation of large amounts of iron hydroxide sludge (Monteil et al., 2018).

$$Fe^{2+} + \cdot OH \rightarrow Fe^{3+} + OH^- \quad (9)$$

3. ELEKTROCOAGULATION

The process of electrocoagulation (EC) is based on the passage of electric current through electrodes in the reactor and immersed in water, which with their dissolved particles (coagulants) dissolve and neutralize the charges of the dispersed (dirt) particles. Such a destabilization process is called coagulation. In flocculation, the destabilized or coagulated particles accumulate into larger clusters (flocs) which separate from the mixture by precipitation. In worldwide practice, iron or aluminum electrodes are mainly used.

In the process of electrocoagulation, several electrochemical reactions take place simultaneously at the an-ode and the cathode. The action of direct current on the electrodes in the electrochemical cell causes the release of cations at the anode and the simultaneous reduction of water to the group OH and hydrogen at the cathode. The released metal cations, together with the OH group, form stable hydroxides that aggregate the pollutant particles from the water, neutralize their charge, and form larger structures with them that are separated by pre-cipitation in solution. Generated hydrogen strengthens the bond between dissolved particles and pollutants, in-creases turbulence in the system and reduces the relative specific gravity of the pollutants (Publication et al., 2015; Orescanin et al., 2018).

Anode:

$$Fe \rightarrow Fe^{2+} + 2e^- \quad (10)$$

$$2H_2O \rightarrow O_2 \uparrow + 4H^+ + 4\,e^- \quad (11)$$

Chatode:

$$2H_2O + 2e^- \rightarrow H_2 \uparrow + 2OH^- \quad (12)$$

Electroreduction:

$$Cr^{6+} + 3Fe^{2+} \rightarrow Cr^{3+} + 3Fe^{3+} \quad (13)$$

Precipitation:

$$Cr^{3+} + 3OH^{-} \rightarrow Cr(OH)_3 \downarrow \quad (14)$$

$$Fe^{3+} + 3OH^{-} \rightarrow Fe(OH)_3 \downarrow \quad (15)$$

$$Fe^{2+} + 2OH^{-} \rightarrow Fe(OH)_2 \downarrow \quad (16)$$

4. EXPERIMENTAL WORK

4.1. Sampling and preparation of oily water

Wastewater is collected in an oil and grease separator designed to treat stormwater from traffic areas (public roads and parking lots). Two cleaning series were performed with low load at low currents (15 A). The second series of tests was performed with higher wastewater load and at higher currents (100 A). The wastewater contained in the IBC tank is also contaminated with oily wastewater. The properties of the wastewater before and after the additional load are shown in **Table 1.**

Table 1. Characteristics of oily wastewater

Parameter	Wastewater from oil and grease separators	Wastewater after additional
pH	6.97	6.98
Electrical conductivity - EC (μS/cm)	599.5	583
Dissolved oxygen - DO (mg/L)	2.23	3.68
Mineral oil (mg/L)	3.955	129.17
Chemical oxygen demand - COD (mg/L)	420	1080

4.2. Equipment and measuring instruments

The first series of experiments concerned the efficiency of the EAOP / EC process at currents of 15 A. The efficiency of stainless steel (SS), iron (Fe) and aluminium (Al) electrodes was tested. The set of stainless-steel electrodes consisted of 12 electrodes (6 pairs), rectangular (400 x 40 mm), active surface 146.7 cm^2, electrodes arranged in parallel, separated by a 10 mm thick insulator (pair 4.5 mm), 2 mm thick. Both sides of the electrodes represent the active surface. Each odd plate was connected as the cathode and the even plate as the anode. The Fe and Al electrodes had the same dimensions as the stainless-steel electrodes, while the distance between them was 5 mm. The thickness of the iron electrode was 3 mm and that of the aluminium electrode was 7 mm. Each set of electrodes was placed on the bottom of the reaction vessel and connected to a laboratory rectifier. A MC Power LBN-1990 laboratory rectifier was used to test the treatment efficiency at low currents, while the Mean Well RSP-3000-12 was used for higher currents. In all experiments, wastewater was mixed with air using a TetraTec APS 400 pump. Electrical conductivity, pH, dissolved oxygen, and temperature were determined using a Hanna Instruments HI98194 multiparameter probe. Concentrations of mineral oil were deter-mined using a Nexis GC-2030 Shimadzu, with samples previously prepared by extraction. Concentrations of heavy metals were determined using an Agilent 5900 ICP-OES instrument.

4.3. Methodology

Homogeneity of the sample was achieved by mixing the effluent before taking the sample for the experiments. All experiments were performed in batches in a plastic reaction vessel (reactor). For the analyzes and laboratory tests of the low flow treatment, 10 dm3 of wastewater was taken. The efficiency of stainless steel (SS), iron (Fe) and aluminum (Al) electrodes was tested. The prepared oily wastewater was treated with 15 A and 21.9 V on stainless steel electrodes for 30 minutes; then a sample was taken. This is followed by 15 minutes of treatment at 15 A and 55.6 V on iron electrodes; then a sample is taken. This is followed by a 15-minute treatment with 15 A, 45.3 V aluminum electrodes: and sampling. After completion of the EAOP treatment, the effluent was gently agitated with air for the next 40 minutes. The effluent was then precipitated and sampled for analysis. In the second

series of experiments, the efficiency of the same electrode materials with prior pretreatment was investigated. 40 dm3 of wastewater was placed in two plastic containers. To each plastic container, 60 g of NaCl was added to obtain enough conductive ions for the current prescribed in the experiments and enough chloride for the generation of chlorine and hypochlorite. Then, both plastic containers were treated simultaneously with iron electrodes for 10 minutes, container 1 (18 A, 13.7 V) and container 2 (22 A, 13.7 V). This was followed by precipitation for 20 minutes and decantation of the wastewater from tanks 1 and 2 into tank 3 until a volume of 40 dm3 was obtained. The wastewater thus prepared was then treated with stainless steel electrodes for 45 minutes. A sample was taken every 15 minutes and the current was measured. Thus, after 15 minutes of treatment, 110 A, 13.7 V was measured; after 30 minutes, 120 A, 13.7 V; after 45 minutes, 130 A, 13.7 V. This was followed by 30 minutes of treatment with 35 A, 13.7 V iron electrodes and sampling. In the final stage of processing, aluminum electrodes were applied at 35 A, 13.7 V.

5. RESULTS

5.1. Wastewater from oil and grease separators

The wastewater samples were stored in 1 m3 IBC tanks at room temperature 22 ºC - 23 ºC. The oily wastewater was slightly contaminated with mineral oil, organic matter, and heavy metals. The values of physico-chemical parameters are given in **Table 2**. The input sample is colorless, odorless and has neutral pH (about pH 6). High levels of COD (420 mg/L) and mineral oils or total carbon (4 mg/L) were measured in the input sample. All heavy metal concentrations in the input wastewater were negligible (ng/L), while the iron concentration was slightly higher (0.21 mg/L).

Table 2. Physico-chemical parameters in wastewater from oil and grease separators before and after treatment with electrodes made of stainless steel (SS), iron (Fe), aluminum (Al) and after aeration with air

Parameter	Initial effluent	SS 30 min	Fe 15 min	Al 20 min	Aeration 40 min
pH	6.97	7.36	8.59	8.2	-
DO (mg/L)	2.23	5.5	3.45	2.68	-
EC (µS/cm)	599.5	466.3	356	245.6	-
COD (mg/L)	420	210	190	200	210
Mineral oil (mg/L)	4	2.8888	1.6	2.22	1.088
Cd (ng/L)	2.552	26.60	1.267	21.35	4.097
Cr (ng/L)	2272	91444	531.1	279.5	1705
Cu (ng/L)	675.0	4702	<0.1	1565	693.5
Fe (ng/L)	205164	843176	335534	73963	202934
Ni (ng/L)	108.8	31115	183.1	<0.1	1259
Pb (ng/L)	112.6	1239	78.62	570.9	459.4
Sn (ng/L)	27,48	131.5	24.91	167.8	230.7
Zn (ng/L)	2704	31280	<0.1	<0.1	11618

The combination of stainless steel, iron, and aluminum electrodes has proven effective in removing organic indicators such as COD and mineral oil. When wastewater is electrooxidized with stainless steel electrodes, Cr^{6+} is formed and the concentration of organic indicators decreases. Chromates released from the sacrificial anode play an important role in the oxidation of the organic load. The ionic form of Cr^{6+} is a very soluble and toxic form of chromium and must be reduced to the more stable Cr^{3+}. During wastewater treatment with iron electrodes, excess Cr^{6+} is reduced to Cr^{3+} by electrochemically generated Fe^{2+} and at the same time Fe^{2+} is oxidized to Fe^{3+}. Water is reduced at the cathode with simultaneous formation of H_2 and OH ions. The reaction of cations and OH ions produce stable hydroxides and electrochemically generated gasses H_2 and O_2, which additionally mix the suspension during mechanical stirring to ensure constant contact of the pollutant with the iron flocs. (Orescanin et al., 2018). Everything described follows the reactions described previously in Chapter 3.

Electrocoagulation using aluminum electrodes resulted in a small increase in organic indicators com-pared to the previous phase. The concentrations of heavy metals Cr, Fe and Ni were further reduced, which is very important when they are present in higher concentrations since electrodes were used in the procedure. After a total treatment

time of 105 minutes at 15 A, more than 50% of COD and 73% of mineral oil were removed. The increased levels of chromium, iron, nickel, and zinc are explained by the electrooxidation of the stainless-steel sacrificial anode, which releases these ions.

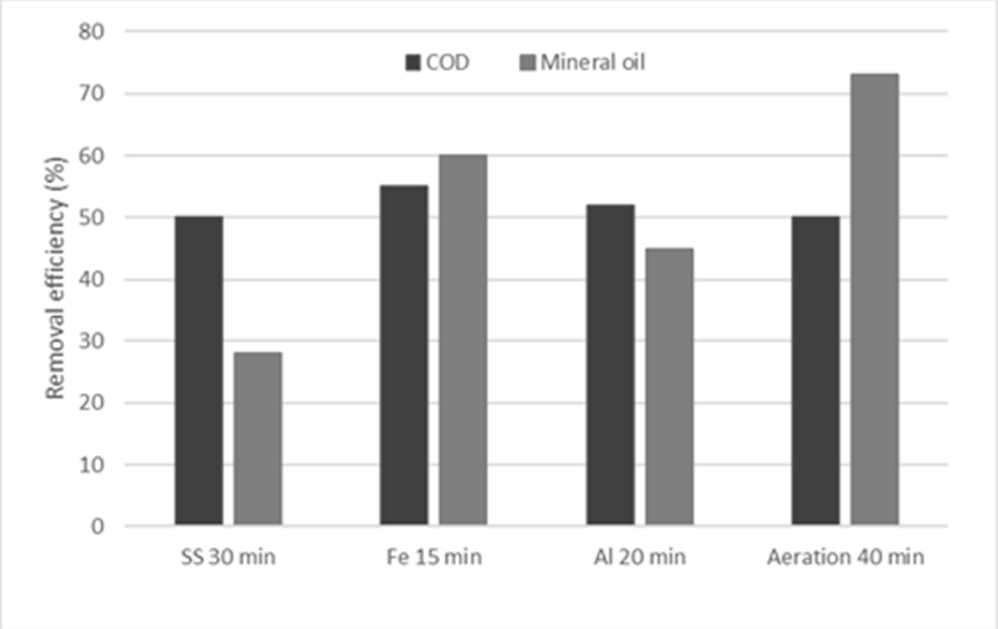

Figure 1. *Removal efficiency of COD and mineral oil from wastewater from oil and grease separators during individual stages of treatment using electrodes made of stainless steel (SS), iron (Fe) and aluminum (Al)*

5.2. Additionally loaded wastewater from oil and grease separators

To conduct studies with higher concentrations of organic loadings, additional loadings were added to the effluent from the previous experiment. 1 L of used motor oil and 0.5 L of emulsion from metallurgic processing were added to the wastewater in the IBC tank. The suspension thus prepared was mixed until homogeneous and allowed to stand for 24 hours. Before taking the effluent sample for conducting the experiments, the suspension was well mixed mechanically. The input sample has a neutral pH (about 6), a dissolved oxygen concentration of 3.68 mg/L, an electrical conductivity of 583 mg/L and is characterized by an intense odor and a gray-black color. High concentrations of COD (1080 mg/L) and mineral oils (129 mg/L) were found. All concentrations of heavy metals in the wastewater were negligible (ng/L).

Table 3. Physico-chemical parameters in additionally loaded wastewater from oil and grease separators before and after treatment with electrodes made of stainless steel (SS), iron (Fe), aluminum (Al) and after aeration with air

Parameter	Initial effluent	SS 15 min	SS 30 min	SS 45 min	Fe 30 min	Al 30 min	Aeration 40 min
COD (mg/L)	1080	-	-	-	243	-	43
Mineral oil (mg/L)	129.17	9.63	10	7,6	15,77	13,47	-
Cd (ng/L)	11.68	17.70	<0.1	22,07	<0.1	3,940	8,946
Cr (ng/L)	838.1	120851	386386	538297	195.3	69.79	354.4
Cu (ng/L)	539.8	<0.1	<0.1	<0.1	77.88	<0.1	495.1
Fe (ng/L)	77269	36979	111353	159492	17610	<0.1	<0.1
Ni (ng/L)	<0.1	43676	62786	53402	427.9	105.3	43.10
Pb (ng/L)	583.3	<0.1	5.859	<0.1	<0.1	<0.1	<0.1
Sn (ng/L)	526.5	263.9	290.7	98.37	331.3	<0.1	69.29
Zn (ng/L)	793.4	<0.1	<0.1	<0.1	<0.1	<0.1	<0.1

In the first stage of processing, which includes processing with stainless steel electrodes after 45 minutes of processing, the reduction efficiency of mineral oil was 94% of tin 80%, while zinc reached 100% efficiency already in the first 15 minutes. The mechanisms of organic indicator removal by indirect oxidation using electrochemically generated chlorine and hypochlorite formed from chlorides added to wastewater are described in detail in Chapter Two (Orescanin et al., 2018).

In the second phase of treatment, there is a marked increase in the removal efficiency of heavy metals, the concentration of which had increased in the previous phase due to the release of metal ions from the stainless-steel electrode. The chromium and iron removal efficiency were 77%. To remove the yellow color, which came from low molecular weight organics, aluminum electrodes were used in the third phase. The removal efficiency of chromium was 92% and of tin 100%. After the fourth treatment phase, which included aeration, results of 96% were obtained COD.

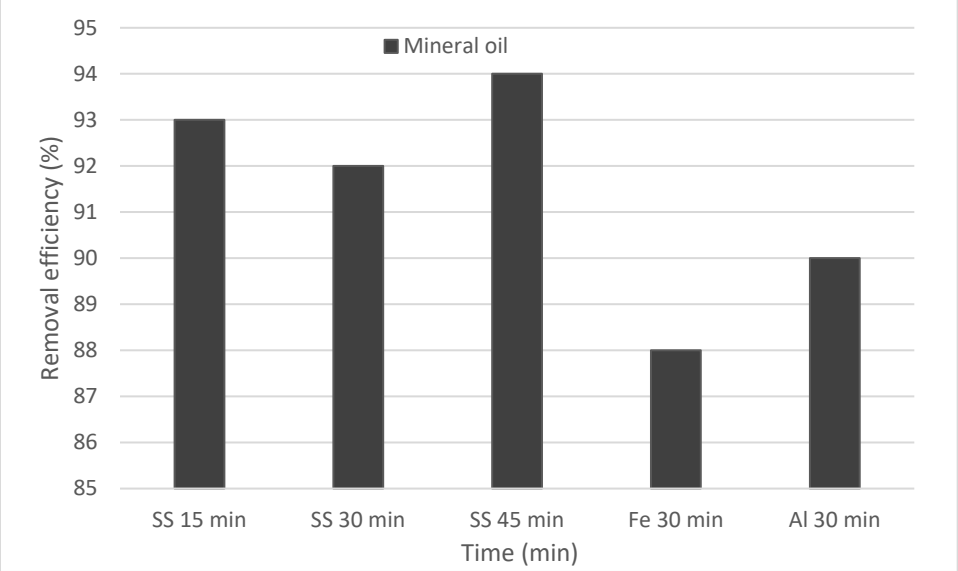

Figure 2. *Removal efficiency of mineral oil from wastewater from oil and grease separators additionally loaded with waste oil during individual stages of treatment using electrodes made of stainless steel (SS), iron (Fe) and aluminum (Al)*

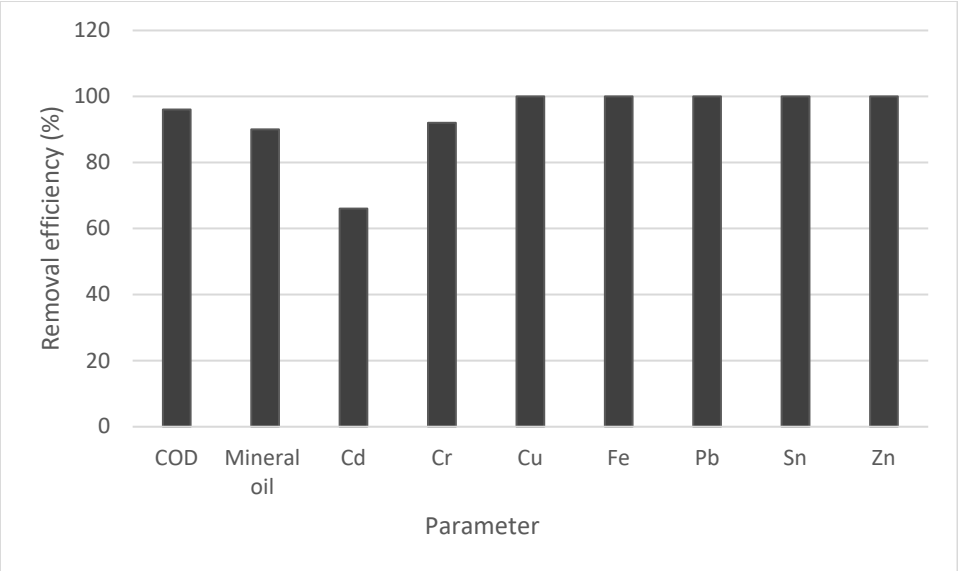

Figure 3. *Removal efficiency of COD, mineral oil, and heavy metals after all stages of processing*

6. CONCLUSION

The strong development of electrochemistry and the numerous research in this field in the 20th century have led to the increasing importance of electrochemical processes as one of the methods for water treatment. In the last 20 years, with a significant reduction in electricity prices and new ways of generating electricity, these processes have become the subject of numerous scientific studies. In this work, the efficiency of electrochemical advanced oxidation processes is tested on wastewater contaminated with mineral oil. The aim of these experi-ments was to show that these processes can achieve sufficiently good efficiency. In order to confirm the effi-ciency of the method, two series of experiments were carried out.

The wastewater from oil and grease separators used in this work was slightly contaminated with organic indicators (COD), mineral oil, and heavy metals, had no colour, no odour, and the pH was neutral. The applied current was 15 A and the efficiencies were 50% for COD and 73% for mineral oil.

Used oil and emulsion was additionally added to the wastewater to test efficiency at higher loads.

To achieve the desired current intensity, 60 g of NaCl was added to the wastewater. The experiments were carried out at a current of 110 A and an efficiency of 96% was obtained for COD and 90% for mineral oil.

High efficiency in removing heavy metals from this type of wastewater was also confirmed. The values for the removal of cadmium, chromium, copper, iron, lead, tin and zinc were almost 100%.

The method has proven successful in this study and can certainly be a confirmation that the answers to the point pollution issues can be very successful with the development of this technology and with additional application of solar energy sources that needs to be further examined in future research.

***Acknowledgments**:* This work has been fully supported by Croatian Science Foundation under the project "IP2019-04-1169 - Use of treated oily wastewater and sewage sludge in brick industry - production of innovative brick products in the scope of circular economy".

7. REFERENCES

Brillas E (2014) Electro-Fenton, UVA Photoelectro-Fenton and Solar Photoelectro-Fenton Treatments of Organics in Waters Using a Boron-Doped Diamond Anode: A Review. J Mex Chem. Soc. DOI:10.29356/jmcs.v58i3.131

Coca Parados J, Gutiérrez G, Benito J (2011) Treatment of oily wastewater. W Puri Manag. DOI:10.1007/978-90-481-9775-0_1

Grymonpré DR, Finney WC, Clark RJ, Locke BR (2004) Hybrid gas-liquid electrical discharge reactors for organic com-pound degradation. Ind Eng Chem Res. DOI:org/10.1021/ie030620j

Jurac Z (2009) Otpadne vode. Veleučilište u Karlovcu, Karlovac.

Orescanin V, Kollar R, Nađ K, Ruk D, Halkijević I, Kuspilić M (2018) Elektrokemijska/ultrazvučna/elektromagnetska obrada zrelog odlagališta eluata. Hrv vode.

Orescanin V, Kollar R, Ruk D, Nađ K (2012) Characterization and electrochemical treatment of landfill leachate. Part A, Tox-ic/hazardous substan. & enviro. Eng. DOI: 10.1080/10934529.2012.646146

Oturan N. and Oturan M.A. (2005) Degradation of three pesticides used in viticulture by electrogenerated Fenton's reagent, Agron. Sustain. Dev. DOI: 10.1051/agro:2005005

Monteil H, Péchaud Y, Oturan N, Oturan MA (2018) A review on Efficiency and Cost Effectiveness of Electro- and Bio-electro-Fenton processes: Application to the Treatment of Pharmaceutical Pollutants in Water. Chem. Eng. J. DOI:org/10.1016/j.cej.2018.07.179

Publication V, Kuokkanen V, Kuokkanen T, Rämö J, Lassi U (2015) Electrocoagulation treatment of peat bog drain-age water containing humic substances. Wat. Res. DOI: 10.1016/j.watres.2015.04.029

INFLUENCE OF SHEAR RATE ON THE SOIL'S SHEAR STRENGTH

Anja Bek [1*], Goran Jeftić [1], Stjepan Strelec [1], Jasmin Jug [1]
[1] *University of Zagreb, Faculty of Geotechnical Engineering, Hallerova aleja 7, 42000 Varaždin, Hrvatska*
*E-mail of corresponding author: anjabek08@gmail.com

Abstract: *One of the most important mechanical properties is shear strength. It is conditioned by the value of the maximum shear stress that the soil can withstand before failure. Exceeding the shear strength causes one particle to slide next to another, causing the failure of soil. The shear strength of the soil for effective stresses is1 a combination of drained strength parameters: internal friction angle (φ) and cohesion (c) defined by the Mohr-Coulomb failure criterion. It is determined "in situ" and by laboratory experiments. Direct shear is the oldest and the simplest laboratory experiment to determine the shear strength of the soil. The first phase of experiment is specimen consolidation under specific vertical stress, and in the second phase specimens are sheared at a given shear rate, depending on the consolidation properties of the soil. Cohesionless soils are sheared at up to 100 times higher shear rate compared to cohesive soils. Shear rate and drainage conditions affect the magnitude of soil strength parameters. The paper is based on the comparison and demonstration of the influence of different shear rates on the peak and residual shear strength in the direct shear device. The tests were performed on two samples of low plasticity clay (CL) and one sample of high plasticity clay (CH).*
Keywords: *shear strength, shear rate, shear strength parameters, direct shear.*

Received: 11.10.2021. / Accepted: 25.11.2021.
Published online: 01.12.2021.

Original scientific paper
https://doi.org/10.37023/ee.8.1-2.6

1. INTRODUCTION

Soil failure occurs due to exceedance of the maximum shear stress that soil can withstand, which makes shear strength highly important for the execution of both designs and construction. When testing the soil's shear strength in a direct shear device, the correct choice of shear rate is very important. Coherent soils shear at a lower rate, and the shear rate for cohesionless soils is up to 100 times higher.

This paper deals with the influence of different shear rates on the peak and residual shear strength of the soil. Increasing the dynamic load causes the soil to slide whereby residual shear strength becomes important. Two samples of low plasticity clay (CL) and one sample of high plasticity clay (CH) were used, in a direct shear device and in consolidated drained conditions, for determining the soils shear strength; the results are presented graphically and tabulated.

2. PREVIOUS RESEARCH

Rouaiguia & Rogers (2001) tested the influence of shear rate on peak and residual values of the internal friction angle and cohesion on three samples of kaolin, two samples of clay and one sample of sludge. All the tested samples showed a higher value of peak cohesion at higher shear rates when compared to lower shear rates, while the peak internal friction angle had a lower value at a higher rate.

Strength tests at three landslide sites in loess areas (Baoqi et al., 2018) showed that samples which were sheared faster also demonstrated a higher value of cohesion than at a lower shear rate. The internal friction angle value is smaller at a slower shear. Soil samples consolidated under lower vertical stress demonstrated a lower value of peak shear stress.

Papić (2014) presented a test of shear strength for two samples of mid to high-plasticity clay after compaction according to the standard Proctor experiment. The results of the conducted experiments demonstrated that a smaller normal stress leads to lower peak shear stress. Likewise, the results demonstrate that an increase in shear rate causes increase in cohesion, and a decrease of the internal friction angle.

3. SHEAR STRENGTH

Shear strength is the highest value of shear stress that can be applied to soil structure in a certain direction. Reaching maximum shear stress, followed by plastic deformations, leads to soil failure, with one particle sliding over another. Due to friction resistance in grain contact, the soil shows the greatest part of shear strength. If there was no friction among grains, the soil's behaviour would be the same as that of a liquid. Shear stress is taken on by the soil's skeleton, while the stress is transferred via contact forces of neighbouring

grains. Pre-consolidated and compacted soils have characteristic peak and residual shear strengths. Loose and normally consolidated soils show peak shear strength reached after larger displacement.

3.1. Failure creation

Terzaghi's modification of Mohr-Coulomb failure criterion defines the shear strength of soil for effective stress (Eslami et al. 2020). Shear strength, shown in Equation 1, is defined by the parameters of drained strength - cohesion and the internal friction angle:

$$\tau_f = c' + \sigma' \cdot tg\varphi' \quad (1)$$

where τ_f is shear stress, c' is drained cohesion, σ' is defined as normal effective stress applied on the soil sample, while φ' is the drained internal friction angle.

Figure 1 illustrates the peak and residual strength and the failure envelope for peak and residual shear conditions.

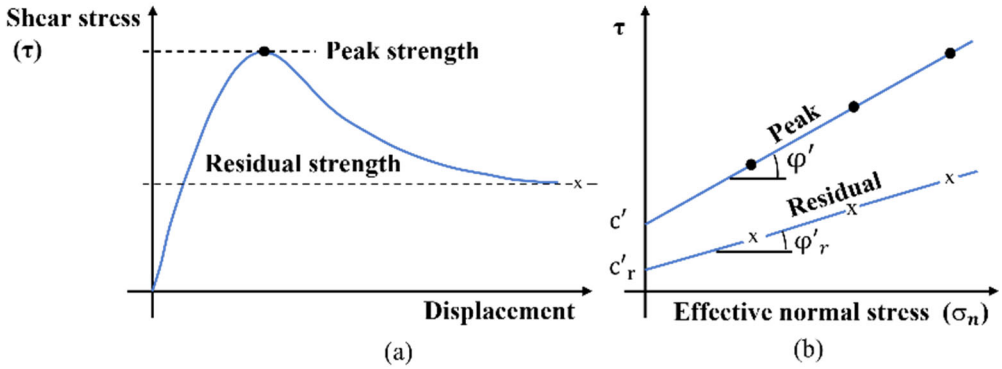

Figure 4. *a) The peak and residual strength and b) the approximated failure envelope for peak and residual conditions (Head & Epps, 2011)*

3.1.1. Cohesion and the internal friction angle

Cohesion is a characteristic of fine-grained (coherent) soil and occurs as a consequence of electric and Wan der Waals forces applied to contact points of neighboring grains. When normal stress equals zero, the soil resists shearing due to cohesion. Cohesion is not a constant soil parameter; its value depends on water (moisture) content of soil. At higher content of moisture, the strength of electrochemical forces is lower, while it completely disappears if the soil is dissolved in water.

In gravel and sand, the internal friction angle is the natural slope angle which can withstand the slope inclination with such material. Soil compaction increases the internal friction angle, depending on particle size, porosity, and consistency state (for coherent soils). The internal friction angle has a higher value in cohesionless soils than in coherent ones (**Table 1**).

Table 1. Values of the internal friction angle in coherent and cohesionless soils (Geotechdata, Angle of friction)

Description	USCS	Internal friction angle [°]		
		Minimum value	Maximum value	Specific value
Well graded gravel	GW	33	40	-
Poorly graded gravel	GP	32	44	-
Well graded sand	SW	33	43	-
Well graded sand – compacted	SW	-		38
Poorly graded sand	SP	30	39	-
High plasticity dust	MH	23	33	-
High plasticity clay	CH	17	31	-
High plasticity clay – compacted	CH	-	-	19
Low plasticity clay	CL	27	35	-
Low plasticity clay – compacted	CL	-	-	28
Peat and other organic soils	Pt	0	10	-

3.2. Drained or slow (CD) direct shear experiment

A consolidated drained (CD) experiment is conducted on three or four specimens of the sample in two different phases. In the first phase each specimen undergoes consolidation under different vertical stress. The first vertical stress is smaller than geological, and each subsequent stress is double the value of the previous one. The second phase of the experiment is specimen shearing under constant vertical stress action.

3.3. Shear rate

Shear rate depends on the sample's consolidation parameters i.e., the drainage condition, permeability, and sample thickness. Sher rate must be slow enough to enable a total drainage of the sample and the dissipation of pore pressures which are not measurable within this type of test. Cohesionless soils shear at higher while coherent soils shear at a lower velocity determined by Equation 2:

$$v = \frac{\delta_f}{t_f} \tag{2}$$

where $\boldsymbol{v}$ is the shear velocity calculated as the ratio between displacement $\boldsymbol{\delta_f}$ and time $\boldsymbol{t_f}$ necessary for failure.

3.3.1. Displacement in failure

Displacement at failure is an estimated value which will mobilize the peak shear strength. **Table 2** shows displacement range at failure for sand and clay in a direct shear device.

Table 2. Direct shear displacement in sand and clay at failure (Head & Epps, 2011)

Soil type	Displacement [mm]
Loose sand	5-8
Compacted sand	2-5
Plastic clay	8
Rigid-plastic clay	2-5
Solid clay	1-2

3.3.2. Time to failure

The time required for failure is determined from the curve of the settlement timeline, yielded during the consolidation phase. Based on the curve, it can be determined the time necessary for 100% (t100) of primary consolidation, as shown on **Figure 2.**

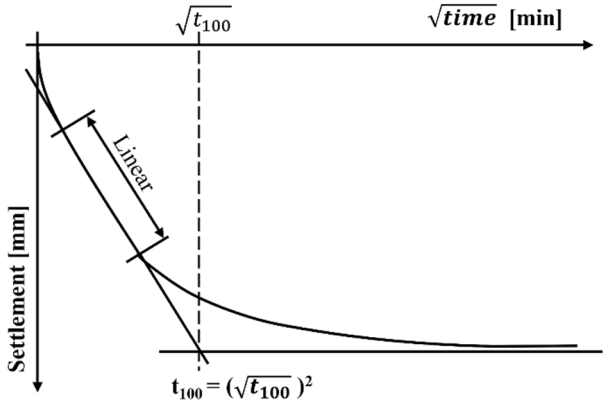

Figure 2. *Graphic representation of determining time* $\sqrt{\mathbf{t_{100}}}$ *(Head & Epps, 2011)*

The time value $\sqrt{t_{100}}$, whose square value is needed to determine time $t_{100,}$ is determined in the following way: a tangent is drawn onto the straight-line part of the primary consolidation. The tangent is elongated to the intersect

point with the horizontal line representing 100% of consolidation. The intersect point between the elongated tangent and the horizontal curve is the value $\sqrt{t_{100}}$.
The time t_f necessary for failure is determined by **Equation 3** (BS 1377 Part 7 :1990):

$$t_f = 12{,}7 \cdot t_{100} \tag{3}$$

4. LABORATORY DETERMINATION OF SHEAR STRENGTH IN A DIRECT SHEAR DEVICE

A laboratory test determined the shear strength of three soil samples. Nine test specimens were prepared from the same soil sample, three for each shear rate. The influence of different shear rates was compared and their influence on the parameters of the soil's shear strength, cohesion (c) and internal friction angle (φ). The tests for all samples were conducted according to the norm BS 1377 Part 7 :1990 Clause 4 – Determination of the shear strength by direct shear (small shear box apparatus). All the tests were conducted in a direct shear device in consolidated drained conditions.

4.1. Soil sample classification

Table 3 lists the characteristics and the classification of the tested intact soil samples, and they are featured in the plasticity chart on **Figure 3.**

Table 3. The classification and the characteristics of the tested soil samples

Sample mark	Moisture	Liquid limit	Plasticity limit	Plasticity index	Consistency index	USCS classification
	w_0 [%]	w_L [%]	w_P [%]	I_P [%]	I_C [-]	
1	24,2	47,5	20,9	26,6	0,88	**CL**
2	24,6	45,3	21,2	25,0	0,87	**CL**
3	38,1	83,3	34,7	48,6	0,93	**CH**

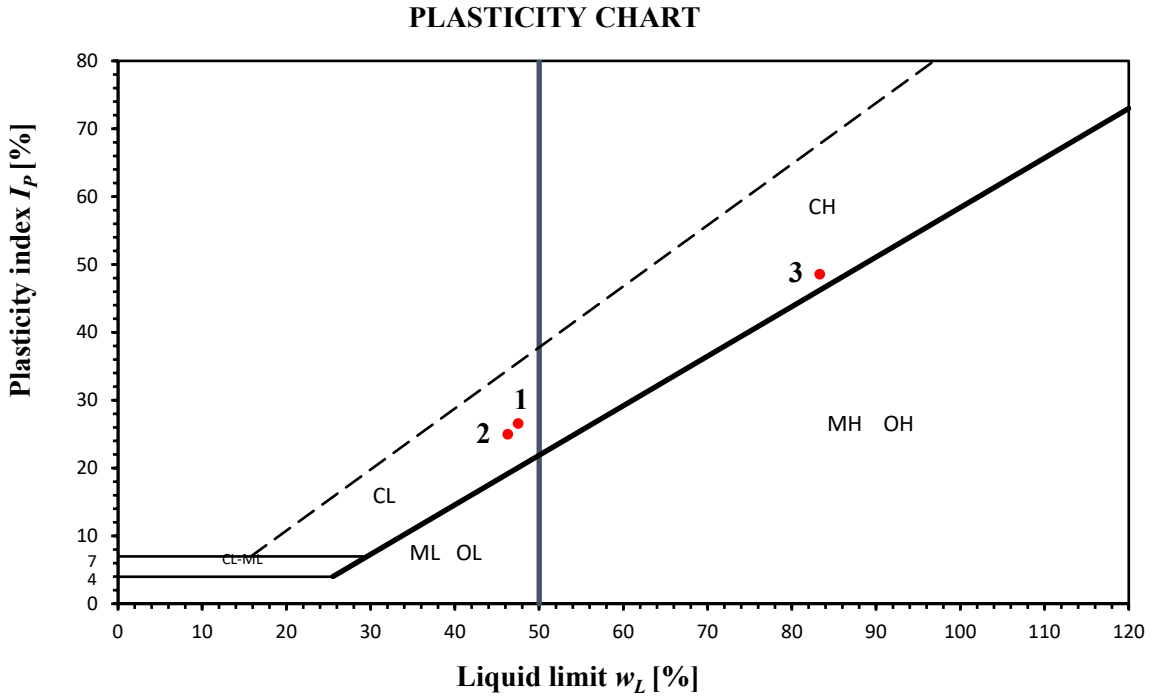

Figure 3. *The plasticity chart for the tested soil samples*

4.2. Processing and installing specimens

Each soil sample was cut into nine smaller soil pieces - soil specimens with dimensions 60x60x20 mm; processing leftovers are left to dry to constant mass, to determine moisture.

A processed specimen (**Figure 4**) is installed into the shearing cell, placing two porous plates on each side of the specimen, which enable water drainage; the cell with the specimen is then placed into the direct shear device (**Figure 5**).

Figure 5. *Specimen processed from the CL sample*

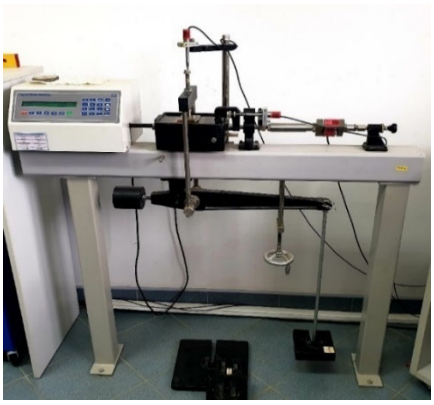

Figure 6. *The direct shear device*

4.3. Testing the specimens

Processed specimens from three soil sample are tested in two phases. The first phase is soil sample consolidation; following the consolidation completion. In the second phase the sample is sheared at a specific rate.

Groups of three specimens from each soil sample to be sheared at the same rate are consolidated under different normal stress. The first specimen is consolidated at a normal stress of 54,5 kPa, the second specimen at 109,0 kPa, and the third at 218,0 kPa. The results of the consolidation phase are entered into the chart of the settlement timeline, which is then used to determine the time necessary for total sample settlement (t_100) and the reference shear rate, in ways described in chapters 3.3 and 3.3.2.

The consolidation phase is followed by specimen shear. Groups of three specimens are sheared at the reference rate, then ten (three) times faster than the reference rate and ten (three) times slower than the reference rate.

4.4. The results of the conducted tests

The results yielded from a direct shear test are interpreted in the form of three charts. The first one is a curve of the settlement timeline which is not shown in the results. The second chart shows the result of direct shear test (shear stress vs horizontal displacement curve). The third shows the values of peak and residual shear stress and the accompanying vertical stress. Through all three points of testing, a regression line is drawn which determines peak and residual values of cohesion and internal friction angle. The greatest achieved value during the shear is taken as the peak value of shear stress, while the values from the almost horizontal part of the curve, towards the end of the horizontal deformation, are accepted as the value of residual shear stress. Slope and intercept of the failure envelope are shear strength parameters of soil: cohesion (c) and internal friction angle (φ). Slope and intercept of the residual envelope are residual shear strength parameters of soil.

After conducting specimen shear tests at different rates, the data and information attained using a computer are processed by applying the appropriate computation operations, and the results are presented both graphically and tabulated. The values of peak and residual shear stress, peak and residual cohesion, and peak and residual internal friction angle, at different shear rates and for three different soil samples, were attained.

Direct shear test results at rate 0,0075 [mm/min] (sample #3) are shown in **Figure 6**. Failure envelope (red line) and residual envelope (blue line) at rate 0,0075 [mm/min] (sample #3) are shown in **Figure 7**. The test results of other soil samples at different shear rates are not shown graphically. The results are presented in a table (**Table 4**).

Table 4. The report of all results attained in the direct shear experiment

Sample - Classification	Shear rate [mm/min]	Specimen	Vertical stress [kPa]	Peak shear strength [kPa]	Residual shear strength	Cohesion [kPa] Peak/ residual	Internal friction angle [°] Peak/ residual
#1 - CL	0,01	A	54,5	48,9	34,4	8,2 5,2	34,7 29,4
		B	109,0	79,1	68,8		
		C	218,0	160,6	127,3		
	0,03	A	54,5	53,0	44,2	24,7 17,3	28,2 23,7
		B	109,0	84,4	60,5		
		C	218,0	141,0	114,4		
	0,1	A	54,5	58,4	35,8	31,0 4,0	24,8 29,1
		B	109,0	78,6	62,3		
		C	218,0	133,2	125,9		
#2 - CL	0,001	A	54,5	42,4	37,9	10,7 9,7	28,9 27,1
		B	109,0	68,5	65,0		
		C	218,0	131,9	121,4		
	0,01	A	54,5	46,5	39,0	18,7 15,5	25,8 21,9
		B	109,0	69,4	56,8		
		C	218,0	125,0	103,8		
	0,1	A	54,5	53,1	36,6	22,9 6,1	25,5 27,1
		B	109,0	68,5	57,8		
		C	218,0	128,8	118,9		
#3 - CH	0,0075	A	54,5	36,2	15,4	21,3 8,3	16,8 10,7
		B	109,0	56,4	33,7		
		C	218,0	86,2	48,0		
	0,075	A	54,5	43,8	19,7	32,1 10,0	13,9 10,0
		B	109,0	61,7	29,1		
		C	218,0	85,2	48,5		
	0,75	A	54,4	61,0	38,7	51,5 30,3	11,5 9,0
		B	109,0	75,1	48,0		
		C	218,0	95,1	64,8		

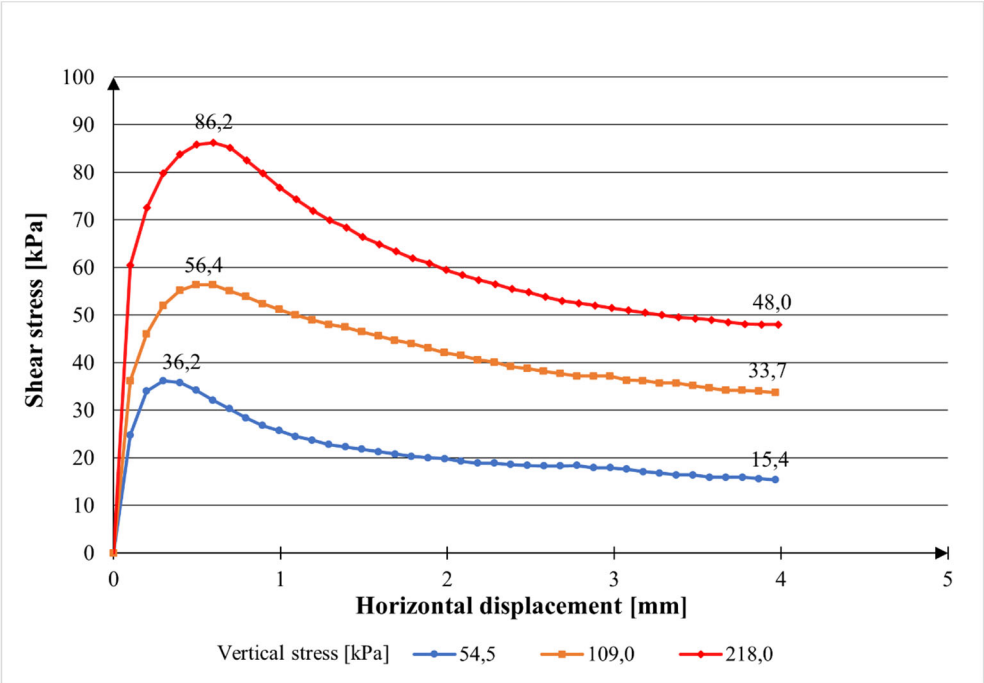

Figure 6. *Direct shear rate test results at rate 0,0075 [mm/min] (sample #3)*

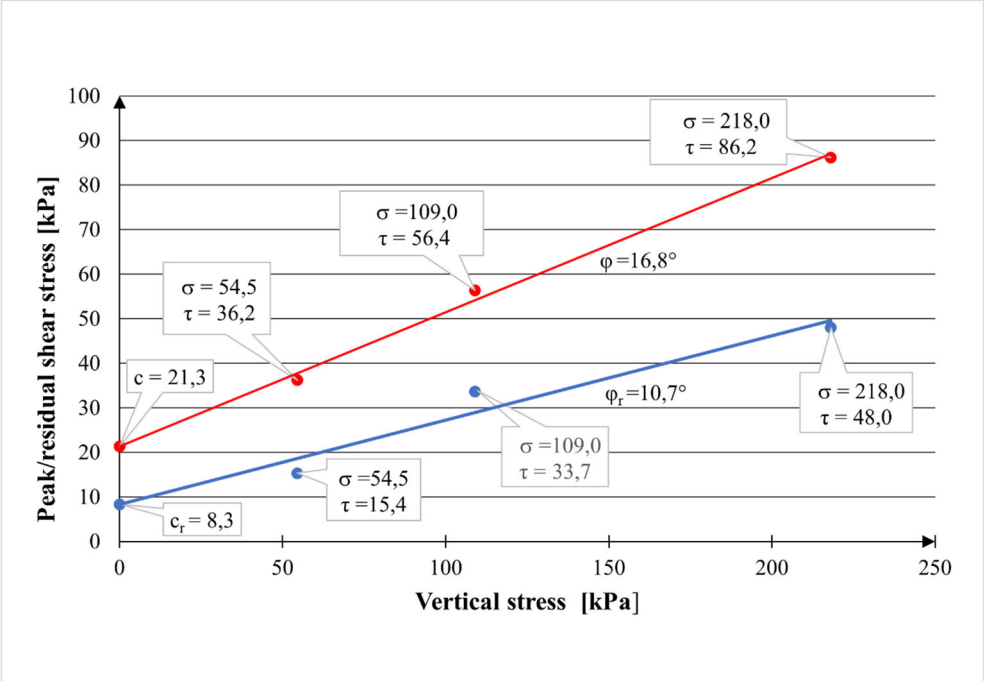

Figure 7. *Failure envelope (red line) and residual envelope (blue line) at rate 0,0075 [mm/min] (sample #3)*

4.4.1. Aggregate visualization of the direct shear experiment results

Shown here are the failure and residual envelopes for different shear rates, in a chart of peak/residual shear stress and vertical stress for teste soil samples. The full lines represent the yielded peak values at different shear rates, and the interrupted lines represent the residual values (**Figure 8, Figure 9, and Figure 10**).

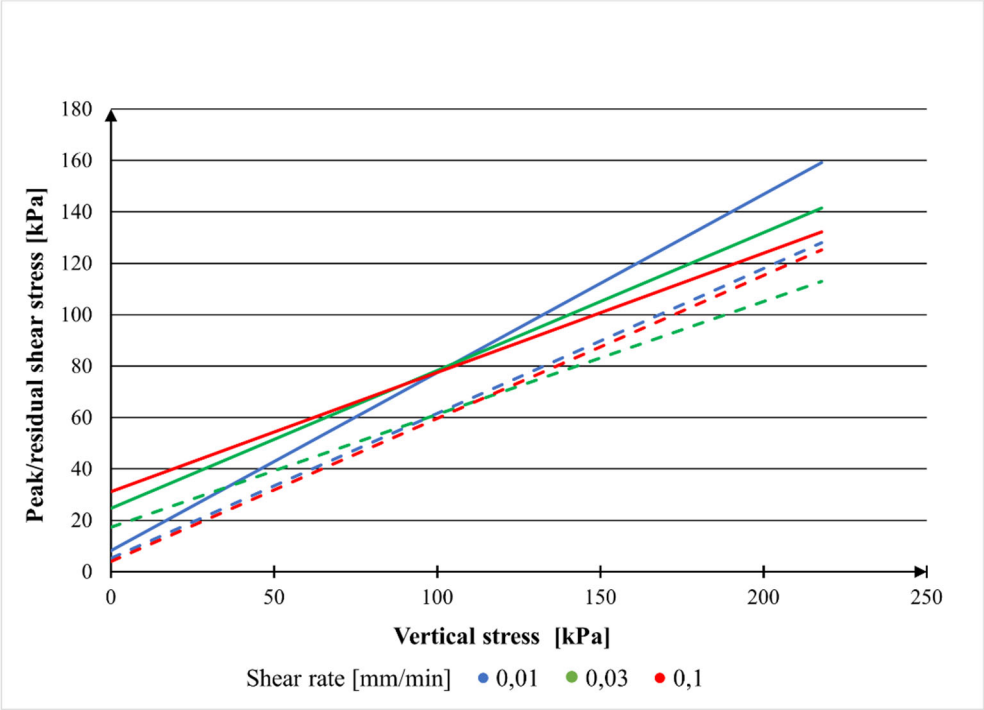

Figure 8. *Failure and residual envelopes for sample #1*

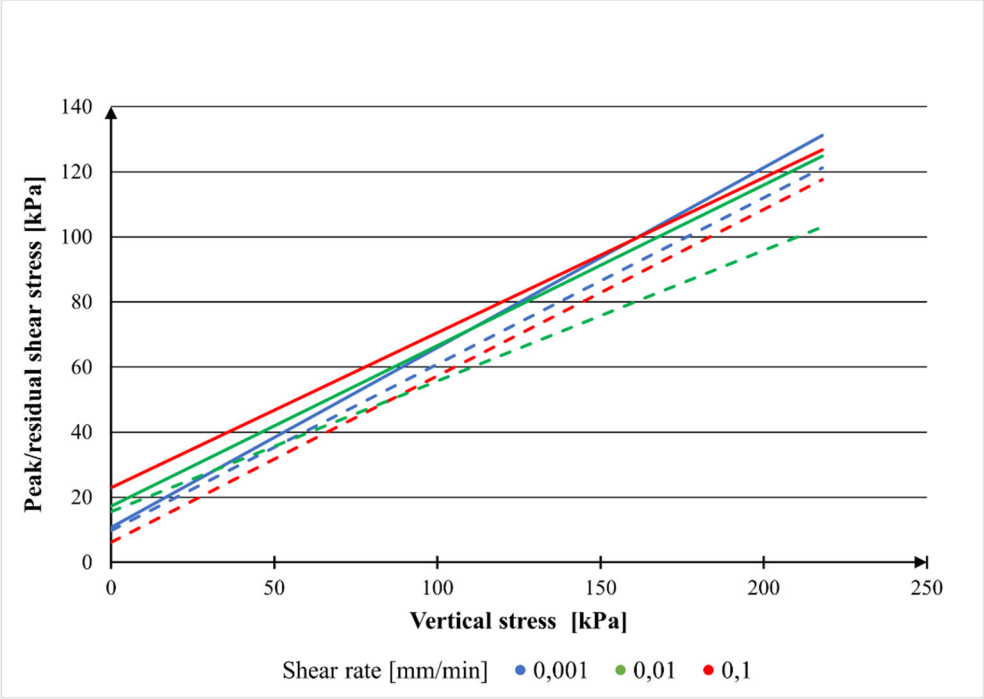

Figure 9. *Failure and residual envelopes for sample #2*

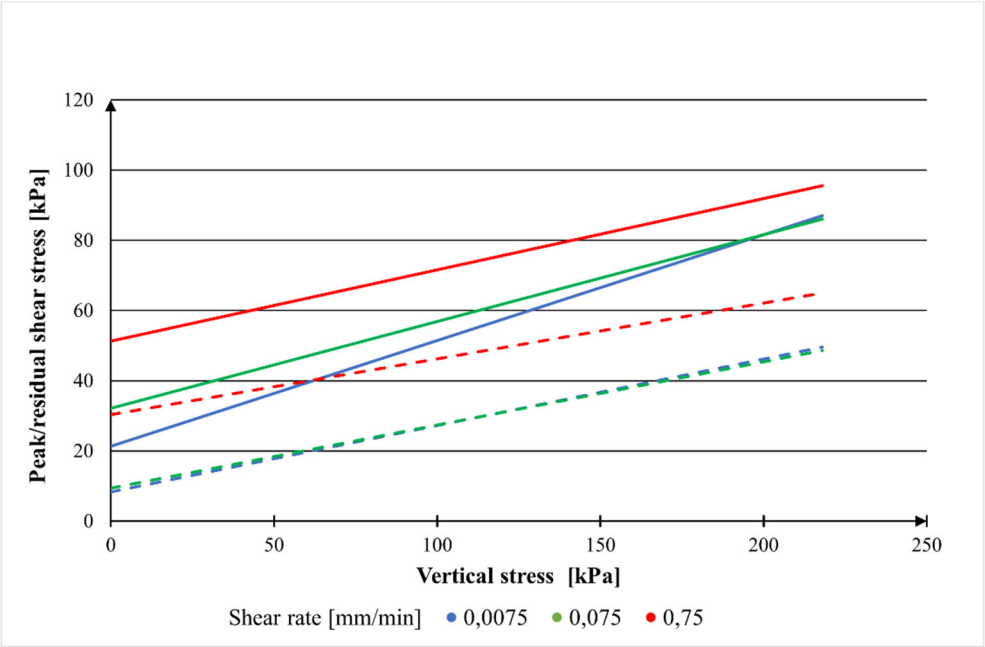

Figure 10. *Failure and residual envelopes for sample #3*

5. CONCLUSION

The results of the laboratory soil test in a direct shear device demonstrate that the parameters of shear strength of soil do not have a constant value, but depend on soil characteristics, drainage conditions, the amount of vertical stress and shear rate. Test conditions must be chosen in a way that they approximate the actual conditions of the sample as close as possible, for the results to be as accurate as possible.

The specimens of low-plasticity clay in sample #1 were sheared at the reference rate, three times slower and three times faster. The specimens from soil sample #2 and soil sample #3 were sheared at the reference rate, ten times faster and ten times slower. The conducted tests of the influence of different shear rates on the shear strength of coherent soil demonstrate that increases in shear velocity increase cohesion and decrease the internal friction angle. If shear rate is too high, the dissipation of pore pressure becomes impossible i.e., there is excess pore water pressure; the test results can lead to bigger construction costs. In the case of a too low shear rate, the result can be unrealistically favourable, which does not benefit the required safety. For these reasons, the choice of appropriate shear rate is of paramount importance.

6. REFERENCES

Rouaiguia, A., Rogers C.D.F.(2001), Fast shear rate effects on the residual shear strength of clay, International Society for Soil Mechanics and Geotechnical Engineering, UK, 261-264

Baoqi, L., Jianbing P., Xingang, W., Qiangbing, H., (2018), Influence of shearing rate on the residual strength characteristic of 2 three landslide soils in loess area, Discussions, X'ian-China

Bek, A., (2020), Utjecaj brzine smicanja na posmičnu čvrstoću tla, Završni rad, Sveučilište u Zagrebu, Geotehnički fakultet; Varaždin

BS 1377 Part 7 :1990 Clause 4 – Determination of the shear strength by direct shear (small shear box apparatus)

Eslami., A., Moshfeghi, S.,MolaAbasi, H., Eslami M.M. (2020) Piezocone and Cone Penetration Test (CPTu and CPT) Applications in Foundation Engineering, First edition

Geotechdata, Angle of friction, available at: http://geotechdata.info/parameter/angle-of-friction

Head K.H, & Epps R. J., (2011), Manual of soil laboratory testing, Volume 2: Permeability, Shear Strength and Compressibility tests, Third edition

Huđek, D.,(2008), Utjecaj brzine posmika na parametre čvrstoće tla, Diplomski rad, Sveučilište u Zagrebu, Geotehnički fakultet; Varaždin

Strelec S., Štuhec D. (2011), Geotehnički laboratorij i primjena u inženjerskoj praksi, Interna skripta, Varaždin: Sveučilište u Zagrebu, Geotehnički fakultet

Papić., M. (2014), Ovisnost posmične čvrstoće koherentnog tla o brzini smicanja, Završni rad, Sveučilište u Zagrebu, Rudarsko-geološko naftni fakultet; Zagreb

FOREST AREA CHANGES THROUGHOUT THE YEARS IN BJELOVARSKO-BILOGORSKA COUNTY

Nikola Kranjčić[1*], Antonio Jaguljnjak [1], Jurica Ivanušec [1], Mihael Heček [1]
[1] *University of Zagreb, Faculty of Geotechnics, Hallerova aleja 7, 42000 Varaždin, Croatia*
*E-mail of corresponding author: nikola.kranjcic@gfv.unizg.hr

Abstract: *The results of forest cover reduction were obtained using raster data and administrative borders for the Republic of Croatia. Examples are taken from other countries to compare the results and show the reduction of cover, both forest and agricultural. The first part of this paper describes the situation in the Republic of Croatia, where Ministry of Environmental Protection provided analysis. The condition of land cover in the Republic of Croatia is presented. The second part of this paper is a description of the task development process in the software package "QGIS". From adding CLC raster data to, the actions performed in the program that were performed until the results arrived. Finally, the interpretation of the obtained data and the conclusion follow.*
Keywords: *Corine Land Cover, QGIS, Bjelovarsko-bilogorska, Forest cover*

Received: 10.07.2021. / Accepted: 15.09.2021.
Published online: 01.12.2021.

Professional paper
https://doi.org/10.37023/ee.8.1-2.7

1. INTRODUCTION

The topic of the paper is reduction of forest cover in Bjelovarsko-bilogorska county from 1990 to 2018. Be-tween 1990 and 2000, data analyses were processed for the several processes were processed in Europe. Urbanization was most noticeable in the Netherlands (2.1% of the total land area), changes in agricultural intensification in Ireland (3.3%), in the Czech Republic extensive agriculture (over 3.5%), afforestation in Portugal (over 4%), whitewashing forests in Portugal (over 3.5%) and water bodies construction in the Netherlands and Slovakia (over 0.1%). (Feranec, 2010) In Romania, the results indicate that almost 7.5 km2 of forests (0.81% of the total forest area) were cutted during 1990-2000. And 5.7 km2 (1.06%) during 2000-2006. Percentages of afforested areas per administrative unit ranged between 0% and 83.8% during 1990-2000. and between 0% and 95.9% during 2000-2006. (Petrişor, 2015) In Bulgaria, CORINE Land Cover changes in land cover for the peri-od 1990-2000 cover an area of 123,080 ha or 1.1% of the country's territory. The most significant changes relate to the forest landscape (58% of the total changed area). Afforested areas are about 10% larger than de-forested forests. (Vatseva, 2006) In Slovakia, for the period from 1976 to 1992, a study of the identification and analysis of landscape changes was conducted. The result of the research was the creation of a database on changes in land cover in certain districts of Slovakia. Deforestation reduced the forest area by 8.6% of the total area of Snina district, extensive agriculture by 3.5% of the total area of Snina district and urbanization together with industrialization by 3.3% of the total area of Dunajska Streda district, and these are the largest identified surface changes. (Feranec, 2002) In the United Kingdom, from 2006 to 2012, land cover change affected al-most 60% more land than from 2000 to 2006. A greater diversity of land cover change of 165 species was found in the period from 2006 to 2012 than 67 species in the period from 2000 to 2006. The area of altered cover increased by over 21,000 ha or 11% but remained at around 1% of the total land area in the UK. (Cole, 2018)

Using Landsat data in west Africa in the period from 1975 to 1990, the change of land cover was studied. Dur-ing the period from 1975 to 1990, the net annual rate of change of dense tree cover was estimated at -0.95%, for other wooded land -0.37% and very low for mosaic tree cover -0.05%. On the other hand, other vegetation cover increased annually by 0.70%, most likely due to the expansion of agricultural land. (Vittek, 2014)

2. CORINE LAND COVER (CLC)

The CORINE program enables us to properly manage our nature and environment, and those who make decisions should be provided with an overview of existing knowledge and information that is up to date on changes in the characteristics of the biosphere. In this case, the three principles of the CORINE pro-gram (coordination of environmental information) are European:

- collect information on the state of the environment regarding certain topics that have priority for all members of the State Union,

- coordinate the collection of data and the organization of information between the Member States or at international level,
- to ensure that the information is consistent, and that the data is compatible.

On 27. June 1985, on a proposal from the Commission, the Council adopted a decision on the CORINE program. This work program of the commission refers to an "experimental project to collect, coordinate and ensure the consistency of information on the state of the environment and natural resources in the Community" (Official Journal L 176, 6.7.1985). To establish community environmental policy, it is appropriate to assess the effects these policies and incorporate the environmental dimension into other policies, understanding the different features of the environment:

- condition of individual environments,
- geographical distribution and condition of natural areas,
- geographical distribution and abundance of wild fauna and flora,
- quality and abundance of water resources,
- soil cover structure and soil condition,
- quantities of toxic substances released into the environment,
- lists of natural hazards, etc.

The next goal is to gather all the numerous attempts made over the years at various levels (international, joint, national, and regional) to obtain as much information as possible about the environment and the way it has changed.

Two main types of complementary actions have been taken to meet the objectives of the program:

- devising procedures for the collection, standardization, and exchange of environmental data in EC Member States.
- creating a geographic information system to provide environmental information that is crucial in the preparation and implementation of community policies.

3. CORINE LAND COVER (CROATIA)

3.1. CLC Cro 2000

The result of the CORINE Land Cover Croatia project is a digital, up-to-date database on land cover according to the CORINE nomenclature, which is the same for the entire European Union. Mapping of land cover in the EU was launched in 1990, and mapping of land changes for 2000 and 2006. The project is funded by the Ministry of Environmental Protection, Physical Planning and Construction, and is also the Croatian national share in the European Environment Agency, which is entrusted with the use of the database. The aim of the project is to provide relevant and up-to-date environmental databases. The maintenance of the database has been carried out by the Environmental Protection Agency since 2005. In 2002, the creation of the CLC database for the years 2000, 1990, 1980 began. IMAGE 2000, 1990, 1980 are based on available satellite imagery, processing and represent a large database. This period was to show an assessment of changes as natural processes and development processes, but also those that were a consequence of the war in the 90s.

Two basic "CORINE" databases that are indivisible and derived from each other:

- IMAGE2000, IMAGE1990 and IMAGE1980: cover all activities related to the acquisition, orthorectification of satellite images (Landsat TM and ETM+), including the production of European and national mosaics (Kušan, 2010)
- CLC2000, CLC1990 and CLC1980: cover all activities related to the establishment of the CLC land cover inventory database based on IMAGE products and interpretation (detection) of changes (Kušan, 2010)

Experts from Europe, from the European Topic Center on Terrestrial Environment, had the basic task of ensuring coordination and implementation of the harmonization of project results at the level of all EU countries and others participating in the project. OIKON d.o.o. and GISDATA d.o.o. were responsible for CLC interpretation with the purpose of creating CLC databases and CLC databases of land cover changes using basic reference originals - satellite images (IMAGE1980, IMAGE1990 and IMAGE2000).

3.2. CLC Cro 2006

With the aim of creating a map and database of land cover CLC 2006, a project of updating the database and changes that occurred on the land cover from 2000 to 2006 with the project implementation period from 2007 to 2008 was implemented. The CLC 2006 Croatia project is part of a larger project "Implementation of CLC 2006 in the West Balkan Countries" coordinated by the European Environment Agency. In a smaller size, the technical specifications were improved compared to CLC 2000, only changes that took up more than 5 ha were mapped. Recent IMAGE 2006 images from IRS and SPOT satellites were used. Which as a result contributed to the improvement of the spatial resolution which went from 30 meters (Landsat 7) to 20 meters (SPOT).

3.3. Land cover in Croatia, examples

For the territory of the Republic of Croatia, a map of land cover was prepared according to the CORINE methodology for the reference years: 1980, 1990, 2000 and 2006, based on these databases, the areas for each CORINE class were calculated (**Table 1**).

Table 1. State of land cover in the Republic of Croatia according to CORINE land use classes in databases for 1980, 1990, 2000 and 2006 (area in ha)

CLC Code	Class Name	CLC 1980.	CLC 1990.	CLC 2000.	CLC 2006.
				ha	
111	Settlements (>80% built)	524	524	550	550
112	Settlements (<80% built)	131 722	134 464	138 791	139 723
121	Industrial or commercial premises	10 565	10 826	11 292	11 853
122	Roads with associated land	797	847	1 398	7 482
123	Ports with associated land	647	699	704	704
124	Airports with associated land	2 481	2 527	2 610	2 610
131	Miners	3 451	3 602	4 380	4 909
132	Landfills	308	308	434	418
133	Construction site	286	409	817	1 562
141	City greenery	1 812	1 812	1 782	1 724
142	Sports and recreational facilities	5 211	5 632	5 667	5 917
211	Arable land	385 633	378 430	368 974	370 262
212	Irrigated agricultural areas	9 443	9 397	9 821	9 821
221	Vineyards	28 200	28 193	28 925	29 055
222	Orchards	9 760	9 410	9 548	9 574
223	Olive groves	18 759	18 705	20 223	20 197
231	Mowing meadows and intensive pastures	475 815	477 566	307 296	298 950
242	Mosaic of different ways of agricultural use	1 034 844	1 026 779	1 017 238	1 022 051
243	Agricultural areas with a significant share of natural vegetation	515 282	510 822	523 509	524 202
311	Deciduous forest	1 706 194	1 695 356	1 695 495	1 682 078
312	Coniferous forest	105 473	102 496	105 702	102 528
313	Mixed forest	273 533	275 465	272 522	271 624
321	Natural grasslands	77 147	77 103	252 102	252 781
322	Screams, cretes and low thickets	6 892	6 916	4 114	4 421
323	Sclerophilic vegetation	134 541	138 026	144 450	143 691
324	Forest succession (land in healing)	567 840	591 160	579 824	592 532
331	Beaches, dunes, sands	563	484	225	225
332	Bare surfaces	12 706	12 714	11 892	11 892
333	Areas with sparse vegetation	65 329	63 989	61 061	60 807
334	Burnt areas	1 333	1 547	3 271	395
411	Land marshes	17 861	17 841	19 014	18 887
421	Salt marshes	517	517	548	538
422	Salt pans	522	522	524	524
423	Areas affected by tides	48	48	48	48
511	Water liquids	23 779	23 167	23 961	23 968
512	Stagnant waters	27 593	29 636	29 695	29 918
521	Coastal lagoons	45	45	44	44
523	Sea	3 163 423	3 159 469	3 156 321	3 156 305
	Total Land	5 657 456	5 657 984	5 658 451	5 658 465
	Total Republic of Croatia	8 820 879	8 817 453	8 814 772	8 814 770

Table 2. State of land cover in the Republic of Croatia according to CORINE databases for 1980, 1990, 2000 and 2006 (area in ha)

Label categories	Rollup Name	Surface (ha)			
		CLC 1980	CLC 1990	CLC 2000	CLC 2006
1a	Man-influenced surfaces	157 804	161 650	168 425	177 452
2a	Arable land and permanent plantations	451 795	444 135	437 491	438 909
2b	Heterogeneous agricultural areas	2 025 941	2 015 167	1 848 043	1 845 203
3a	Forests and thickets	2 653 543	2 664 477	2 653 543	2 648 762
3b	Shrub and grass vegetation	298 511	300 779	477 115	474 212
4a	Swamp	18 948	18 928	20 134	19 997
5a	Inland waters	51 417	52 848	53 700	53 930
	altogether	5 657 456	5 657 984	5 658 451	5 658 465

The largest part of the land area in the Republic of Croatia is occupied by forests and thickets with a share of about 47%. Heterogeneous agriculture decreased by 3.2% between 1980 and 2006. The following category by share is shrub and grass vegetation of 8.4% in 2006. This group also includes natural grasslands, shrubs of vegetation and areas that were burned in summer fires. Areas where there were forests in the past are now occupied by bushy vegetation, and this is especially true for coastal areas. The following category is intensive agriculture, which occupies 7.8% of the total area of the Republic of Croatia in 2006, and other categories occupy a very small share. Figures 1 to 4 shows changes of landscape in Croatia from 1980 till 2006.

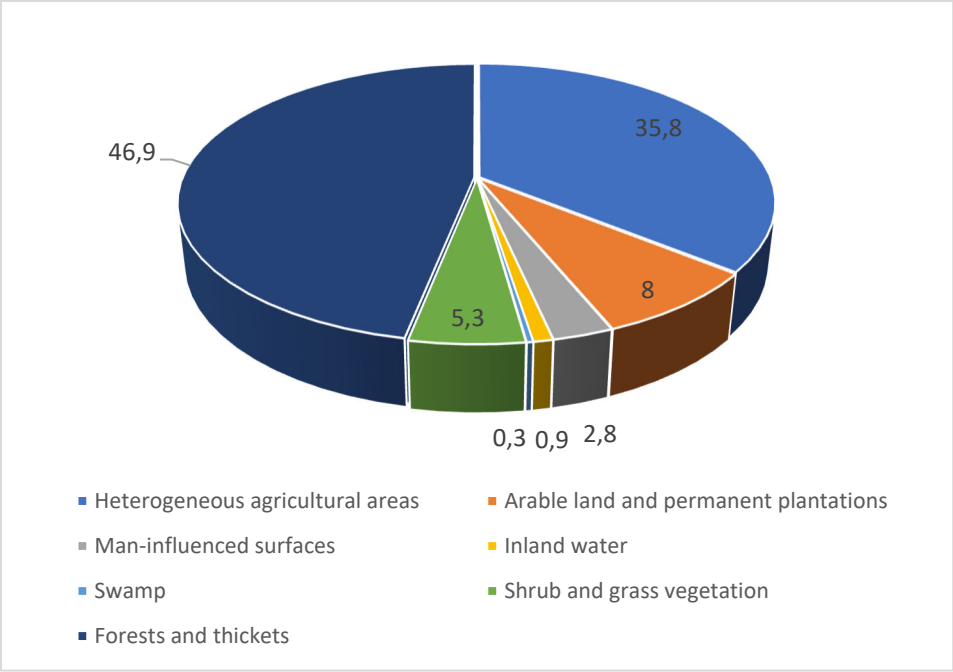

Figure 1. *Structure of land cover by area in the Republic of Croatia (without sea) in 1980*

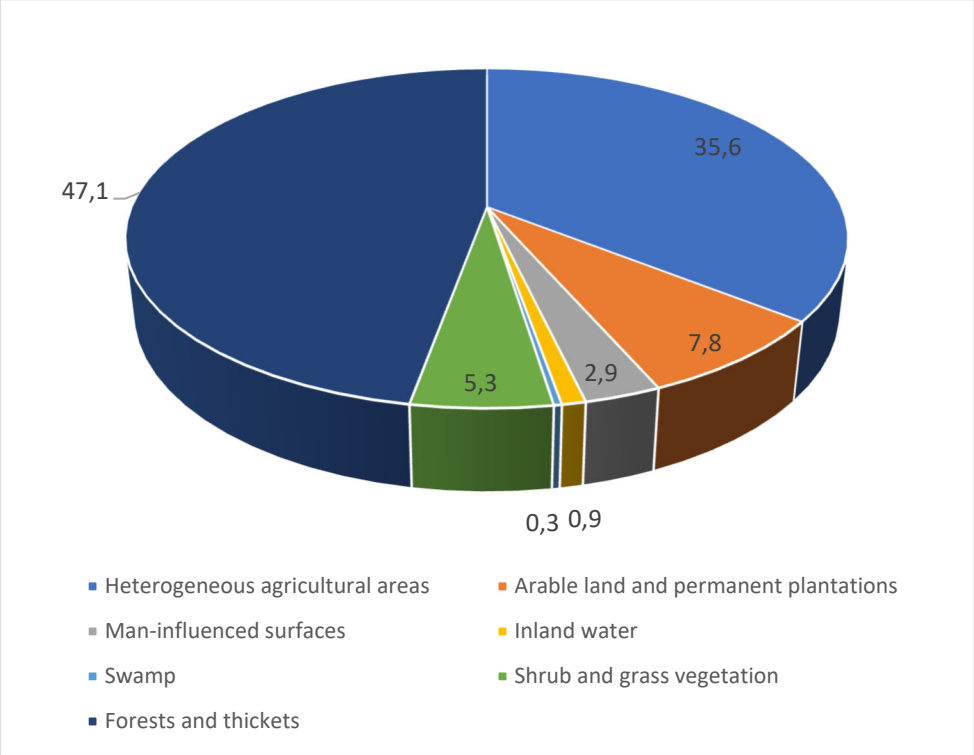

Figure 2. *Structure of land cover by area in the Republic of Croatia (without sea) in 1990*

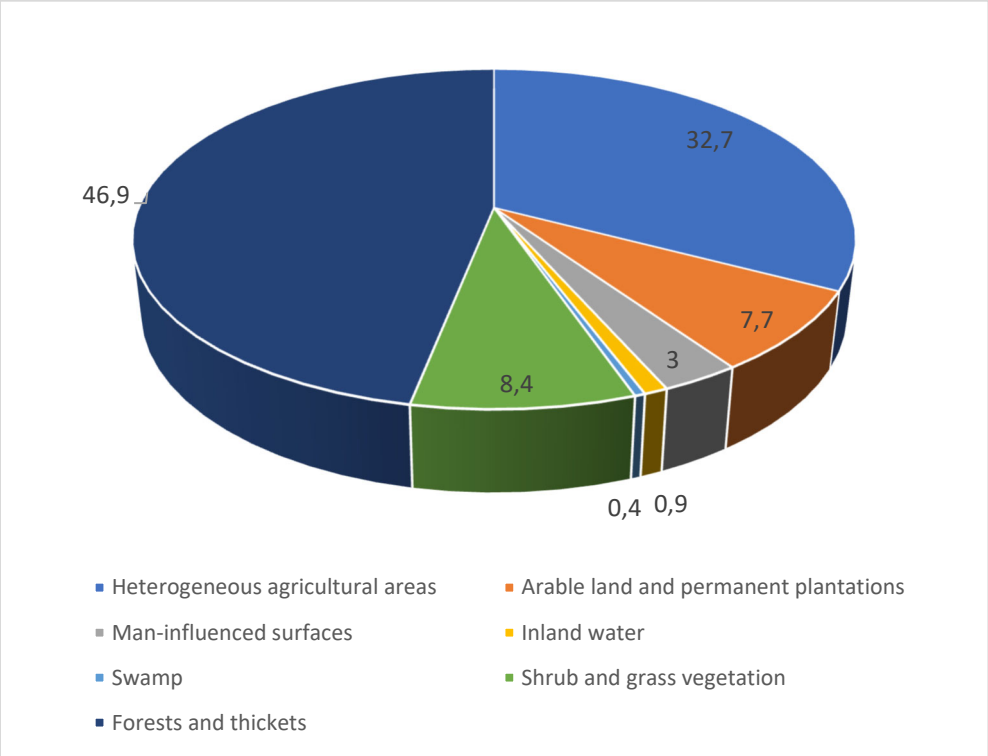

Figure 3. *Structure of land cover by area in the Republic of Croatia (without sea) in 2000*

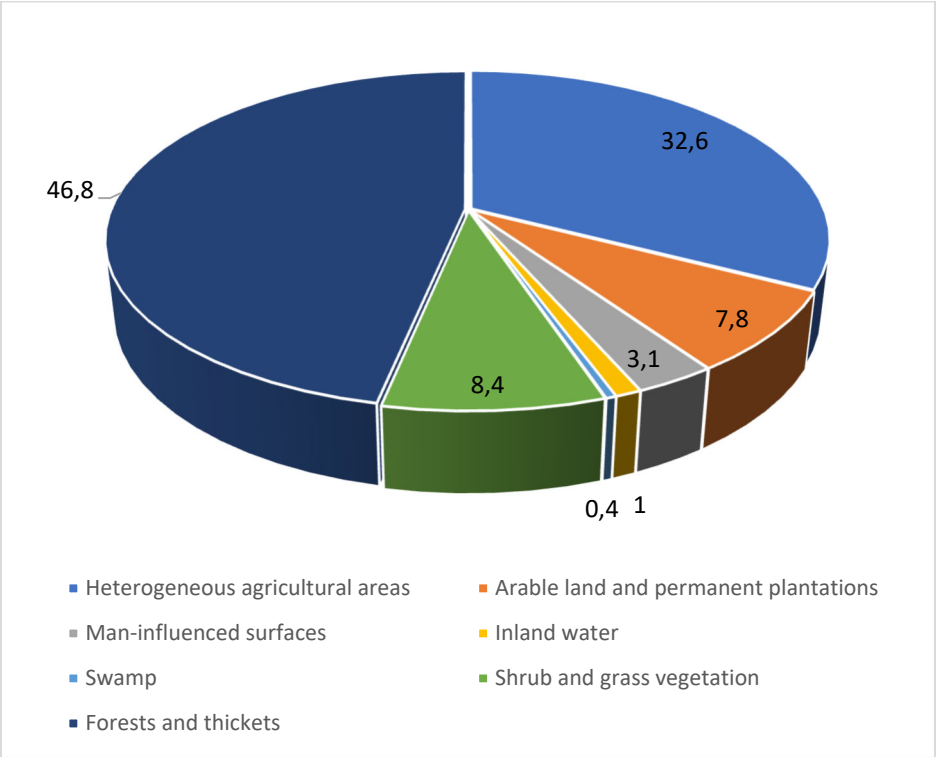

Figure 4. *Structure of land cover by area in the Republic of Croatia (without sea) in 2006*

Forests and thickets and heterogeneous agricultural areas are the categories in which the change in area is greatest, the reason being that these categories occupy the largest part of the land area of the Republic of Croatia with a share of about 80 percent. The change in forest and shrub areas in the first two periods amounted to more than 10,000 ha, and after that in the third period it amounted to 5,000 ha, due to the occurrence of neglect of agricultural land and forest management. Changes in heterogeneous agricultural areas are a consequence of the neglect of intensive agricultural areas. Due to human influence, large changes have occurred in the areas, because of the construction of infrastructure, urbanization. Arable land and permanent crops decreased until 2000, after which there was a gradual increase in their area.

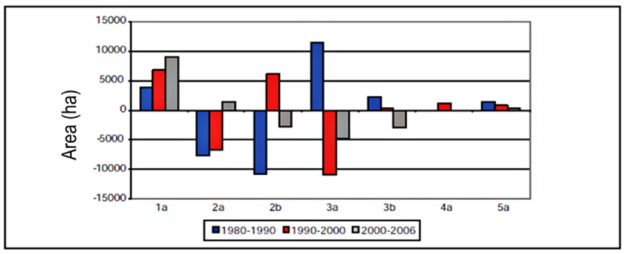

Legend

Label categories	Rollup Name	Label categories	Rollup Name
1a	Man-influenced surfaces	3a	Forests and thickets
2a	Arable land and permanent plantations	3b	Shrub and grass vegetation
2b	Heterogeneous agricultural areas	4a	Swamp
		5a	Inland waters

Figure 5. *Differences in land use areas in the period 1980-2006.*

4. METHODOLOGY

The first step is to download the raster data from the CORINE land cover website for each year separately (1990, 2000, 2006, 2012, 2018), and for the period between two years (1990.-2000., 2000.-2006., 2006.-2012., 2012.-2018.). We can notice that it is CLC raster data, while on the other hand for the period between two years there is CHA raster data. Each type of raster data is processed in the QGIS program in a different way, which will be described and explained in more detail below. After all the data for each year have been downloaded and unpacked, it is necessary to download the administrative boundaries, which is added as vector data. Let's open "QGIS Desktop with GRASS" and create a new document. First, we add the raster CLC data (TIFF image) that is

in the downloaded DATA folder for each year separately (Figure 6). It should be noted that a separate document is prepared for each year in the QGIS to avoid confusion in the calculation of areas.

Figure 6. *CORINE land cover layer*

Furthermore, we add administrative boundaries for Croatia (SHP file) as vector data. After that vector data is filtered based on desired county to crop raster layer to be more suitable for processing. Figure 7 presents Bjelovarsko-bilogorska county on raster map.

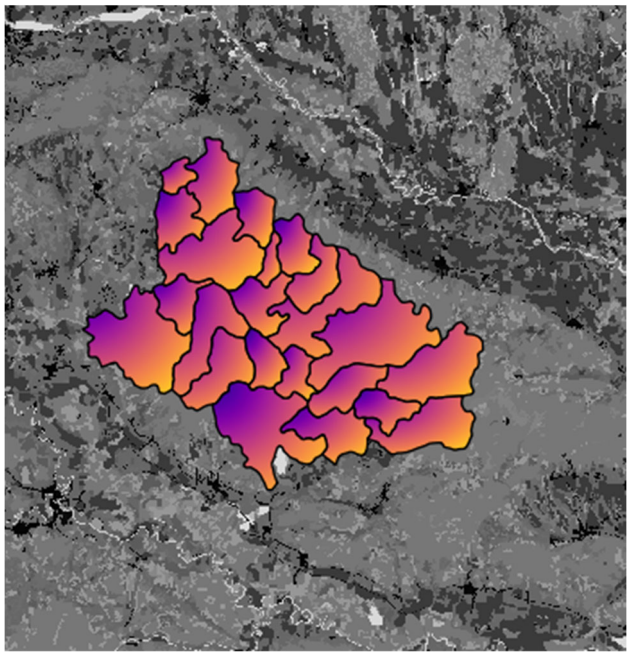

Figure 7. *Separated county*

After the raster is cropped there can be different selections performed. To establish connection between forest areas we chose dark green for the broadleaf forest, red for the coniferous, and orange for the mixed forest. Figure 8 presents only forest areas for selected county.

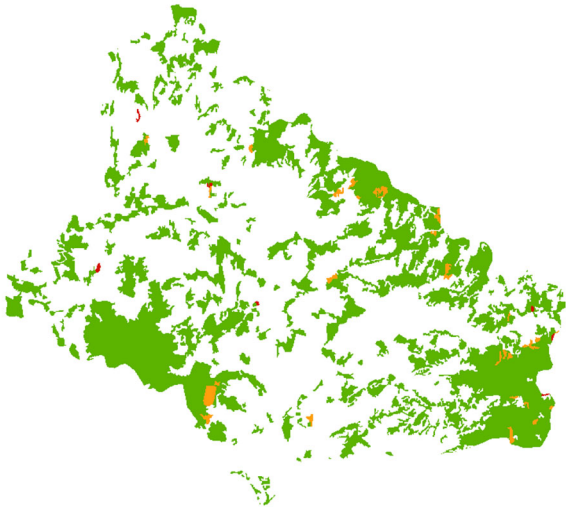

Figure 8. *Forest areas for Bjelovarsko-bilogorska county*

After forest areas have been filtered, it is necessary to calculate areas for each year, using raster report function. Figure 9 shows one raster report, where areas in square meters have been calculated.

```
+-------------------------------------------------------------------------------+
|                          RASTER MAP CATEGORY REPORT                           |
|LOCATION: temp_location                              Fri May 07 17:45:35 2021  |
|-------------------------------------------------------------------------------|
|          north: 2577400    east: 4902600                                      |
|REGION    south: 2508900    west: 4824900                                      |
|          res:       100    res:      100                                      |
|-------------------------------------------------------------------------------|
|MASK: none                                                                     |
|-------------------------------------------------------------------------------|
|MAP: (untitled) (rast_6095609ea1bc03 in PERMANENT)                             |
|-------------------------------------------------------------------------------|
|                     Category Information                      |       square|
|         #|description                                         |       meters|
|-------------------------------------------------------------------------------|
|0.996078-1|from  to . . . . . .                                |  910,160,000|
|0-0.003922|from  to . . . . . .                                |4,412,290,000|
|-------------------------------------------------------------------------------|
|TOTAL                                                          |5,322,450,000|
+-------------------------------------------------------------------------------+
```

Figure 9. *Raster map category report*

In next section, there are graphical representation of forest areas for Bilogorsko-bjelovarska county. Table 3 presents forest areas and other surfaces for years 1990, 2000, 2006, 2012 and 2018.

Table 3. Total forest areas for different years

Year	Forest area (km^2)	Other areas (m^2)	Total (m^2)
1990	879,83	4442,62	5322,45
2000	884,61	4437,84	5322,45
2006	885,80	4436,65	5322,45
2012	910,16	4412,29	5322,45
2018	890,01	4432,44	5322,45

Based on the Table 3, we can see how the forest area of Bjelovarsko-bilogorska county has changed over the years, and the reasons for this can be numerous, from afforestation to logging etc. On Figure 10 changes in forest areas in m^2 are presented.

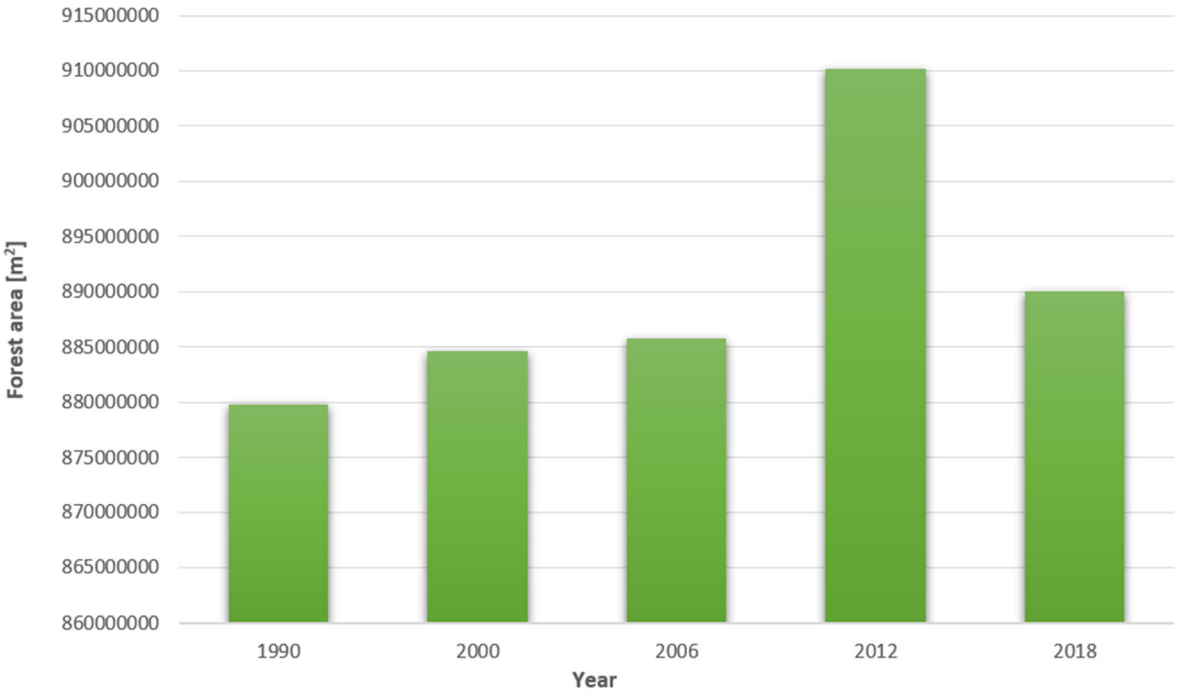

Figure 10. *Forest area changes over the years in m^2*

In conclusion, we can observe that the forest area has increased with age which was not expected. From 2012 to 2018, logging probably took place, but an increase in forest areas is still visible for a period of 28 years (Figure 11).

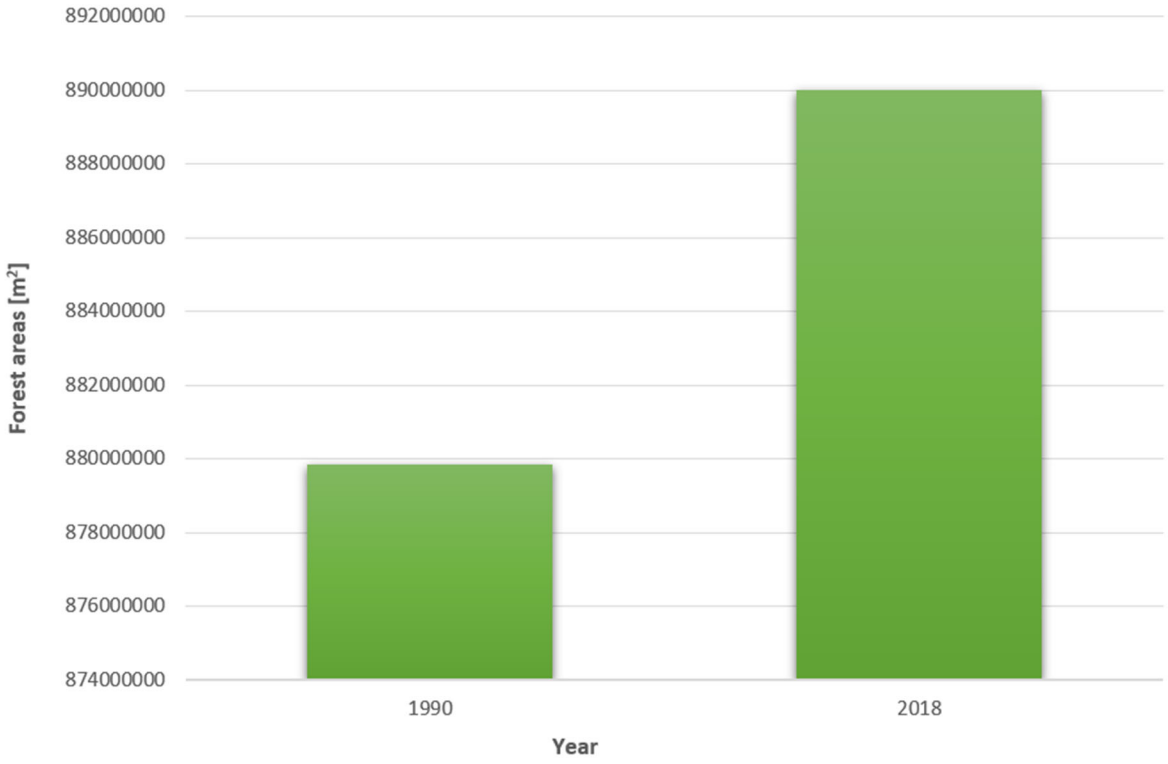

Figure 11. *Forest areas difference from year 1990 to year 2018 in m^2*

5. CONCLUSION

Databases created according to the CORINE methodology, and their analysis have shown many advantages that these data provide. All data, for all periods, were obtained by the same methodology, are complete and processed with the same intensity in all parts of Europe, and the Republic of Croatia. The changes were mapped directly on satellite images, which enables the analysis of transitions of individual mapped classes and their tracking throughout the period. In this paper, an analysis of changes in forest cover in Bjelovar-Bilogora County is made. By working in the computer program "QGIS Desktop with GRASS" and processing the obtained raster CLC data, we obtained the results of the size of the areas covered with forest cover. There has been a noticeable increase in forest areas over the years. The increase was not expected, due to the trend of increasing deforestation in the world, but also in the Republic of Croatia. Only in the period from 2012 to 2018, the forest area was reduced, which is a direct result of logging. In general, in the period from 1990 to 2018, we can talk about an increase because of the overgrowing of some other areas, the expansion of forests and afforestation that took place in the Bjelovar-Bilogora County. Working in the program "QGIS Desktop with GRASS" gave us an insight into the situation in the field, without having to go to the field to record "manually" all the necessary data. Due to severe deforestation results presented in this paper are surprising. However, based on CORINE land cover data results are as presented. Increase in forest areas could be result of reduced agricultural areas and then shrubs and lower plants are labeled as forests. Further work should establish in detail changes in landscape.

6. REFERENCES

Cole, B. S. G. &. B. H., 2018. Acceleration and fragmentation of CORINE land cover changes in the United Kingdom from 2006–2012 detected by Copernicus IMAGE2012 satellite data. s.l.:an.

Feranec, J. J. G. S. T. &. H. G., 2010. Determining changes and flows in European landscapes 1990–2000 using CORINE land cover data. s.l.:an.

Feranec, J. S. M. C. T. &. O. a. J., 2002. Methodological aspects of landscape changes detection and analysis in Slovakia applying the CORINE land cover databases. s.l.:an.

Kušan, V., 2010. Pokrov i namjena korištenja zemljišta u Republici Hrvatskoj–stanje i trendovi, s.l.: Agencija za zaštitu okoliša.

Petrişor, A. I., 2015. Using CORINE data to look at deforestation in Romania: Distribution & possible consequences. INCD URBAN-INCERC.

Vatseva, R. &. S. A., 2006. Spatial analysis of land cover and land use changes in Bulgaria for the period 1990-2000 based on image and CORINE land cover data. s.l.:an.

Vittek, M. B. A. D. F. S. D. &. D. B., 2014. Land cover change monitoring using Landsat MSS/TM satellite image data over West Africa between 1975 and 1990. s.l.:an.

MULTI-OBJECTIVE OPTIMIZATION OF RETAINING WALL USING GENETIC ALGORITHM

Filip Dodigović [1], Krešo Ivandić [1*], Jasmin Jug [1], Krešimir Agnezović [1]
[1] *University of Zagreb, Faculty of Geotechnical Engineering, Hallerova aleja ,7 42000 Varaždin, Croatia*

*E-mail of corresponding author: kreso.ivandic@gfv.unizg.hr

Abstract: *The paper investigates the possibility of applying the genetic algorithm NSGA-II to optimize a reinforced concrete retaining wall embedded in saturated silty sand. Multi-objective constrained optimization was performed to minimize the cost, while maximizing the overdesign factors (ODF) against sliding, overturning, and soil bearing resistance. For a given change in ground elevation of 5.0 m, the width of the foundation and the embedment depth were optimized. Comparing the algorithm's performance in the cases of two-objective and three objective optimizations showed that the number of objectives significantly affects its convergence rate. It was also found that the verification of the wall against the sliding yields a lower ODF value than verifications against overturning and soil bearing capacity. Because of that, it is possible to exclude them from the definition of optimization problem. The application of the NSGA-II algorithm has been demonstrated to be an effective tool for determining the set of optimal retaining wall designs.*
Keywords: *Geotechnical analysis, NSGA-II, optimization, retaining wall, Eurocode 7.*

Received: 01.09.2021. / Accepted: 15.11.2021.
Published online: 01.12.2021.

Professional paper
https://doi.org/10.37023/ee.8.1-2.8

1. INTRODUCTION

The classic approach to geotechnical design is an iterative process to find the optimal solution that meets prescribed safety margins at a minimal cost. Complex geotechnical analyses often involve many decision variables and limit states verifications, resulting in a large number of feasible designs in the design space. In the classical approach, the search for the optimal designs in the solution space is done manually, which may lead to the selection of a suboptimal design. The use of multi-objective optimization using the NSGA-II genetic algorithm enables the automated search for optimal designs in the entire solution space. The algorithm is based on the dominance principle (Čupić, 2013), and it produces a set of non-dominated designs, referred to as the Pareto front.

Several authors explored the possibility of optimizing geotechnical structures by combining various optimization techniques with reliability theory (Dodigović et al., 2021; Gong et al., 2017, 2014; Juang et al., 2012; Juang and Wang, 2013; Khoshnevisan et al., 2016, 2014a, 2014b). Numerous advantages of such an approach have been emphasized in the literature. Still, due to the complexity of applying structural reliability theory principles, it is not often applied in engineering practice. Optimization of geotechnical structures using the NSGA-II algorithm can be performed without the use of reliability theory. For example, in this case, the overdesign factors (ODF) (Frank et al., 2005) can be maximized while minimizing the cost of the structure.

Islam and Rokonuzzaman (2018) use a genetic algorithm to optimize the design of a footing. They compare the obtained results with the results of the classical approach and conclude that the application of a genetic algorithm can reduce the structure cost by 68%.

Yazadani et al. (2016) investigate the ant colony optimization method for raft piled foundation design. They developed the ACO algorithm for finding optimal solutions of piled-raft foundations. Shahin (2015) investigates the applicability of evolutionary computation for use in complex geotechnical analyzes. They evaluate the application of evolutionary polynomial regression (ERP) to various geotechnical tasks. The obtained results are compared with the results of in-situ tests, from which they conclude that the studied method is suitable for use in complex geotechnical analyzes. This paper investigates the possibility of applying NSGA-II (Non-Dominated Sorting Genetic Algorithm II) to optimize the embedment depth and foundations width of a retaining wall. In this case, the feasible design space consists of all designs that satisfy the ultimate limit state criteria according to Eurocode 7, design approach 3 (European Committee for Standardization, 2012). In the optimization procedure, materials and actions are characterized by mean, characteristic and design values (European Committee for Standardization, 2011). The result of the NSGA-II algorithm is a Pareto front from which the final design is selected.

2. MATERIALS AND METHODS

2.1. Retaining wall geometry and geotechnical properties of soil

Geotechnical analyzes were carried out on the reinforced concrete retaining wall with the geometry showed in **Figure 1**. In accordance with the ultimate limit state criteria, the wall is designed for a given change in ground elevation of 5.0 m. The wall is embedded in a saturated silty sand (SM). A drainage layer behind the wall consists of well graded gravel (GW). Water pressure on the stem is not expected due to the drainage pipe installed at its base.

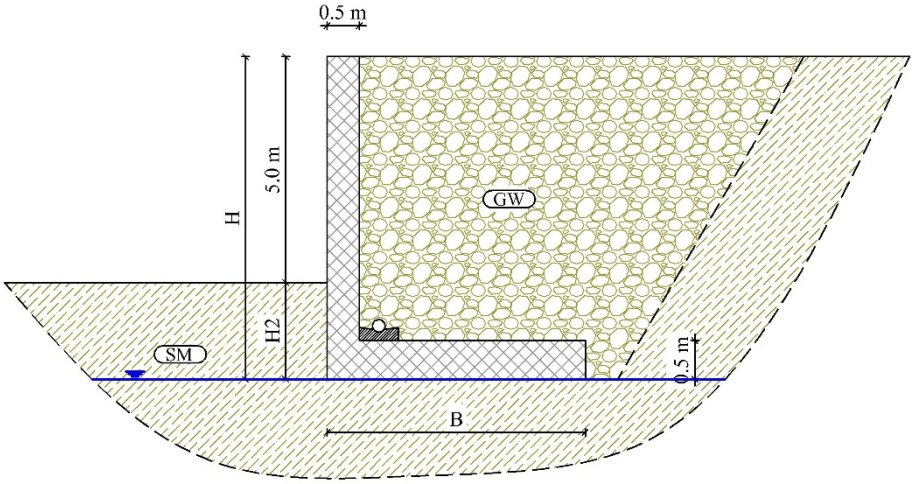

Figure 1. *Geometry of the wall*

Table 1 summarizes the features of the geotechnical parameters used in the analyses. Coefficients of variation were chosen in accordance with the recommendation of Duncan (2000). Geotechnical random variables are assumed to be normally distributed. From the mean values, the characteristic values of geotechnical parameters were calculated according to the following equation Schneider (1999):

$$X_k = X_m \cdot (1 - 0.5 \cdot COV_X) \qquad (1)$$

where:
X is the variable symbol,
X_m is the mean value of X,
COV_X is the coefficient of variation of X.

Design values are calculated from the characteristic values using partial factors according to Eurocode 7, design approach 3.

Table 1. Statistical properties of geotechnical random variables

SYMBOL	DESCRIPTION	SOIL UNIT WEIGHT $[kN/m^3]$	EFFECTIVE ANGLE OF INTERNAL FRICTION	
			$\phi'_m[°]$	$COV_{\phi'}$
GW	Well-graded gravel	20	33	0.1
ML	Silty sand	19	28	0.1

2.2. Verification of ultimate limit states according to Eurocode 7

Figure 2 shows the forces acting on the retaining wall. Up to the freezing depth, the effect of passive soil resistance is neglected. The force V_d is the sum of the weight of the soil above the foundation and the weight of the retaining wall. Since the vertical force is eccentric, the bearing capacity is calculated for the effective area of the footing.

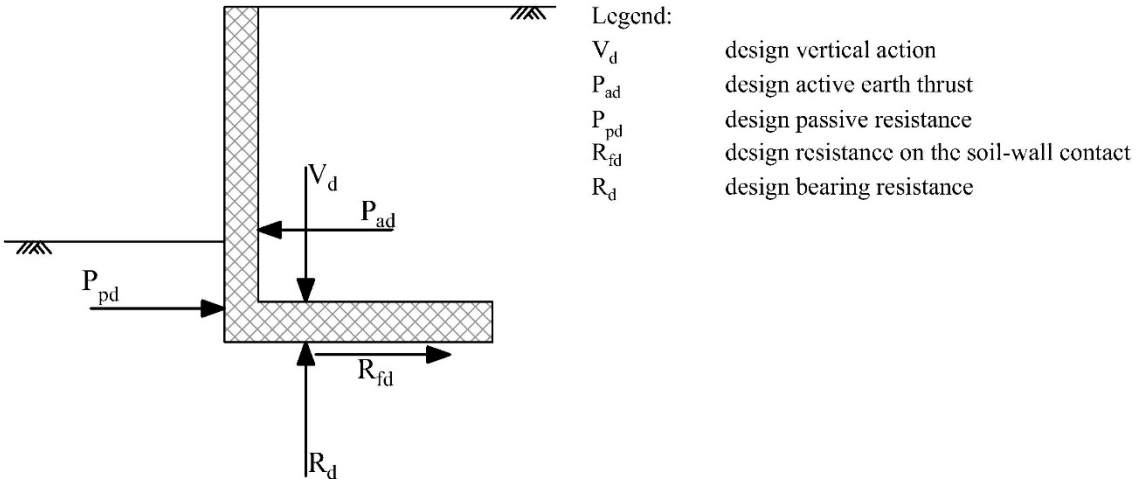

Figure 2. *Forces acting on the retaining wall*

Verification of bearing capacity and resistance against sliding is carried out using **Equations 2 and 3**.

$$V_d \leq R_d \quad (2)$$

$$P_{ad} \leq F_{fd} + P_{pd} \quad (3)$$

To establish the influence of each ultimate limit state on the required minimum wall dimensions, preliminary geotechnical analyses were conducted. The findings of these investigations are not included in this paper. Due to a negligible influence, it was determined that the verification against overturning may be excluded from subsequent analyses.

Design values of active earth thrust P_{ad}, passive resistance (P_{pd}), resistance at wall-soil contact (R_{fd}), vertical action (V_d) and bearing capacity (R_d) are determined using **Equations 4-8**.

$$P_{ad} = K_{ad} \cdot \gamma_s \cdot \frac{H^2}{2} \cdot L \quad (4)$$

$$P_{pd} = K_{pd} \cdot \gamma_s \cdot \frac{H^2}{2} \cdot L \quad (5)$$

$$V_d = \gamma_{G,unfav} \cdot V_k = \gamma_{G,unfav} \cdot G_{wall} + G_{soil} \quad (6)$$

$$R_{fd} = V_k \cdot 0.67 \cdot tan\phi_d \cdot B \cdot L \quad (7)$$

$$R_d = [q' N_q s_q + 0.5\gamma' B' N_\gamma s_\gamma] \cdot A' \quad (8)$$

Where:
K_{ad} and K_{pd} are Rankine's earth pressure coefficients,
γ_s is the weight of the gravel,
$\gamma_{G,unfav}$ is the partial factor for an unfavorable permanent action,
V_k is the characteristic value of vertical load,
G_{wall}, G_{soil} are weights of the wall and soil,
ϕ_d is the design value of angle of internal friction of gravel,
q' the design effective overburden pressure at the level of the foundation base,
N_q, N_γ are dimensionless factors for the bearing capacity,
s_q, s_γ are dimensionless factors for the shape of foundation,
A' is the design effective foundation area.

2.3. The optimization problem

The decision variables in the optimization task are foundation width (B) and wall embedment depth (H2). Two-objectives and three-objective optimizations were performed. In the first case, the wall cost is minimized while the ODF for wall sliding (ODF_{sl}) is maximized. In addition to the above, the ODF for wall bearing capacity (ODF_{bc}) is maximized in the second case. Design space is divided into feasible and infeasible design spaces, setting up four optimization constraints.

The optimization problem can be set up as follows:

Find:	d=[B, H2]
Subject to:	$B \in \{3.0m, 3.1m, \dots, 8.0m\}$ and
	$H2 \in \{0.8m, 0.9m, \dots, 2.5m\}$
	$ODF_{sl} \leq 1.0$
	$ODF_{bc} \leq 1.0$
	$A_{s1} \leq A_{s,max}$
Objective:	Maximizing ODF_{sl} and ODF_{bc}
	Minimizing cost of the retaining wall

The cost of the foundation was estimated using the following equation:

$$Z = Q_e c_e + Q_f c_f + Q_c c_c + Q_r c_r \qquad (9)$$

Where Q_e, Q_f, Q_c and Q_r are quantities of excavation, compacted backfill, concrete and reinforcement, respectively, c_e, c_f, c_c and c_r are the associated unit prices. Unit prices are expressed in Croatian kuna (HRK). They are estimated according to the author's experience.

2.3. NSGA-II algorithm

Multi-objective optimization is performed using the NSGA-II algorithm (Deb, 2001). It is a variant of the genetic algorithm that applies the principle of dominance to the optimization problem. In the algorithm, parents are selected from the parent population and combined by crossover. The mutation operator is applied to the solutions obtained by the crossover operaton. Then, the procedure is repeated until a children population with the same number of elements as the parent population built. The parent population is deleted, and children become new parents (Čupić, 2013). The procedure is carried out until the termination criterion is met. In this paper, the number of generations is selected as the termination criterion. The convergence of the algorithm was checked using a hypervolume indicator (Beume et al., 2007). The NSGA-II algorithm flowchart is shown in **Figure 3**. Optimization was performed using the Python programming language and the Pymoo library (Blank and Deb, 2020).

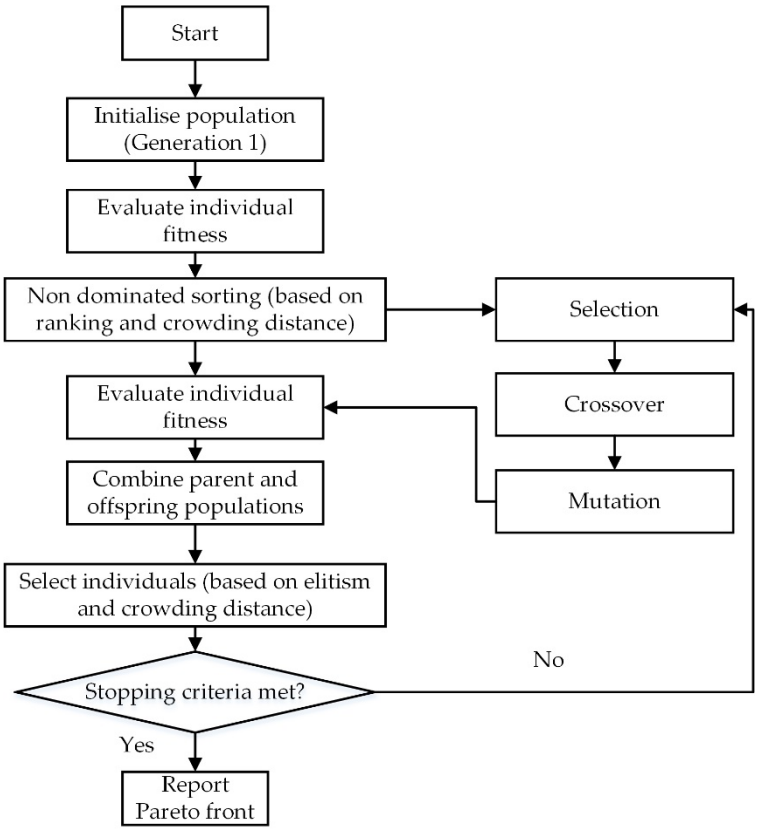

Figure 3. *A flowchart of the NSGA-II algorithm*

3. RESULTS

Figure 4a shows the Pareto front for the case of three-objective optimization, and **Figure 4b** shows its projection on the plane $ODF_{sl} - ODF_{bc}$. Design space comprises 738 designs, of which 290 are in the Pareto front. The ODF_{sl} range is from 1.0 to 2.0, and ODF_{bc} ranges from 1.3 to 3.5. The lowest construction price is 14700, and the highest is 26000 HRK/m'.

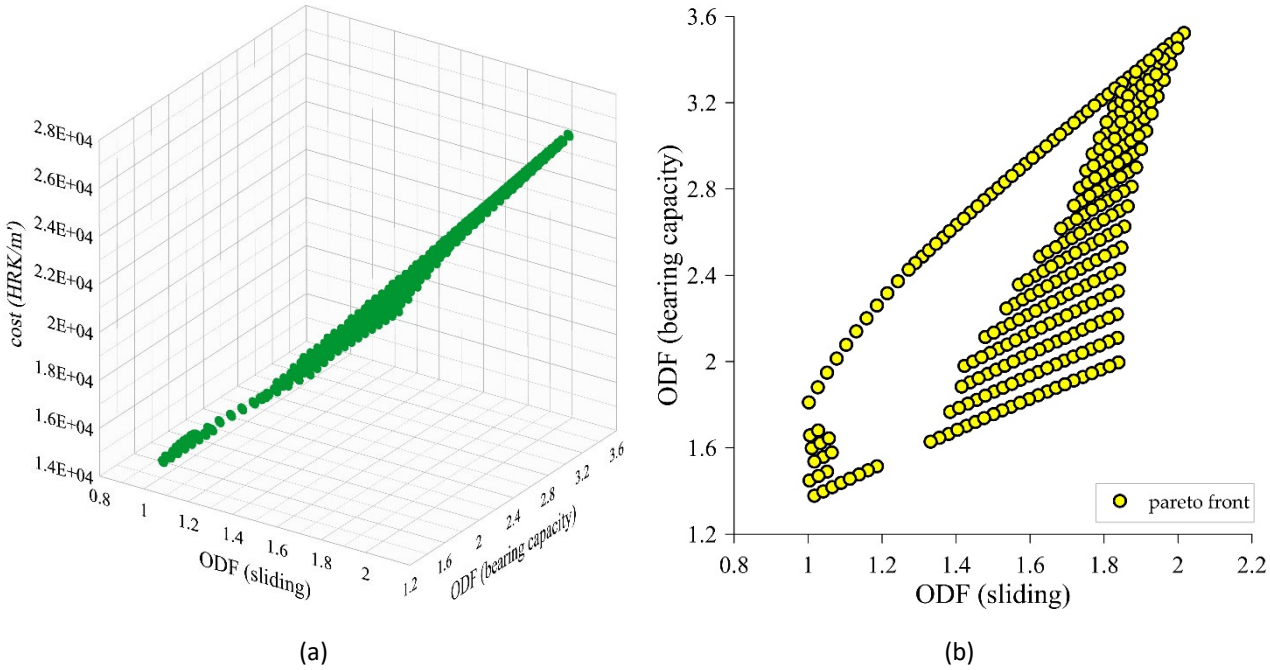

Figure 4. *Pareto front for the case of three-objective optimization (a), projection of the Pareto front on the plane $ODF_{sl} - ODF_{bc}$ (b)*

Figure 5 shows the Pareto front determined by two-objective optimization that comprises 63 non-dominated designs. Out of a total of 738 designs, 26 are infeasible, and 712 are feasible designs. The values of ODF_{sl} and construction costs are the same as in the case of three-objective optimization.

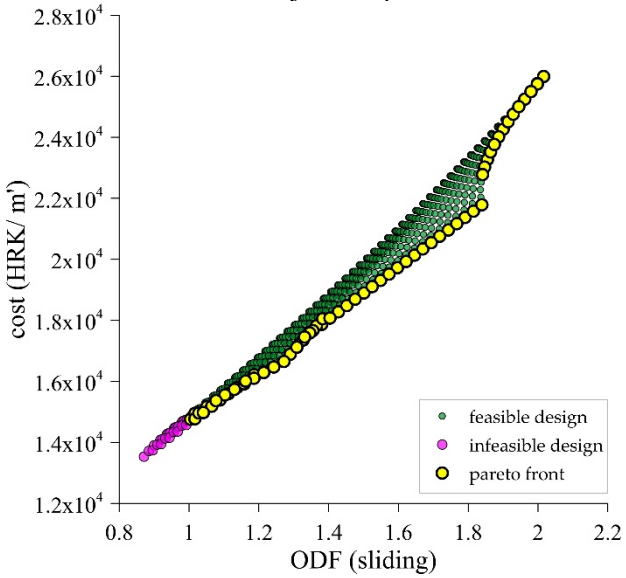

Figure 5. *Pareto front along with feasible and infeasible designs for the case of two-objective optimization*

Figures 6a and 6b shows the non-dominant designs in the decision space, resulting from two-objective and three-objective optimization. For the same number of decision variables, there is a significant difference in the number of non-dominated solutions between the two considered examples.

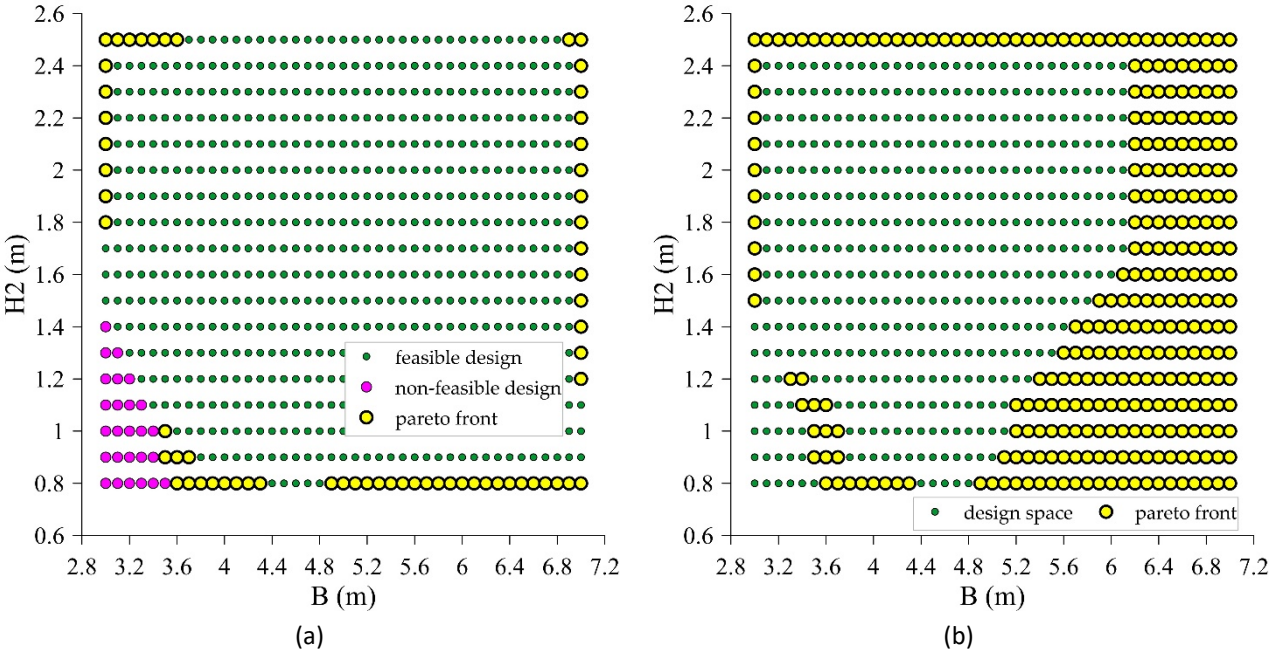

Figure 6. *Pareto front in decision space for the case of two-objective (a) and three-objective (b) optimization.*

Figures 7a and 7b shows the convergence of the NSGA-II algorithm for the two-objective and three-objective optimization cases. In the first case, the algorithm converged after 480, and in the second after 835 generations.

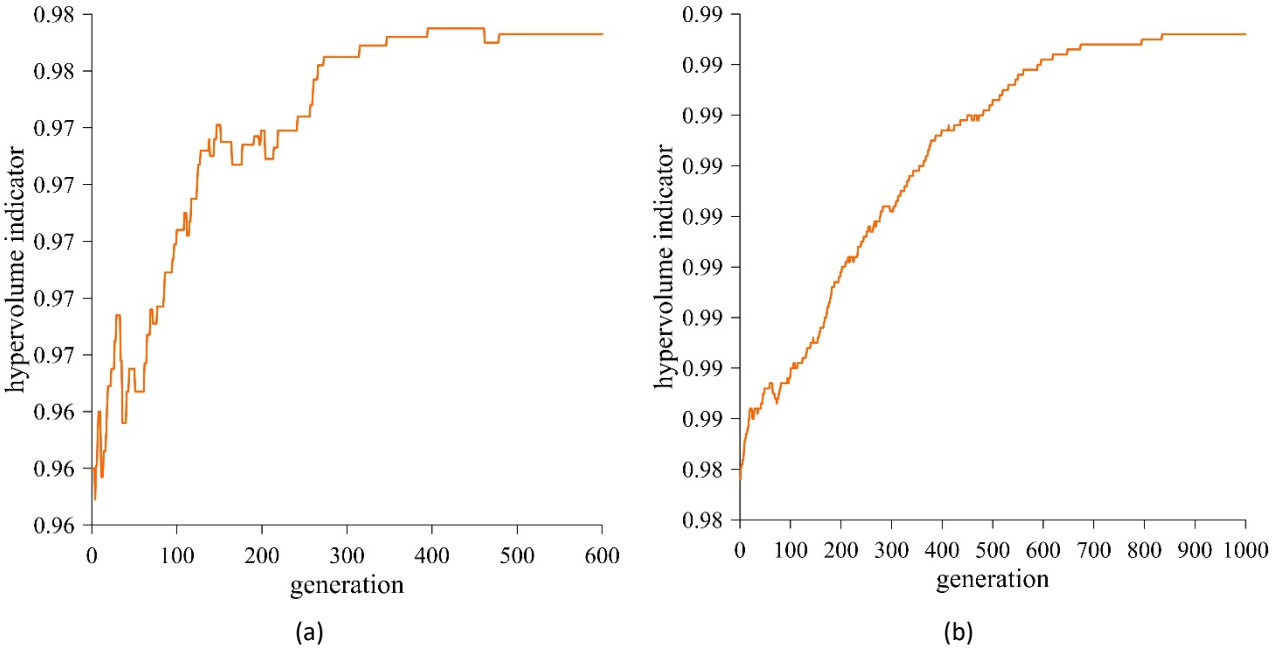

Figure 7. *Convergence of the NSGA-II algorithm for the case of two-objective (a) and three-objective (b) optimization*

4. DISCUSSION AND CONCLUSIONS

The paper investigates the possibility of applying the genetic algorithm NSGA-II to optimize the design of a reinforced concrete retaining wall. The wall is embedded in a saturated silty sand (SM), with the groundwater level at the base of the footing. A drainage layer of well-graded gravel (GW) is installed behind the wall. For a 5.0 m change in ground elevation, the foundation width and embedment depth are optimized. A minimum embedment depth is 80 cm and is determined from the conditions related to the depth of soil freezing. To harmonize the results with Eurocode 7, four constraints are defined in the optimization problem. The goal of optimization is to determine a set of non-dominant designs, i.e., the Pareto front.

Two-objective and three-objective optimizations were performed with the aim of minimizing costs and maximizing overdesign factors for wall verification against sliding and bearing capacity. An additional objective in the three-objective optimization was found to significantly affect the convergence rate of the NSGA-II algorithm. In the case of two-objective optimization, the algorithm converged after 480 and three-objective after 835 generations, as shown in **Figures 7a and 7b**. **Figures 6a and 6b** shows that the Pareto front obtained by performing three-objective optimization consists of Pareto front of two-objective optimization with the addition of the designs that have higher ODF_{bc} values for the same cost. Only 26 of the 738 designs are infeasible, as shown in **Figure 5**. The reasons for that are appropriate assumptions of minimum and maximum values of decision variables. The difference in the number of designs in the Pareto front can be seen in **Figures 6a and 6b**. Two-objective optimization yielded 63 optimal designs, while three-objective optimization yielded 290. The ultimate limit state verification against sliding controls the wall designs in the case of the retaining wall studied in this paper. Because of this reason, objectives related to verifications of other ultimate limit states are excluded from the optimization problem. The optimization procedure and graphical representations of the Pareto front were greatly simplified by reducing the number of objectives.

From the obtained Pareto front, the final design is selected. There are various options for selecting a final design. In the literature, the knee point concept is frequently employed (Gong et al., 2017; Ravichandran and Shrestha, 2020; Zhou et al., 2020). According to this concept, the final design is selected in the knee point Pareto front. It is possible to choose a final solution by reducing the multi-objective optimization problem to a single-objective problem by forming a composite objective function as the weighted sum of the objectives (Deb, 2001).

The implementation of the genetic algorithm NSGA-II allows for the quick and straightforward determination of the Pareto front in the case of retaining wall optimization. Preliminary geotechnical analyses are proposed to reduce the number of objectives and decision variables for defining the optimization problem. In this way, it is possible to simplify optimization, speed up the algorithm's convergence, and facilitate the selection of the final design.

5. REFERENCES

Beume, N., Naujoks, B., & Emmerich, M. (2007). SMS-EMOA: Multiobjective selection based on dominated hypervolume. European Journal of Operational Research, 181(3), 1653–1669. https://doi.org/10.1016/j.ejor.2006.08.008

Blank, J., & Deb, K. (2020). Pymoo: Multi-Objective Optimization in Python. IEEE Access, 8, 89497–89509. https://doi.org/10.1109/ACCESS.2020.2990567

Čupić, M. (2013). Prirodom inspirirani optimizacijski algoritmi. Metaheuristike. Zagreb, Croatia: Faculty of Elecetrical Engineering and Computing Zagreb.

Deb, K. (2001). Multi-Objective Optimization using Evolutionary Algorithms Kalyanmoy. John Wiley & Sons, 16(9), 1689–1699.

Dodigović, F., Ivandić, K., Kovačević, M.-S., & Soldo, B. (2021). Modified, Reliability-Based Robust Geotechnical Design Method, in Accordance with Eurocode 7. Applied Sciences, 11(18), 8423. https://doi.org/10.3390/app11188423

Duncan, J. M. (2000). Factors of Safety and Reliability in Geotechnical Engineering. Journal of Geotechnical and Geoenvironmental Engineering, 126(April), 307–316. https://doi.org/https://doi.org/10.1061/(ASCE)1090-0241(2000)126:4(307)

European Committee for Standardization. (2011). Eurocode: Basis of structural design (EN 1990:2002+A1:2005+A1:2005/AC:2010).

European Committee for Standardization. (2012). Eurocode 7: Geotechnical design -- Part 1: General rules (EN 1997-1:2004+AC:2009).

Frank, R., Bauduin, C., Driscoll, R., Kavvadas, M., Ovesen, N. K., Orr, T., Schuppener, B., & Gulvanessian, H. (2005). Designers' Guide to EN 1997-1 Eurocode 7: Geotechnical Design – General Rules (H. Gulvanessian, Ed.). Thomas Telford Publishing. https://doi.org/10.1680/dgte7.31548

Gong, W., Huang, H., Juang, C. H., & Wang, L. (2017). Simplified-robust geotechnical design of soldier pile–anchor tieback shoring system for deep excavation. Marine Georesources & Geotechnology, 35(2), 157–169. https://doi.org/10.1080/1064119X.2015.1120369

Gong, W., Khoshnevisan, S., & Juang, C. H. (2014). Gradient-based design robustness measure for robust geotechnical design. Canadian Geotechnical Journal, 51(11), 1331–1342. https://doi.org/10.1139/cgj-2013-0428

Islam, M. S., & Rokonuzzaman, M. (2018). Optimized design of foundations: an application of genetic algorithms. Australian Journal of Civil Engineering, 16(1), 46–52. https://doi.org/10.1080/14488353.2018.1445437

Juang, C. H., & Wang, L. (2013). Reliability-based robust geotechnical design of spread foundations using multi-objective genetic algorithm. Computers and Geotechnics, 48, 96–106. https://doi.org/10.1016/j.compgeo.2012.10.003

Juang, C. H., Wang, L., Atamturktur, S., & Luo, Z. (2012). Reliability-based robust and optimal design of shallow foundations in cohesionless soil in the face of uncertainty. Journal of GeoEngineering, 7(3), 75–87. https://doi.org/10.6310/jog.2012.7(3).1

Khoshnevisan, S., Gong, W., Wang, L., & Juang, C. H. (2014a). Robust design in geotechnical engineering – an update. Georisk, 8(4), 217–234. https://doi.org/10.1080/17499518.2014.980274

Khoshnevisan, S., Gong, W., Wang, L., & Juang, C. H. (2014b). Robust design in geotechnical engineering – an update. Georisk: Assessment and Management of Risk for Engineered Systems and Geohazards, 8(4), 217–234. https://doi.org/10.1080/17499518.2014.980274

Khoshnevisan, S., Wang, L., & Juang, C. H. (2016). Simplified procedure for reliability-based robust geotechnical design of drilled shafts in clay using spreadsheet. Georisk: Assessment and Management of Risk for Engineered Systems and Geohazards, 10(2), 121–134. https://doi.org/10.1080/17499518.2016.1146305

Ravichandran, N., & Shrestha, S. (2020). Performance- and cost-based robust design optimization procedure for typical foundations for wind turbine. International Journal of Geotechnical Engineering, 14(4), 395–408. https://doi.org/10.1080/19386362.2018.1428387

Schneider, H. R. (1999). Definition and determination of characteristic soil properties. Fourteenth International Conference on Soil Mechanics and Foundation Engineering. Proceedings, 2271–2274. https://www.issmge.org/uploads/publications/1/31/1997_04_0032.pdf

Shahin, M. A. (2015). Use of evolutionary computing for modelling some complex problems in geotechnical engineering. Geomechanics and Geoengineering, 10(2), 109–125. https://doi.org/10.1080/17486025.2014.921333

Yazdani, H., Hatami, K., & Khosravi, E. (2013). Ant Colony Optimization Method for Design of Piled-Raft Foundations (DFI 2013 Student Paper Competition Winner). DFI Journal - The Journal of the Deep Foundations Institute, 7(2), 17–27. https://doi.org/10.1179/dfi.2013.7.2.002

Zhou, X., Huang, W., Li, J., & Chen, D. (2020). Robust Geotechnical Design for Soil Slopes considering Uncertain Parameters. Mathematical Problems in Engineering, 2020, 1–11. https://doi.org/10.1155/2020/5190580

COMPOSTING OF FINE FRACTION AFTER MECHANICAL-BIOLOGICAL TREATMENT OF MUNICIPAL SOLID WASTE

Aleksandra Anić Vučinić [1*], Valentina Tuk [2], Snježana Šimunić [3], Ivana Presečki [1]
[1] *Faculty of Geotechnical Engineering, University of Zagreb, Hallerova aleja 7, 42000 Varaždin, Croatia*
[2] *Hrvatske vode, Međimurska ulica 26b, 42000 Varaždin, Croatia*
[3] *Ministry of economy and sustainable development, Radnička cesta 80, 10000 Zagreb, Croatia*
*E-mail of corresponding author: aav@gfv.hr

Abstract: *One of most common types of municipal solid waste treatment is mechanical-biological treatment (MBT), which in practice has many variations depending on the method of conducting the technological process and it is possible to get different output fractions. In this paper is analysed waste generated after the MBT with biodrying, where waste after mechanical treatment undergoes process of biodrying, and then is RDF (recovery derived fuel) separated. Fine fraction remains with a high content of organic matter that without additional processing cannot be disposed of on a landfill.*
The aim of this research was to determine the possibility of fine fraction composting in different conditions – in the open, in the open and covered area, and indoors. In each area are formed three compost piles: 100% fine fraction (KH1, KH4, and KH7), 70% fine fraction and 30% wood chips (KH2, KH5, and KH8), 50% fine fraction and 50% wood chips (KH3, KH6, and KH9). Moisture content, temperature and dissolved organic carbon (DOC) were monitored.
Results show that after 13 weeks samples KH1, KH4, and KH7 (100% content of fine fractions) did not achieve DOC value less than 3 000 mg/l. The most effective composting in terms of reducing the DOC is achieved in samples KH3, KH6, KH9.
Based on results obtained, it can be concluded that by adding wood chips in fine fraction in ratio 50:50, the most effective and fastest reduction of organic matter is achieved in the analysed samples.
Keywords: *composting, mechanical – biological treatment (MBT), fine fraction, dissolved organic carbon (DOC)*

Received:18.08.2021. /Accepted: 27.10.2021.
Published online: 01.12.2021.

Professional paper
https://doi.org/10.37023/ee.8.1-2.9

1. INTRODUCTION

Developed countries pay great attention to the waste disposal and management. The European Union requires that municipal solid waste should be processed prior of its disposal on sanitary landfills (Law on Waste Management OG 84/21). This processing is defined by physical, chemical, thermal or biological processes, including sorting, that changes the characteristics of waste in the form of reduction of its volume and its hazardous components, thus facilitating its processing (Williams, 2005).

Several countries across Europe, including Germany, Austria, Netherlands, Belgium, etc., use mechanical-biological waste treatment (MBT) as technology to treat municipal solid waste. The aim of mechanical – biological treatment of municipal solid waste is to minimise environmental impact of the disposal, to ensure separation of recyclable materials, to reduce emissions, to reduce the amount of leachate and to reduce the volume of the landfill (Soyez & Plickert, 2002; Williams, 2005). The biological treatment in MBT refers to the microbial degradation of the organic portion of biodegradable fraction of waste that can be held with the presence of oxygen (composting) or without the presence of oxygen (anaerobic digestion), while mechanical treatment includes shredding and sorting of materials in order to separate recyclables (Williams, 2005).

One of most common types of municipal solid waste treatment is mechanical-biological treatment (MBT), which in practice has many variations depending on the method of conducting the technological process and it is possible to get different output fractions. In this paper is analysed waste generated after the MBT with biodrying, where waste after mechanical treatment undergoes process of biodrying, and RDF (refuse derived fuel) is separated. Fine fraction remains with a high content of organic matter that without additional processing cannot be disposed of on a landfill.

The aim of this research was to determine the possibility of fine fraction composting remained after biodrying in different conditions – in the open, in the open and covered area, and indoors, mixed with wood chips and without wood chips.

2. COMPOSTING

The technological process of aerobic composting is complex biological – chemical process where feedstock decomposes through the action of microorganisms, mainly bacteria and fungi (Miller, 1996) during which carbon dioxide, water and heat are generated (Diaz et al., 2002; Williams, 2005; Danon et al., 2008). Microorganisms that decompose organic matter in composting process originate from the environment. They are present in composting substrates, but also in water, air, soil and in processing equipment used during the entire process. These different sources ensure presence of different groups of microorganisms which helps to maintain activity of microbial population during composting despite chemical and physical changes in material characteristics, e.g., changes in pH values, temperatures, moisture and organic content.

Continuous composting process can be viewed as a sequence of four phases, where each has different physical, chemical, and biological characteristics (Insam & de Bertoldi, 2007). Mesophilic phase is characterized by a temperature range of 25°C to 45°C. Bacteria, actinomycetes and fungi during this phase decompose easy degradable molecules e.g., sugars and proteins. Due to their biochemical activity temperature increases inside composting pile, while their activity decreases with temperature increase. From 45 °C to 65°C during thermophile phase mesophilic microorganisms are replaces by thermophile microorganisms. This phase is important due to sanitation, respectively hygienisation of raw compost. Most of pathogenic microorganisms and weed seeds and insect eggs are removes at high temperatures, and to sanitation comes also due to actinomycetes that are used for antibiotics. Temperature starts to decrease after biodegradable substrate is exhausted in thermophile phase and cooling phase or second mesophilic phase follows. Mesophilic microorganisms are activated from remained spores and in this phase the number of microorganisms that break down cellulose and starch increases, unlike the initial mesophilic phase. In maturity phase comes to a complete change of microbial communities; number of fungi increases while number of bacteria decreases. During maturity phase are formed and dominate substances which are not degradable such as complex lignin-humus compounds. Evolution of temperatures is indicator of microbial activity during composting and this parameter can be used as a good indicator for end of bio-oxidative phase (Iglesias Jiménez & Pérez Garcia, 1991).

The primary factors that affect the optimal environment of microbial composting process, respectively period of time and the course of the process, are: oxygenation (aeration), temperature, moisture, C: N ratio, pH value in composting pile and state of the original material (de Bertoldi et al., 1983). The optimal pH value in compost is in range between 5,5 and 8. Concentrations of organic acids increase during the initial phase of composting due to activity of bacteria which decompose organic matter and produce organic acids. In successful composting and maturation of compost, pH values rise to 8-9 (Sundberg et al.,2004). Since the composting is biological oxidation, the availability of oxygen is very important to microorganisms. Function of aeration of compost piles includes the supply of oxygen so that it does not become a limiting factor, and this is done by mechanical turning of the piles ("windrow" systems) or by inserting perforated pipes in a compost pile that remains intact (i.e. forced aeration) (Williams, 2005).

Continued forced ventilation gives satisfactory results and enables better control over temperature and moisture of compost pile. For successful aerobic composting oxygen content should not fall below 18% (de Bertoldi et al., 1983). Moisture content and aeration are closely related, and the optimal amount of moisture in the compost pile depends on the physical condition and particle size.

Biodegradation of small-sized substrates occurs with greater speed because of larger total area available to microorganisms. If the particles are too fine, due to finer space between them, flow and diffusion of air are hindered and anaerobic conditions can occur. If the particles are too large, process is slowed down (de Bertoldi et al., 1983). Waste material used in composting needs to be shredded if particle size is too large. Dusty materials are mixed with other, larger materials or inert materials are added to ensure ventilation of compost pile and reduction of moisture (Silva & Naik, 2006).

3. METHODOLOGY

The sample on which the research was conducted is a fine fraction remained after biodrying process and RDF separation from the MBT plant. The size particles were smaller than +25 mm.

Analysis was conducted on nine composting piles of different composition which depended on content of subsequently added wood chips. Piles were located on three locations, in outdoor uncovered area, outdoor covered area and indoors. Temperature and moisture were measured, and laboratory measurements of dissolved organic carbon were conducted (DOC) in compost piles.

The research included daily monitoring of air temperature, precipitation, temperature, and moisture of compost piles, while on weekly basis was performed additional moistening and loosening or turning the compost piles. Compost piles were placed on three different locations and their initial characteristics (initial mass, height, and moisture content) are shown in Table 1.

Table 1. Measurements results of compost piles (KH) before composting process

Location	Outdoor uncovered area			Outdoor covered area			Indoors		
	KH 1	KH 2	KH 3	KH 4	KH 5	KH 6	KH 7	KH 8	KH 9
Process setting date	8/27/15	8/27/15	8/27/15	8/27/15	8/27/15	8/27/15	8/27/15	8/27/15	8/27/15
Initial mass, kg	5,280	5,048	5,560	6,336	7,352	6,950	5,280	5,718	5,838
Height, m	1	1.1	1.5	1	1.2	1.2	1.5	1.6	1.6
Moisture content, %	61.5	67.7	67.5	59.3	53	61.7	59.3	57.6	56.6

Samples were taken on the beginning of the experiment from compost piles and were analysed according to Croatian regulations (Ordinance on the methods and conditions for the landfill of waste, categories and operational requirements for waste landfills, OG 114/2015).

First laboratory analysis has shown that fine fraction meets all the requirements, except that contains excessive concentration of dissolved organic carbon (DOC) and because of this, it was decided that waste is not suitable for disposal on sanitary landfill. According to the prior mentioned Ordinance, concentration of dissolved organic carbon cannot exceed 3.000 mg kg^{-1}.

On weekly basis samples were collected and analysed to determine changes in DOC concentration. Compost piles on outdoor uncovered area (KH 1, KH 2, KH 3) were under the atmospheric influence which had great impact on the temperature and moisture inside the composting system. Into account were taken precipitations because research was conducted in autumn and compost piles did not have to be often humidified. The rain was falling 21 days out of total 78 days. On this location were analysed three substrates of different composition (Table 2). Fine fraction of biodegradable non-hazardous organic waste was mixed with composted wooden chops in different ratios, which affected the composting process. All compost piles were turned 14 times for aeration and that process took app. 25 minutes. Temperature of KH 1 was in range 20 – 65 °C, and of KH 2 and KH 3 in range of 10 – 60 °C.

In outdoor covered area were analysed three compost piles (KH 4, KH 5, KH 6) of different composition in which fine fraction of biodegradable waste was mixed with composted wooden chops in different ratios. This compost piles were turned 12 timed for aeration. Temperature of KH 4 was in range 20 – 65 °C, of KH 5 in range 10 – 60°C and of KH 6 in range 20 – 70 °C.

Three substrates (KH 7, KH 8, KH 9) of different composition were placed indoors and for 14 weeks were turned 12 times for aeration. Temperature of pile KH 7 was in range 20 – 70 °C, and of piles KH 8 and KH 9 in range 30 – 70 °C.

4. RESULTS AND DISCUSSION

From total of three compost piles, containing 100% fraction of biodegradable substrate, two compost piles have not been satisfactory for further disposal on the landfill. The compost pile KH 1 was under the atmospheric influence because it was in the open uncovered area, and it is the only compost pile that managed to lose enough DOC in 14 weeks so it could be disposed on the landfill. The compost piles, KH 4 and KH 7 at the end of the research did not have a sufficiently low concentration of DOC for disposal on the landfill. All compost piles to which were added composted wood chips in different ratios (70:30 and 50:50), regardless of location, have shown satisfactory results, as presented in Table 2. Wood chips were added to stabilize the compost material. In case that particles within the compost pile have weakened structural strength, they deform under pressure, thus reducing the volume of the air within the system. On the other hand, compost piles which contain substrate with a strong structural strength, whose individual particles will consolidate under pressure (such as wood chips, various shells, straw and hay), are more stable and less prone to deformation. If the compost material "collapsed", anaerobic conditions could occur during which composting process can slow down. Fruit waste, sludge and fertilizer are weak or have no structural strength. In that case, it is necessary to add other material which could improve the structural strength of composting material (Silva & Naik, 2006). Any material that has a greater structural connection could be added to compost pile, whether raw or previously processed. Mass and volume of the compost pile have decreased due to the disintegration of the structure of organic materials and mineralization of organic matter during which a formation of CO2 and H20 was occurred (Breitenbeck & Schellinger, 2004). In Table 3 are

shown results of measurements after the end of composting process for all substrates, of which KH 4, KH 5, KH 6, KH 7, KH 8 and KH 9 have lost the weight. The compost piles of KH 1, KH 2 and KH 3 have greater weight than they had at the beginning of the experiment because they were exposed to atmospheric influence during the entire research.

Table 2. Measured concentrations of dissolved organic carbon (DOC)

Composition material	Date / Parameter	27.08.15.	09.09.15	25.09.15.	07.10.15.	22.10.15	05.11.15	19.11.15	Trend
KH 1	100% fine fraction	DOC, mgkg-1	16,709	15,368	16,469	11,791	13,118	6,770	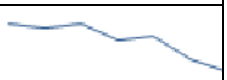
KH 2	70% fine fraction: 30% wood chips	DOC, mgkg-1	14,815	9,774	13,326	7,340	11,484	2,999	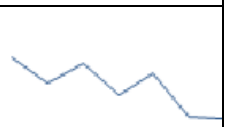
KH 3	50% fine fraction: 50% wood chips	DOC, mgkg-1	7,862	9,809	16,624	10,311	6,002	2,637	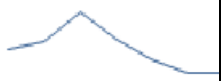
KH 4	100% fine fraction	DOC, mgkg-1	16,709	20,396	22,307	23,558	14,559	12,905	
KH 5	70% fine fraction: 30% wood chips	DOC, mgkg-1	14,815	11,815	16,341	15,447	10,048	3,587	
KH 6	50% fine fraction: 50% wood chips	DOC, mgkg-1	7,862	7,317	12,237	9,068	5,917	2,650	
KH 7	100% fine fraction	DOC, mgkg-1	16,709	19,635	26,911	24,196	19,664	10,076	
KH 8	70% fine fraction: 30% wood chips	DOC, mgkg-1	14,815	12,857	14,431	8,154	7,522	3,416	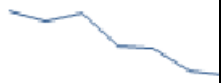
KH 9	50% fine fraction: 50% wood chips	DOC, mgkg-1	7,862	7,304	13,343	12,317	6,025	3,046	

Table 3. The measurement results after the end of composting process for all compost piles (KH)

	Open uncovered area			Open covered area			Indoors		
	KH 1	KH 2	KH 3	KH 4	KH 5	KH 6	KH 7	KH 8	KH9
Ending date	11/19/15	11/19/15	11/19/15	11/19/15	11/19/15	11/19/15	11/19/15	11/19/15	11/19/15
Mass at the end of composting process, kg	5,500	5,440	6,140	5,360	6,020	5,900	4,160	4,960	5,440
Height of compost pile, m	1.28	1.28	1.28	1.20	1.28	1.28	1.28	1.28	1.28
Moisture content, %	40.30	41.07	43.26	36.51	32.07	37.03	40.91	37.53	39.82

The moisture content is very important variable in the composting process for bacteria because they absorb the necessary nutrients which can be dissolved in water. Too high moisture content can squeeze the air out of pore space from compost pile and lead to anaerobic conditions that do not favour composting. Too low moisture content can lead to the termination of microbial activity, regarding their deaths (Silva & Naik, 2006).

Some research shows that total duration of organic matter of municipal solid waste (MSW) bio stabilization ranged from 42 to 135 days, including the intensive phase carried out in closed reactors for 18 to 84 days, and the phase of saturation in windrows, which lasted for 13 to 63 days (Jedrezak&Suchowska-Kisielewicz 2018) what this research confirmed for heavy fraction of MSW after MBT treatment.

5. CONCLUSION

This research was conducted to determine possibilities of processing the fine fraction of biodegradable substrate of non-hazardous organic waste that should be suitable for landfill disposal. In this research, "windrow" composting method was used, which main characteristic is that the raw material is accumulated in compost piles that occupy a lot of space, so it is necessary to loosen it. Satisfactory supply of aeration is necessary for almost all composting system. Starting aeration process in 'windrow' compost method is achieved with the processing and stacking of raw waste. Composting was conducted on three different locations with different ratios of wooden chips. Fourteen weeks were determined for composting process and in that time in almost all compost piles (except compost piles KH 4 and KH 7) value of DOC has been decreased and the requirement for disposal on the landfill was met. As the best location for composting has proven to be an open area for all compositions since all analysis results of compost piles have met the limit values of the effluent parameters of the waste defined with the Ordinance (OG 114/15).

6. REFERENCES

Bertoldi, M. de, Vallini, G. & Pera, A. (1983) The Biology of Composting: A review. Waste managment & research, 1, 157-176.

Breitenbeck G. A., & Schellinger D. (2004) Calculating the Reduction in Material Mass And Volume during Composting. Compost Science & Utilization, 12:4, 365-371.

Danon, M., Franke-Whittle, I. H., Insam, H., Chen, Y. & Hadar, Y. (2008) Molecular analysis of bacterial community succession during prolonged compost curing. FEMS Microbiol Ecol, 65, 133-144, Blackwell Publishing Ltd.

Diaz, L.F., Savage, G.M. & Golueke, C. G. (2002) Chapter Twelve, Composting of Municipal Solid Wastes. In: Handbook of Solid Waste Management, Second Edition (eds.: Tchobanoglobus, G. & Kreith, F.), 12.1-12.70, McGraw-Hill Companies, Inc., New York.

Iglesias Jiménez, E. & Pérez Garcia, V. (1991) Composting of domestic refuse and sewage sludge. I. Evolution of temperature, pH, C/N ratio and cation-exchange capacity. Resources, Conservation and Recycling, 6, 45-60, Elsevier Science Publishers B. V./Pergamon Press Plc.

Insam, H. & Bertoldi, M. de (2007) Microbiology of the Composting Process. In: Compost science and technology, Waste Managment Series, V 8 (eds.: Diaz, L.F., Bertoldi, M. de, Bidlingmaier, W. & Stentiford, E.), 26-45, Elsevier Ltd.

Jadrezak, A. &Suchowska-Kisielewicz, M. (2018) A Comparison of Waste Stability Indices for Mechanical-Biological Waste Treatment and Composting Plants. Internationa Journal of Environmental Research and Public Health, 1-13, MDPI.

Miller, F. C. (1996) Composting of Municipal Solid Waste and its Compopnents. In: Microbiology of Solid Waste (eds.: Palmisano, A. C. & Barlaz, M. A.), 115-154, CRC Press Inc.

Ordinance on the methods and conditions for the landfill of waste, categories and operational requirements for waste landfills, OG 114/2015

Silva M. R. Q. & Naik T. R. (2006): Overview of Composting – Fundamentals and Processes (https://www4.uwm.edu/cbu/Papers/2006%20CBU%20Reports/REP-613.pdf (accessed April 13, 2016)

Soyez, K. & Plickert, S. (2002) Mechanical-Biological Pre-Treatment of Waste: State of the Art and Potentials of Biotechnology. Acta Biotechnol, 22, 3-4, 271-284.

Sundberg, C., Smårs S. & Jönsson H. (2004) Low pH as an inhibiting factor in the transition from mesophilic to thermophilic phase in composting. Bioresource Technology, 95, 145-150, Elsevier Ltd.

Williams, P.T. (2005) Waste Treatment and Disposal, Second edition. I-IX, 1-375, John Wiley & Sons Ltd, Chichester.

The Law on Sustainable Waste Management (Offical Gazette NN 94/13)

URBAN SPACE CHANGE AND FUTURE PREDICTION OF KANPUR NAGAR, UTTAR PRADESH USING EO DATA

Shubham Sharma [1], Suraj Kumar Singh [2], Shruti Kanga [1], Nikola Kranjčić [3*], Bojan Đurin [4]
[1] *Centre for Climate Change and Water Research, Suresh Gyan Vihar University, Jaipur 302017, India*
[2] *Centre for Sustainable Development, Suresh Gyan Vihar University, Jaipur 302017, India*
[3] *Faculty of Geotechnical Engineering, University of Zagreb, 42000 Varaždin, Croatia*
[4] *Department of Civil Engineering, University North, 42000 Varaždin, Croatia*
*E-mail of corresponding author: nikola.kranjcic@gfv.unizg.hr

Abstract: *Urban Land use changes, measurements, and the analysis of rate trends of growth would help in resources management and planning, etc. In this study, we analyze the urban change dynamics using a support vector machine model. This method derives the urban and rural land-use change and various components, such as population growth, built-up areas, and other utilities. Urban growth increases rapidly due to exponential growth of population, industrial growth, etc. The population growth also affects the availability of various purposes in its spatial distribution. In this present study, we carried out using multi-temporal satellite remote sensing data Landsat MSS (Multispectral scanner), ETM+ (Enhanced thematic mapper), OLI (Operational land imager) for the analysis of urban change dynamics between years 1980-1990, 1990-2003, 2012-2020 in Kanpur Nagar city in the state of Uttar Pradesh in India. In our study, we used SVM (Support Vector Machine) Model to analyze the urban change dynamics. A support vector machine classification technique was applied to generate the LULC maps using Landsat images of the years 1980, 1990, 2003, and 2020. Envi and ArcGIS software had used to identify the land cover changes and the applying urban simulation model (CA- Markov model) in Idrisi selva edition 17.0 software. The LULC maps of 2003 and 2020 were used to simulate the LULC projected map for 2050 using (Cellular automata) CA- Markov based simulation model.*
Keywords: *Urban growth, Support vector machine, Change detection, Urban simulation model, and CA- Markov model.*

Received:02.09.2021. / Accepted: 03.11.2021.
Published online: 01.12.2021.

Professional paper
https://doi.org/10.37023/ee.8.1-2.10

1. INTRODUCTION

According to Clark (1982), urban growth is a demographic and spatial process which refers to the increased importance of town and cities with dense population within a specific type of economy and society. Urban land covers about 2% or 3% of the earth's land surface (Poelmans and van Rompaey 2010). Therefore, the relevant information by urban planners and scholars to evaluate the intensity and future direction of urban expansion is essential. Hence to monitor, analyze and identify urban expansion initially, satellite images are used.

India, a highly developing country, and a country with high developing nature the people migrate from rural to urban on a large scale, and hence the urban growth is very high. The era of 1970s and 1950, when industrial revolution and globalization respectively were at a boom and had provided India momentum for urbanization. Due to rapidly growing urbanization in India especially in 'megacities' the lifestyle of normal human beings has been improved. But because of rapidly growing urbanization, it has created many problems which include ecological unbalance, loss of agricultural land, pollution, increase in temperature, etc. These types of problems can be solved by requiring information at various levels, such as population growth patterns, local housing patterns, etc. However, these solutions can only be analysed by the proper channel between new technologies and in-situ observations. All the traditional methods can help us in gathering demographic data, census data, and other required information for mapping urban growth. But these methods and techniques may not be relevant for modern urban management.

The population growth, migration, and development of basic infrastructures caused by urbanization and such growth led to the development of hamlet into villages, villages into towns, towns into cities, and cities into megacities. Identification of urban growth knowledge of extent and pattern of growth is required to make development with well-planned infrastructure. All these development techniques require the use of geospatial spatial techniques such as Remote Sensing, Geographic Information systems (GIS), and Global Positioning Systems (GPS). To detect the change in the recent decades remote sensing data are being used in a large amount. With the help of satellite images, we can view the large area at a specific period this cannot be done by any other conventional method. Remote Sensing and Geographic Information System (GIS) were used in mapping urban change dynamics to detect the changes that had taken place during a time. Remote sensing is the science of obtaining information about objects or phenomena without making physical contact with them.

In this research, the aim to analyse the urban change dynamics using a support vector machine classifier. Support Vector Machine classifiers are being used for analysing the urban change dynamics. One of the Machine Learning techniques that are being used by many researchers in the geospatial analysis is known as a Support Vector Machine which works on statistical learning theory data and formalizing these data.

Machine Learning is a type of learning in which a system is programmed in such a way that it learns and improves automatically by gaining experience. Learning refers to understating and recognizing the supplied data and making a wise decision based on the data provided. There are different types of algorithms used in machine learning to handle various types of problems such as deciding on various types of input provided. By using statistics, probability theory, logic, combinatorial optimization, search, reinforcement learning, and control theory algorithms take the specific data and analysis experience to build knowledge.

Machine learning can be used in many places and can appear in day-to-day life. Machine learning is an art of learning in which a group of data is supplied and based on some algorithm a fairly set of prototypes are provided to us. Support vector machines are a great example of machine learning which works on analysing data and recognizing patterns.

2. STUDY AREA

2.1. Location and size

Kanpur Nagar is located on the Ganga and Yamuna doab track. It is situated on the Ganga's bank. It is located between the latitudes of 25° 26'and 26°58'north, and the longitude of 79° 31'and 80° 34' east. It is bounded in the north by the districts of kanuuaj and Hardoi, in the east by the district of Unnao, in the south by the district of Fatehpur and Hamirpur, and in the west by the district of Kanpur dehat. It is divided from district Unnao in the east by the holy Ganga River, which serves as a natural barrier. It is separated from the districts Kanpur dehat and Fatehpur in the west and south, respectively, by the Pandu River.

2.2. Demography

According to census 2011 Kanpur had a population of 4,581,268 in 2011 with 2,459,809 males and 2,121,462 females. Kanpur Nagar had a population of 4,167,999 in the 2001 census with 2,247,216 males and 1,920,783 females. When compared to the population in 2001, there was a 9.92 percent change. In comparison to the population in 2001, there was a 9.92 percent increase in the population. According to the previous census of India 2001, Kanpur Nagar's population recorded increased by 28.11 percent compared to 1991.

2.3. Physiography

The district of Kanpur Nagar is in the middle Ganga plain- west, which covers an area of 1,065 sq. km. The Ganga's course is a wide and sandy bed that changes on occasion. A belt is formed by new alluvium deposits, in addition to sand. Alluvium deposits are mostly found above flood level and are referred to as 'kachhar'. Many ravines are formed by the high cliffs that run along the Ganga. The Pandu and Rind rivers both flow through the district. Geologically, the district is made up of alluvium and recent Dun gravels. The district has been divided into some sub-micro-regions based on geology, soils, topography, climate, and natural vegetation (likes- Ganga khaddar, Kanpur plain, Rind plain).

2.4. Drainage

The two major rivers of the district are Ganga and the Yamuna. The Isan and Non are Ganga tributaries, and the Rind is the major Yamuna tributary. Pandu is the next significant river.

The Ganga enters the village of Chita Mau and flows along the district's northeast boundary for its entire length, skirting the tehsils of Bilhaur and Kanpur. It has a broad and sandy belt that changes its channel almost as its sandbanks form and is washed away. When it rains, the Ganga has a huge width, but when it gets cold, it shrinks to much smaller dimensions. The river leaves the district at village Purwa Mir in Kanpur tehsil.

Yamuna River separates the district from Hamirpur in the south and flows for almost 58 kilometers from Kanpur in the north.

2.5. Climate

The district's climate is characterized by a hot summer and general dryness, except during the monsoon season. The summer season lasts from March to about the middle of June, followed by the monsoon season until the end of September, October, and the first half of November. The cold season lasts from about the middle of November

to the beginning of February. This climate is classified as Cwa, according to Koppen and Geiger. Kanpur has an average annual temperature of 25.3°C/ 77.5°F.

2.6. Flora and fauna in Kanpur

In Kanpur, you can expect to see a lot of migratory birds. These birds are regularly seen in the locations around Bithoor, the Ganges canal, and the IIT campus. In the various parts of the city, peacocks and nilgais can be observed in great numbers. Wolves, chikaras, black bull, hyena, fox, and jackals are among the important wild creatures that can be found in the area. The district, which was once rich in vegetation, is now devoid of it. Flora in the district is limited to patches of Dhak, Babul, Siras, and Termind (Imli). **Figure 1** presents location of study area.

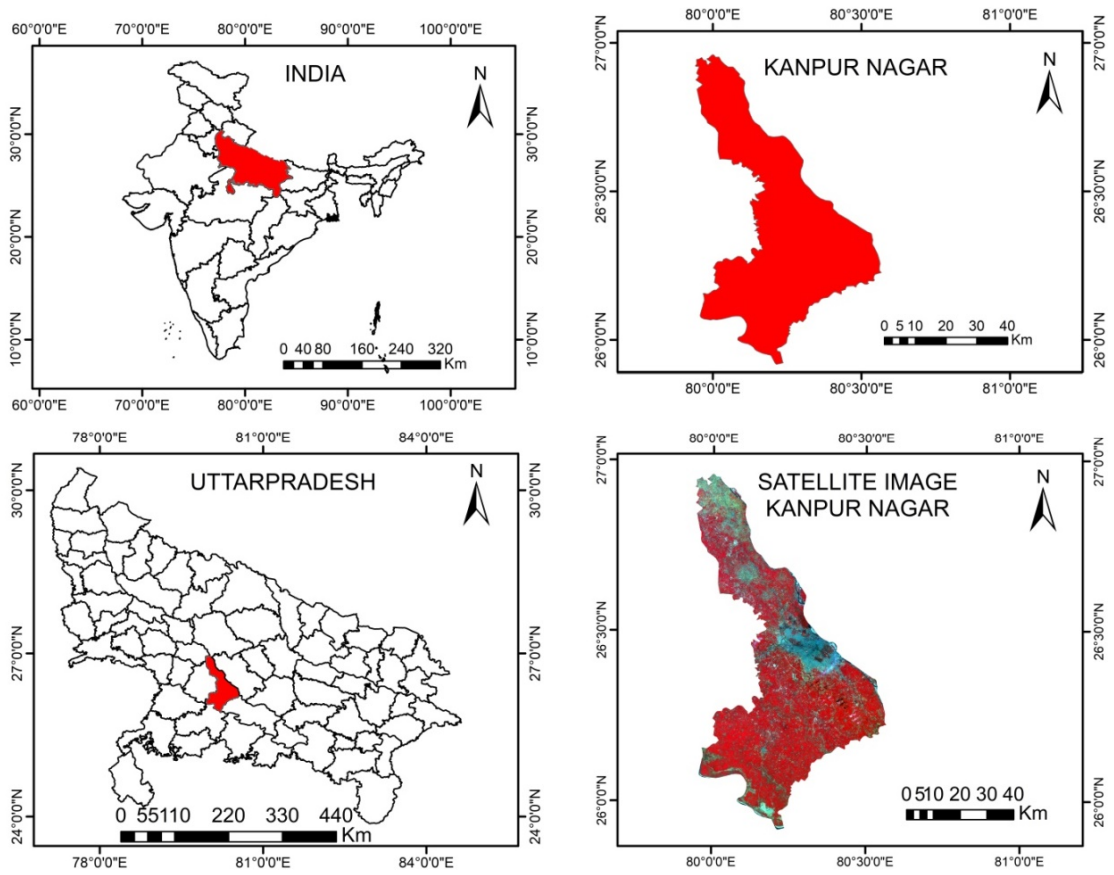

Figure 1. *Location map of study area*

3. DATA USED AND METHODOLOGY

3.1. Software used

The task of image correction, pre-processing, and support vector machine classification are done in ENVI 5.3 software. urban changes and using urban simulation model are performed by IDRISI Selva 17. The preparation of various data layer maps is carried out in ArcGIS 10.6. For Ground Validation: Google Earth

3.2. Data used

3.2.1. Raster data

The satellite images are the main sources of data that are used for urban change dynamics. The remote sensed data used in the study area. The images were cloud-free with excellent quality.

In this study, we use Landsat satellite datasets. The Landsat data are the main sources for monitoring and extracting information about urban change dynamics. Landsat datasets are used for modelling urban change dynamics with the help of a support vector machine classifier. With the help of these datasets, spatiotemporal maps are prepared. The Landsat program is series of Earth-observing satellite missions are combined managed by NASA and the U.S Geological survey. On 23 July 1972 the Earth Resources Technology (ERTS-1) Satellite was launched,

later named was Landsat-1. On March 5, 1978, Landsat 3 MSS was launched. Landsat 7 was launched in 1999 and Landsat 8 was launched on February 11,2013.

The data for the four time periods (1980, 1990, 2003, and 2020) are made availed by the website USGS Earth Explorer.

3.2.2. Vector data and pre-processing

The state and district boundaries of Uttar Pradesh and Kanpur city are provided by Data meet open sources. The cardinal step toward the use of remote sensing data for the preparation of the GIS database is to geometrically correct the maps and satellite image data sets. This process has been formed a very important step in the data preparation because formation- temporal datasets and maps of master plans. Pre-processing operations are referred to as image restoration and rectification purposes to correct radiometric and geometric distortions of the data. the research was carried out using Landsat imageries to identify changes in LULC in Landscape changes over 40 periods of 1980 to 2020 years. To observe and discriminate surface features, all the input satellite images were composed using the RGB color composition. The images provided comprehensive coverage of the area of study and layer stacking of bands, mosaicking, and extraction of the image had done using ENVI 5.3 software. The satellite image covers a large area. However, in practice, most of the area in the satellite image is not required for the research, so we extract the study area in satellite images. This step is carried out in ArcGIS 10.6 software. In this study we put the shapefile of Kanpur Nagar boundary overlay on the satellite image then we extract the study area. The primary aim of image enhancement is not to maintain image fidelity. It turns out that image enhancement is used to improve the visual interpretation of images, with the main goals being to improve image definition and contrast, as well as to emphasize the necessary information in the image.

3.2.3. Classification and support vector machine

The land use and land cover categorization developed in the classification system presented in this report can be related to a system for classifying land capability, vulnerability to certain management techniques, and potential for any activity or land value, either intrinsic or speculative (Anderson et al., 1976). The method of assigning land cover classes to pixels is known as image classification. For example, classes include urban, forest, water, agriculture, etc. The supervised classification method was used in this thesis. during the supervised classification process, we assign the training sets of the areas and give classes name such as agriculture, vegetation, settlement, and so on.

The Urban dynamics were performed using the Support Vector Machine (SVM). The SVM method was familiarized inside the Context of the Statistical Learning Theory evolved utilizing (Cauwenberghs and Poggio 2001). A Support Vector Machine is a supervised non-parametric statistical learning technique that becomes formerly designed for binary classification (Mathur and Foody, 2008). Support Vector Machine is a very useful method for the classification of remotely sensed data.

SVMs have regularly been found to offer higher classification results than other broadly used sample popularity techniques, including the maximum likelihood and neural network classifiers (Melgani and Bruzzone 2004, Theodoridis and Koutroumbas 2003). The Support Vector Machine is a classifier that detects a hyperplane or a function that divide into two classes with a maximum distance (margin).

3.2.4. Accuracy assessment

The easiest way to know the classification result is to check everything in each class, which ENVI could do with the accuracy assessment function. To ensure that the random points were disputed exactly from each class, exactly equal random was used for parameter distribution, and the number of random samples set. A class code in the reference column was assigned to each point on the images, the class value was then displayed to check for agreement. The data was tabulated, and the error matrix was used to describe the finding.

3.2.5. Factors driving the urban growth and analysis of the future urbanization areas

The land-use issue is influenced by several geographical factors such as accessibility, proximity, and the physical nature of the land as it exists. The model is based on land parameters within the domains of planning areas delineated by the town and country planning department, with all variables defined within these domains. The urban growth models have some key factors like' road structure (major, minor), railways, airports, built-up, etc. for this key factor we prepared the Distance maps to each factor in the study area. Analysis of the future urbanization areas can be performed based on the two time-period land cover maps for the earlier and later years and feeding them into the Markov chain process. A pair of land cover images are analyzed by the Markov chain method, which produces a transition probability matrix, a transition areas matrix, and a set of conditional probabilities images. The transition probability matrix and transition areas matrix are found in a text file that records the category of the change in other category and numbers of pixels.

3.2.6. CA-Markov model

Both the Markov chain and the CA are discrete dynamics models in time and state. One of Markov's inherent flaws is that it lacks a sense of geography. The transition probabilities may be correct on a per-category basis, but the spatial distribution of occurrences within each land use category is unknown. In this paper, we use Idrisi software to predict land use in this region.

- Land use data of 2020 is specified as a basic image. The transition probabilities area from the years 2003 to 2020 were used for Markov conditional probability matrix
- A CA filter is used to generate a spatial explicit contiguity-weighting factor to change the state of cells based on their neighbours. The filter is a 5X5 contiguity filter. **Figure 2** presents whole methodology workflow.

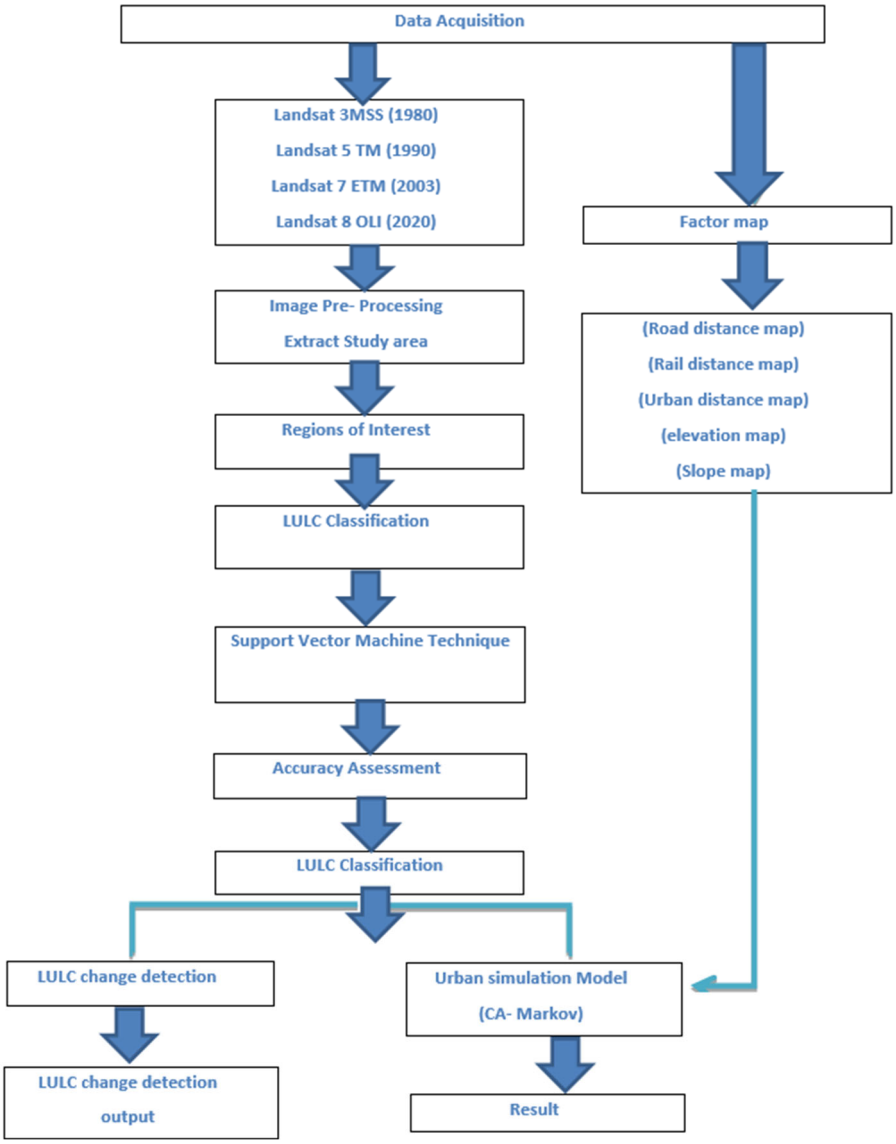

Figure 2. *Methodology flowchart*

4. RESULTS AND DISCUSSION

This research aims to obtain land use and land cover mapping of the Kanpur Nagar District, Uttar Pradesh. In this research, we use a support vector machine classifier for accuracy. After processing the satellite images, the land use and land cover area were analyzed using Support Vector Machine classification. Raster data has been classified and analyzed with different tools in ENVI5.3 software. **Figure 3** presents land use and land cover map from 1980.

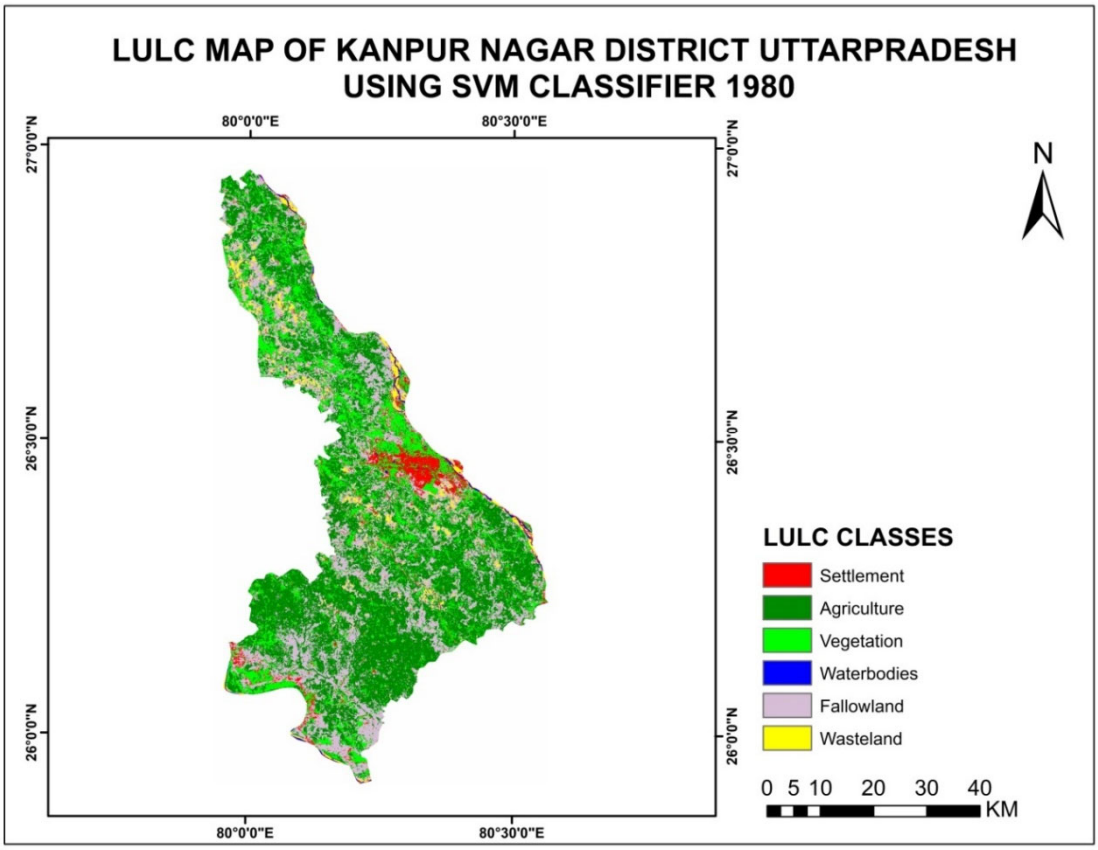

Figure 3. *Land use and land cover map in 1980*

In the year 1980, out of the total area of 2877sq.km, the settlement covered 120sq.km which is 4.17% of the total area, whereas a major share of the total area is coved by agricultural land which is 1332 sq. km and 46.29% of the total percentage. 525 sq. km area covers by vegetation which is 18.25% of the total area than water bodies, fallow land, and wasteland cover 12, 825, and 63 sq. km, which 0.42%, 28.67%, and 2.20% respectively. The overall accuracy is commonly given as a percentage, with 100 percent accuracy indicating that all references sited were correctly categorized and the overall accuracy is an average and does not provide information about the error between classes. The accuracy of the user essentially informs us how often the class on the map will appear on the ground. This is referred to as trustworthiness. The Commission Error is the complement of the User's Accuracy, so User's Accuracy = 100% - Commission Error. The user's Accuracy is calculated by dividing the total number of correct classifications for a class by the total number of rows. Producer's Accuracy is the opposite of Omission Error. Producer's Accuracy= 100% - Omission Error. It's also the number of accurately classified reference sites divided by the total number of reference sites in the class.

Producer and user accuracy of the SVM classified image are given below. Water bodies have the highest producer accuracy and settlement has the lowest producer accuracy. On the other hand, in the case of user accuracy, agriculture has the highest user accuracy, and settlement has the lowest user accuracy. The overall classification accuracies for the year 1980 were 85.48% and the kappa statistics as 82.377% respectively. **Table 1** presents accuracy assessment for the classification in year 1980.

Table 1. Accuracy assessment for the classification in 1980

CLASSES	PRODUCER	USER
Settlement	80.70%	77.97%
Agriculture	83.05%	92.45%
Vegetation	81.16%	82.35%
Water	94.44%	87.18%
Fallow land	88.00%	89.80%
Wasteland	93.75%	85.71%

Figure 4 shows land use and land cover in year 1990.

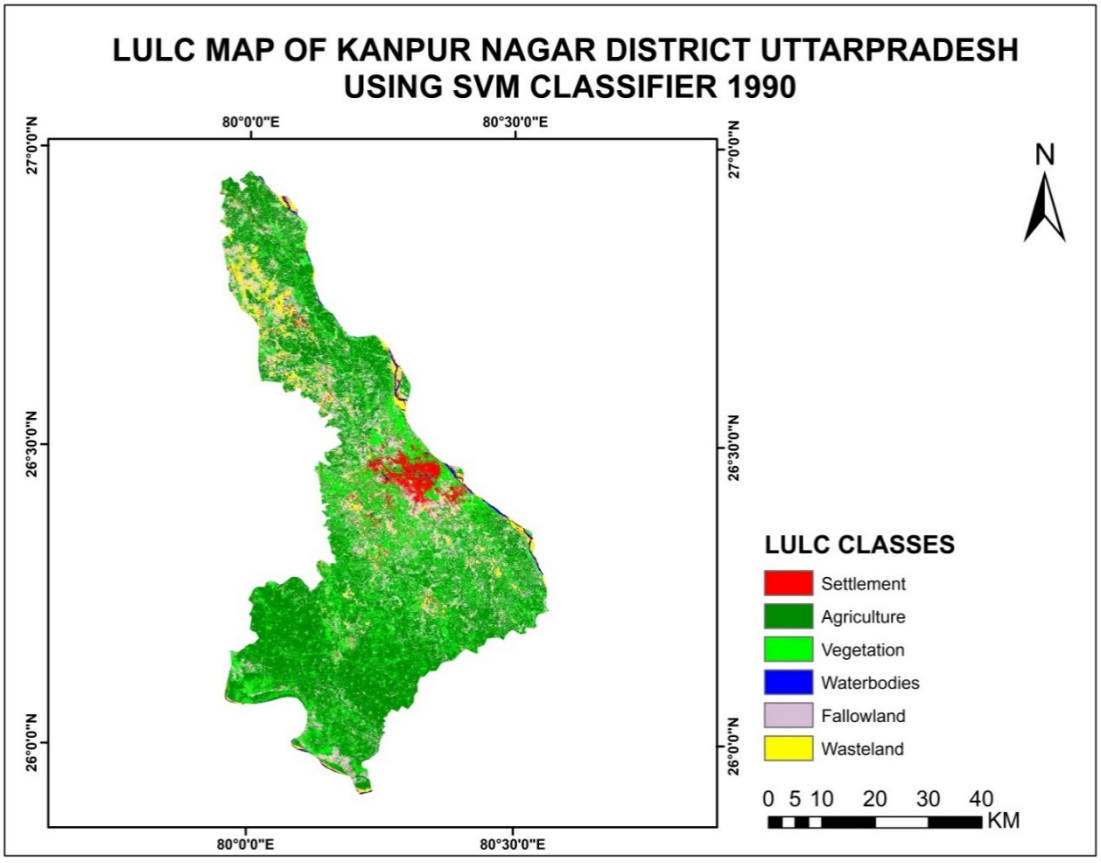

Figure 4. *Land use and land cover map in 1990*

It is quite evident that there was an increase of 0.82% in the settlement from 1980 to 1990. The percentage of settlement rises from 4.17 in 1980 to 5% in 1990. A decrease can be seen in agriculture compared to the 1980 due and fallow land increased. The percentage of land cover classed as fallow remained the same.

Producer and user accuracy of the SVM classified image are shown in the **Table 2** given below. Agriculture has the highest producer accuracy and water bodies have the lowest producer accuracy. On the other hand, in the case of user accuracy, water bodies have the highest user accuracy, and wasteland has the lowest user accuracy. The overall classification accuracies for the year 1990 were 84.38% and the kappa statistics as 81.216% respectively.

Table 2. Accuracy assessment for the classification in 1990

CLASSES	PRODUCER	USER
Settlement	84.78%	78.00%
Agriculture	96.23%	78.46%
Vegetation	78.08%	91.94%
Water	76.47%	100.00%
Fallow land	79.37%	84.75%
Wasteland	95.74%	77.59%

Figure 5 presents land use and land cover in year 2003.

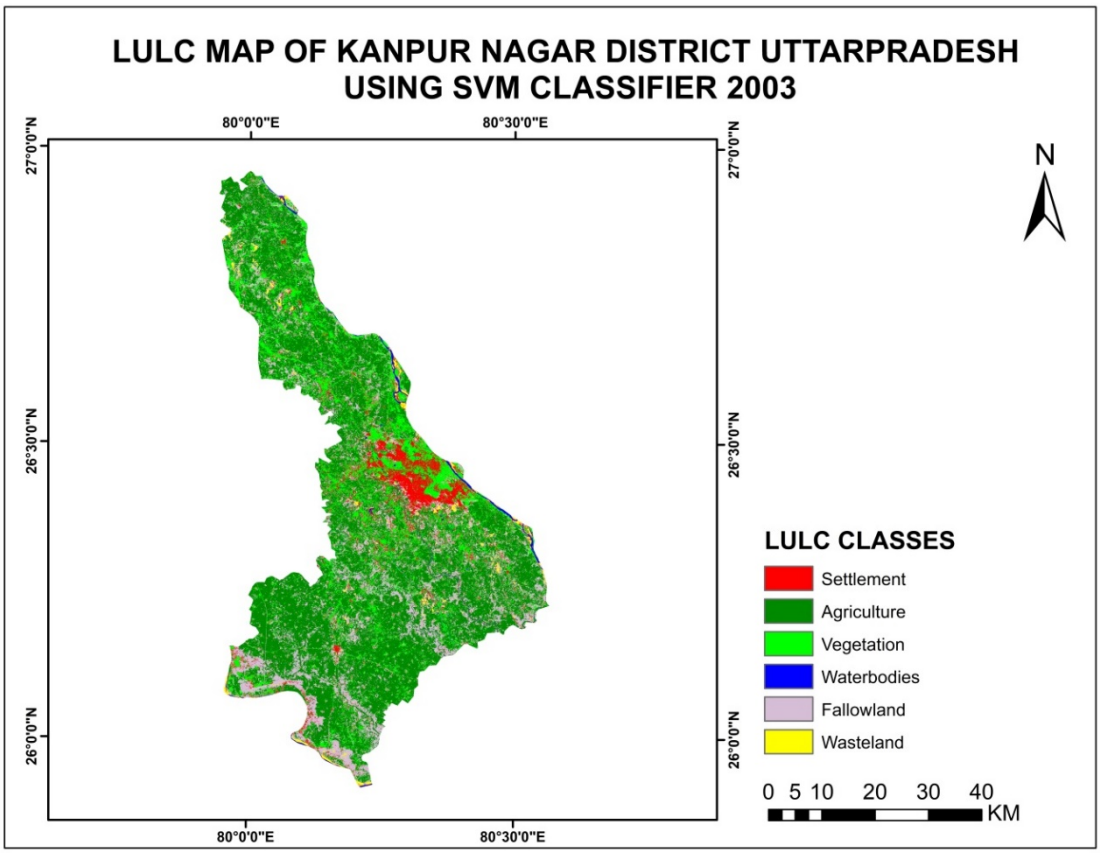

Figure 5. *Land use and land cover map in 2003*

The land cover map for the year 2003 as shown in Figure 5 clearly shows the growth of the settlement area concerning the previous years. The rapid urbanization in the latest period is attributed to the increasing availability of higher-level facilities, better employability, infrastructure, and industrialization.

In the year 2003, out of the total area of 2877sq.km, the settlement covered the 201 sq.km, which is 7.00% of the total area, whereas a major share of the total area is coved by agricultural land which is 1525 sq. km and 53.03% of the total percentage. 536 sq. km area covers by vegetation which is 18.64% of the total area than water bodies, fallow land, and wasteland covers 29, 550, and 33 sq. km, which 1.01%, 19.14%, and 1.18% respectively.

Producer and user accuracy of the SVM classified image are shown in the **Table 3** given below. Wasteland has the highest producer accuracy and settlement has the lowest producer accuracy. On the other hand, in the case of user accuracy, water bodies have the highest user accuracy, and settlement has the lowest user accuracy. The overall classification accuracies for the year 2003 were 86.11% and the kappa statistics as 83.202% respectively.

Table 3. Accuracy assessment for the classification in 2003

CLASSES	PRODUCER	USER
Settlement	77.59%	83.33%
Agriculture	93.75%	89.55%
Vegetation	87.93%	83.61%
Water	88.89%	93.02%
Fallow land	79.66%	83.93%
Wasteland	94.87%	88.10%

Figure 6 presents land use and land cover in the year 2020.

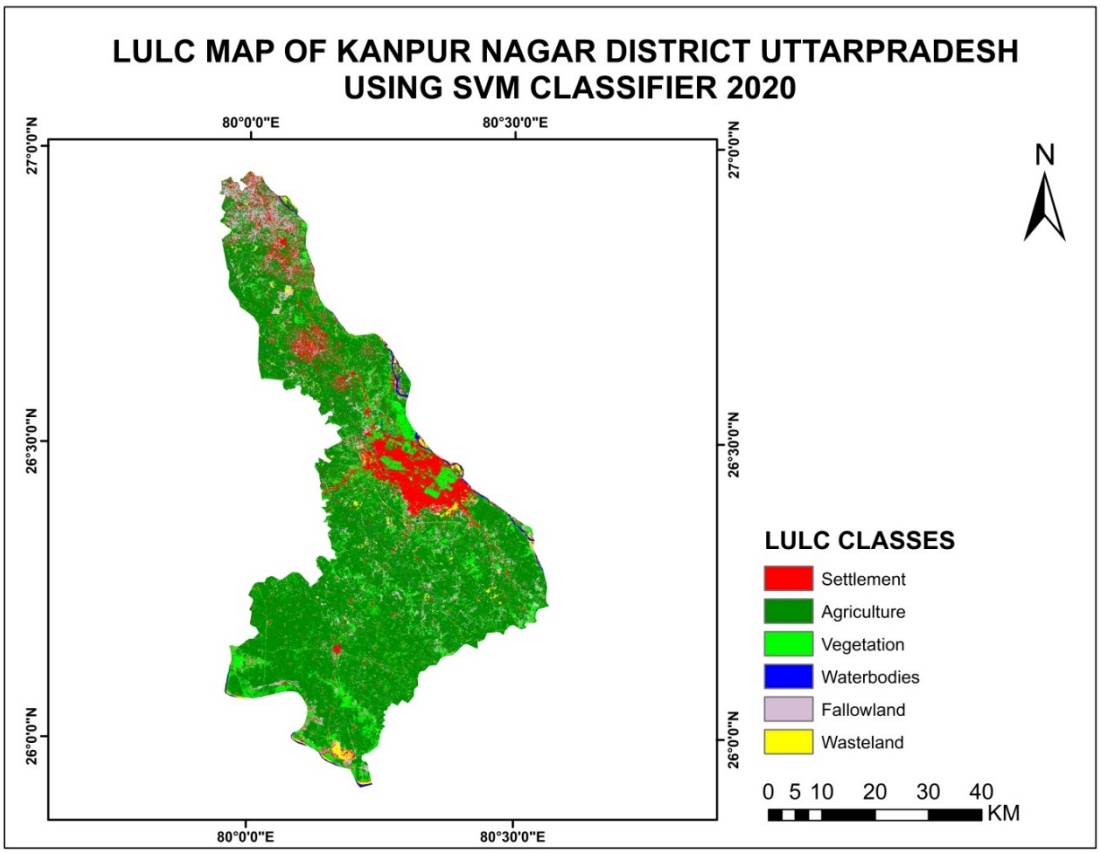

Figure 6. *Land use and land cover map in 2020*

In the year 2020, out of the total area of 2877sq.km, the settlement covered 324sq.km which is 11.25% of the total area, whereas a major share of the total area is coved by agricultural land which is 1786 sq. km and 62.10% of the total percentage. 417sq. km area covers by vegetation which is 14.52% of the total area then water bodies, fallow land, and wasteland cover 29, 272 and 47 sq. km, which 1.01%, 9.47%, and 1.65% respectively.

Producer and user accuracy of the SVM classified image are shown in the **Table 4** given below. Agriculture has the highest producer accuracy and water bodies have the lowest producer accuracy. On the other hand, in the case of user accuracy, the settlement has the highest user accuracy, and fallow land has the lowest user accuracy. The overall classification accuracies for the year 2020 were 86.11% and the kappa statistics as 83.202% respectively.

Table 4. Accuracy assessment for the classification in 2020

CLASSES	PRODUCER	USER
Settlement	89.47%	92.73%
Agriculture	94.00%	85.45%
Vegetation	83.33%	86.21%
Water	81.25%	96.30%
Fallow land	88.64%	78.00%
Wasteland	77.78%	81.40%

4.1. Land use and land cover change detection

This section shows the result of land use and land cover change detection. The landscape growths in this thesis were monitored using change detection. The changes in the areas from 1980 to 2020 were showing the categorized maps of Kanpur Nagar district. These pie-graph and tables are representing the statics the LULC changes. **Figure 7** shows land cover changes from period 1980 to period 1990.

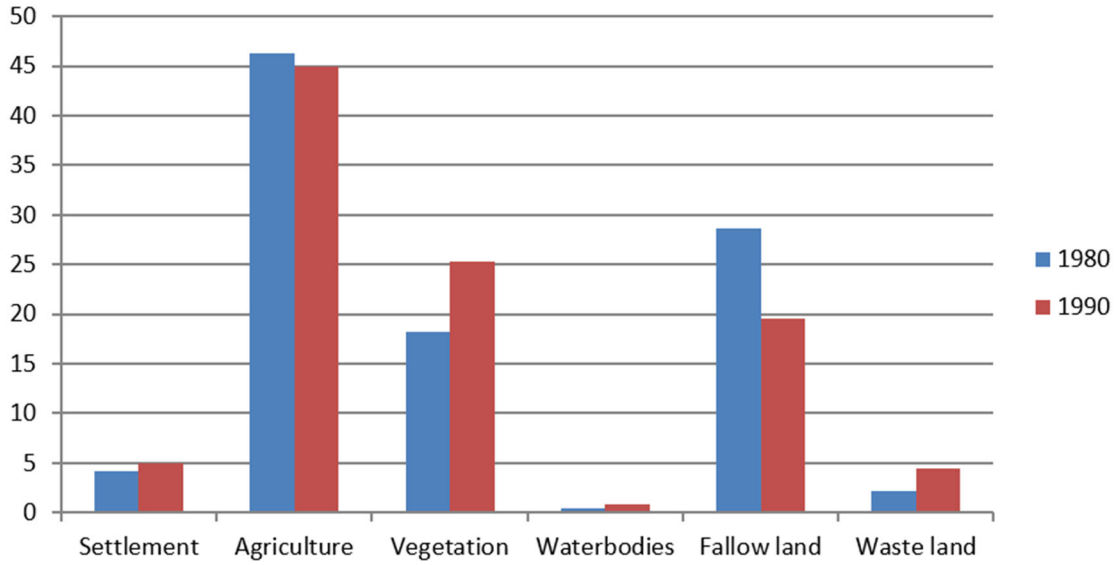

Figure 7. *Land cover changes graph 1980 - 1990*

From the comparison of Figure 7 for the year 1980- 1990, it is quite evident that there were a total increase of 21 sq. km and 0.82% in the settlement area and huge changes can be seen in vegetation, the total increment vegetation classes are 7% and 203 sq. km. agricultural land is decreasing and the fallow land also decrease. In Kanpur mostly bilaur, bithoor, chubepur, Kanpur cantonment and along the major rivers here we found a huge amount of vegetation.

Figure 8 presents land cover changes from year 1990 to 2003

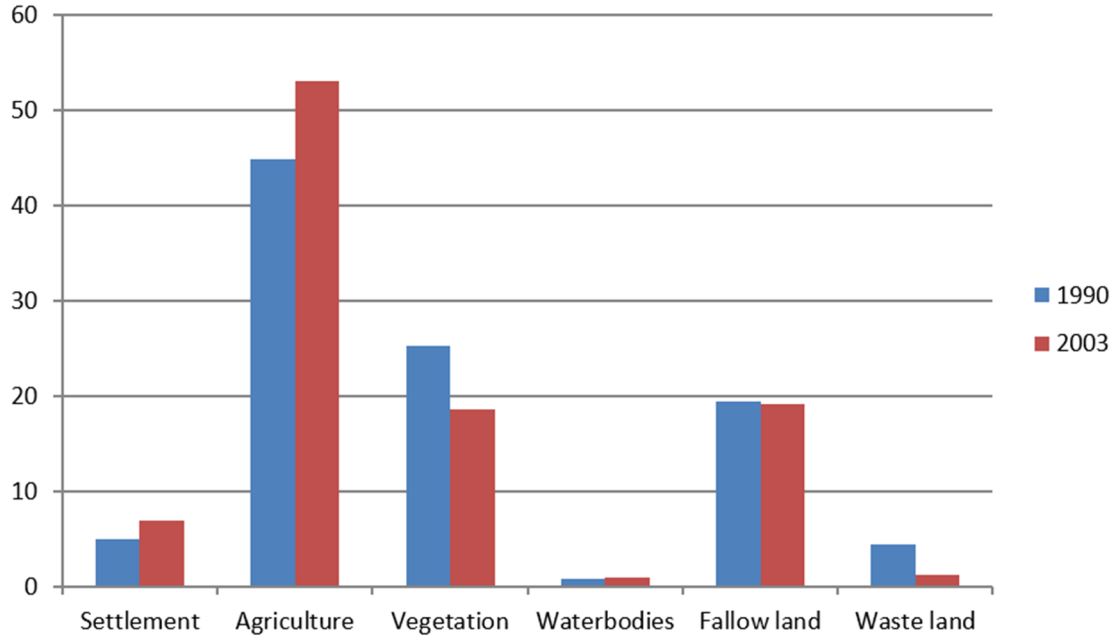

Figure 8. *Land cover changes graph 1990 - 2003*

In 2003 the settlement area is increased compared to previous years; the settlement increased 58 sq. km (2%). Vegetation area is decreasing 192 sq.km and agriculture are increased 234 sq. km. **Figure 9** presents land cover change from year 2003 to year 2020.

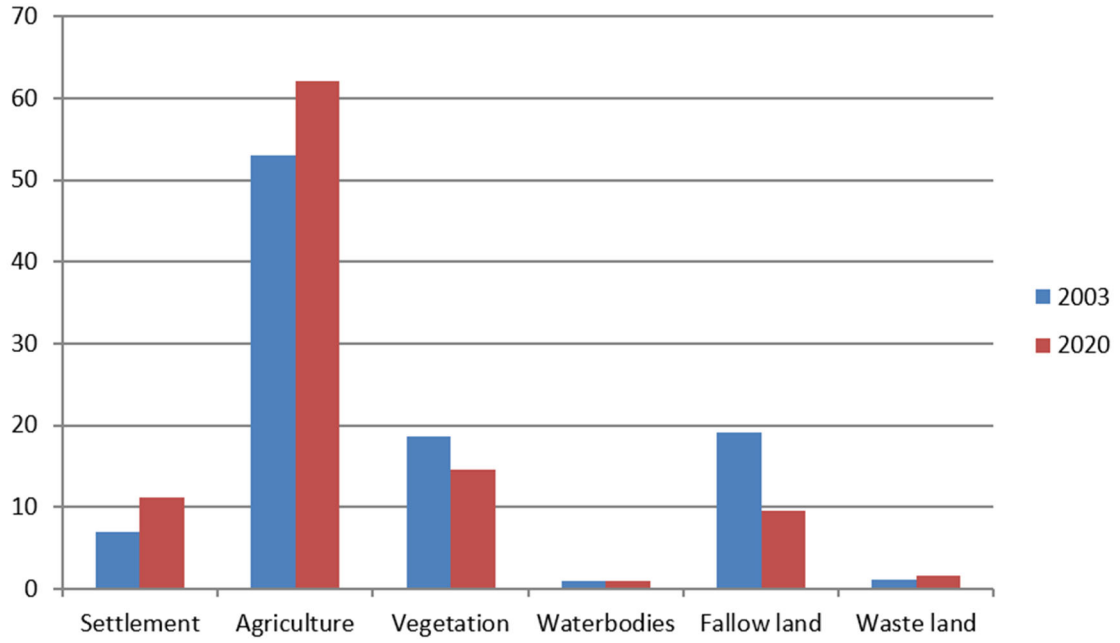

Figure 9. *Land cover changes graph 2003 - 2020*

The result shows that between 2003 and 2020, approximately 22% of vegetation and 50% of fallow land were transformed to other classes. The land cover changes show the latest period increase the utilities, better employability, infrastructure, and industrialization. Many projects are under-processed to make Kanpur a smart city, but most projects are based are only Kanpur urban areas and on the other side Kanpur rural are undeveloped and no found a better infrastructure and better employments. Most people who live in rural areas depend on agriculture.

4.2. Factor inducing urban growth in the study area

The result shows that between 2003 and 2020, approximately 22% of vegetation and 50% of fallow land were transformed to other classes. The land cover changes show the latest period increase the utilities, better employability, infrastructure, and industrialization. Many projects are under-processed to make Kanpur a smart city, but most projects are based are only Kanpur urban areas and on the other side Kanpur rural are undeveloped and no found a better infrastructure and better employments. Most people who live in rural areas depend on agriculture. **Figures 10 – 13** presents as it follows: elevation map, slope map, rail network map and road network map. Table 5 presents probability matrix of possible changes in the future.

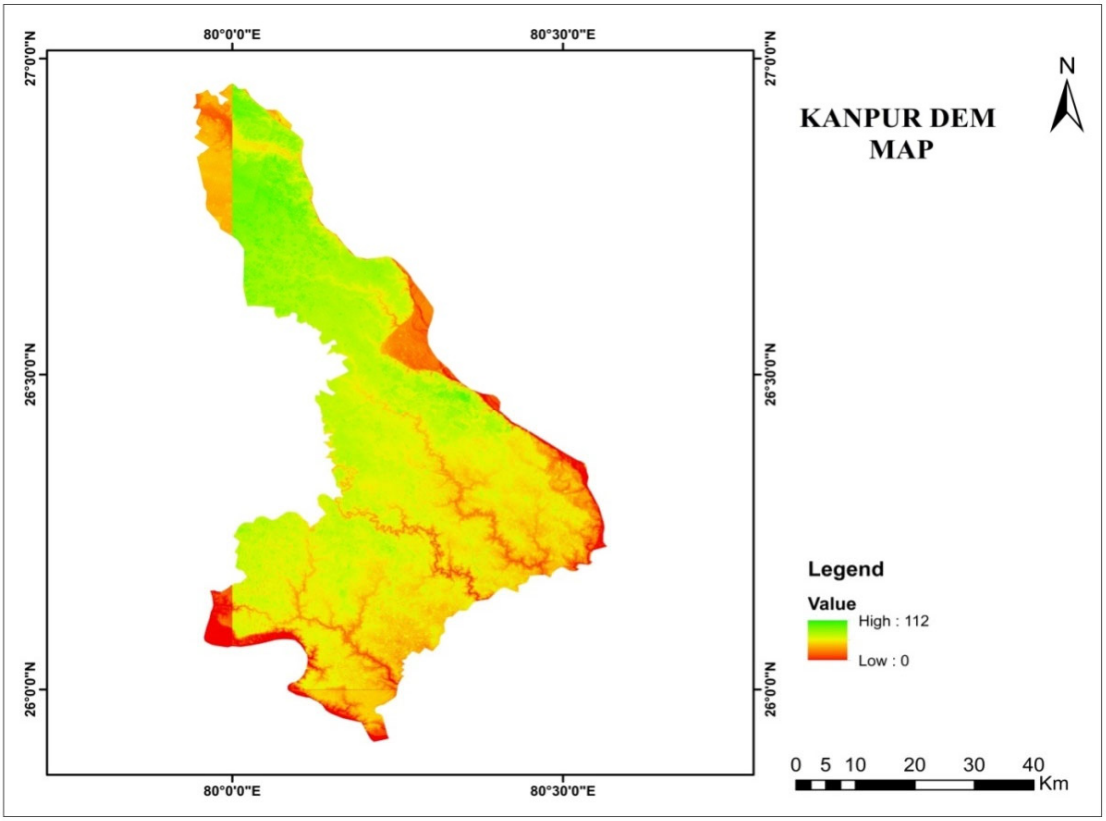

Figure 10. *Kanpur elevation map*

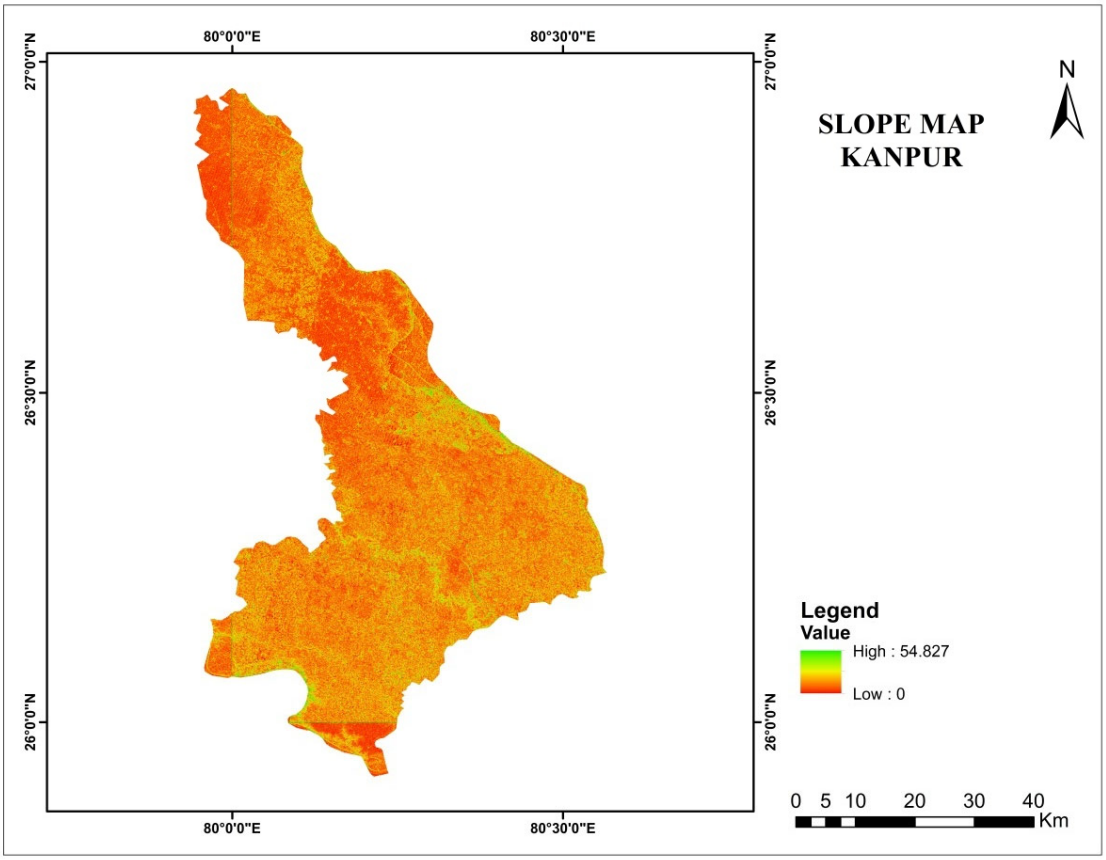

Figure 11. *Kanpur slope map*

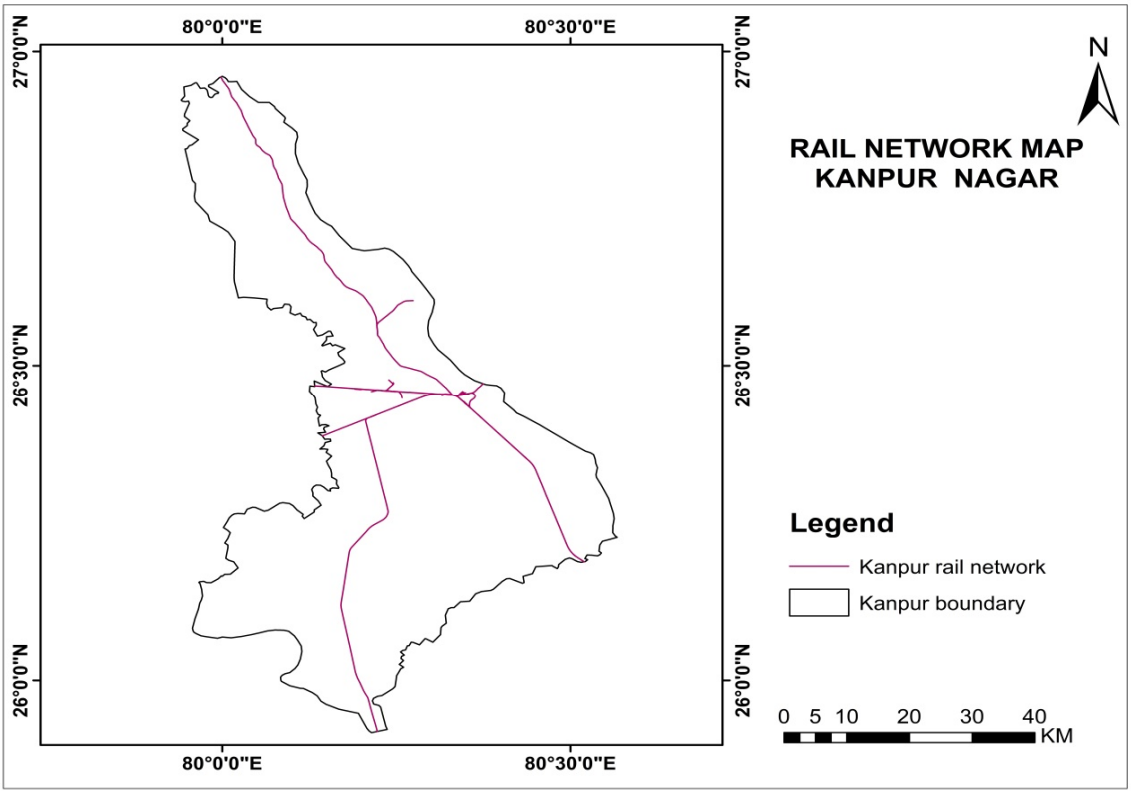

Figure 12. *Kanpur rail network map*

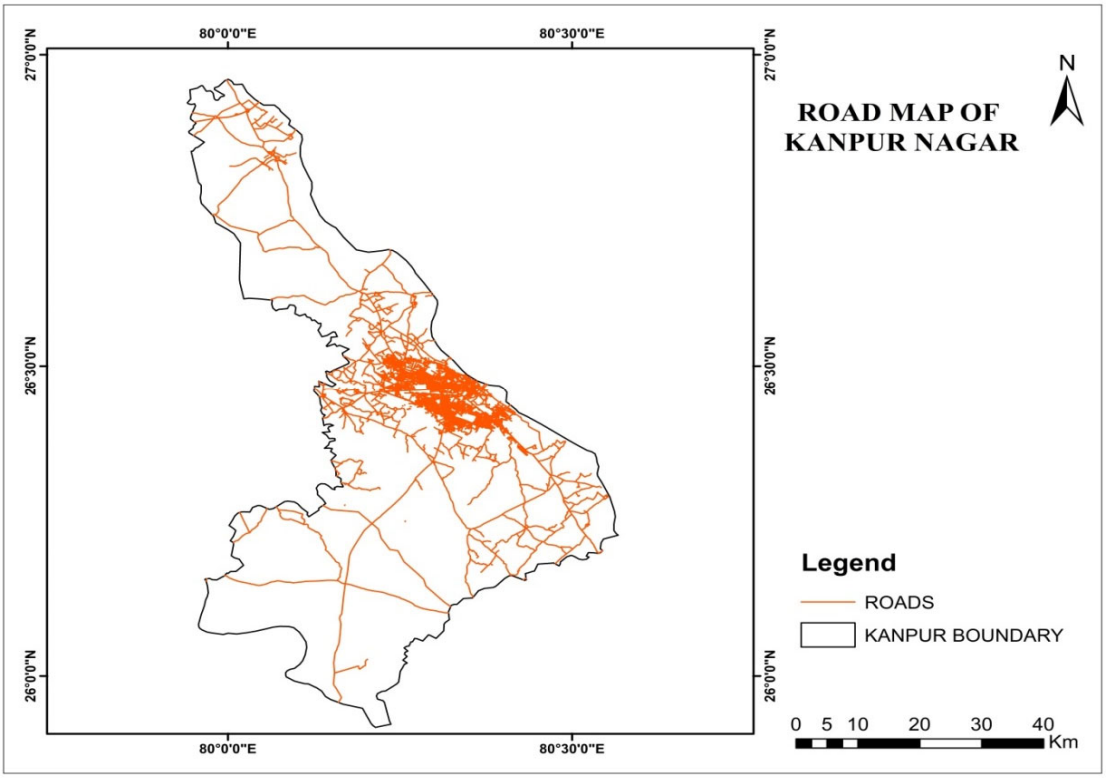

Figure 13. *Kanpur road network map*

Table 5. Transition probability matrix

CLASSES	1. Settlement	2.Agriculture	3. Vegetation	4. Water	5. Fallow land	6. Wasteland
1. Settlement	0.23	0.50	0.16	0.02	0.07	0.02
2. Agriculture	0.10	0.69	0.11	0.01	0.08	0.01
3. Vegetation	0.15	0.60	0.14	0.01	0.08	0.02
4. Water	0.16	0.49	0.18	0.02	0.08	0.03
5. Fallow land	0.13	0.62	0.13	0.01	0.08	0.02
6. Wasteland	0.15	0.54	0.15	0.03	0.10	0.04

The Markov chain calculates the rate of change by comparing earlier and later land cover maps as well as the date specified. The procedure calculates how much land is expected to transition from a later date to the prediction date based on a future projection of transition potentials and generates a transition probability file. The transition probabilities file is a matrix that records the probability that each land cover class will change to other classes. This figure shows the land cover classes change into another class.

Then apply the CA model for generating the future projected land cover map. According to this projected land cover images the settlement increases approximately 437 sq. km and agriculture, vegetation, water bodies, fallow land, wasteland cover 1728, 388, 29, 252, 42 sq. km of the land. **Figure 14** presents projected land use and land cover map for year 2030 of Kanpur Nagar.

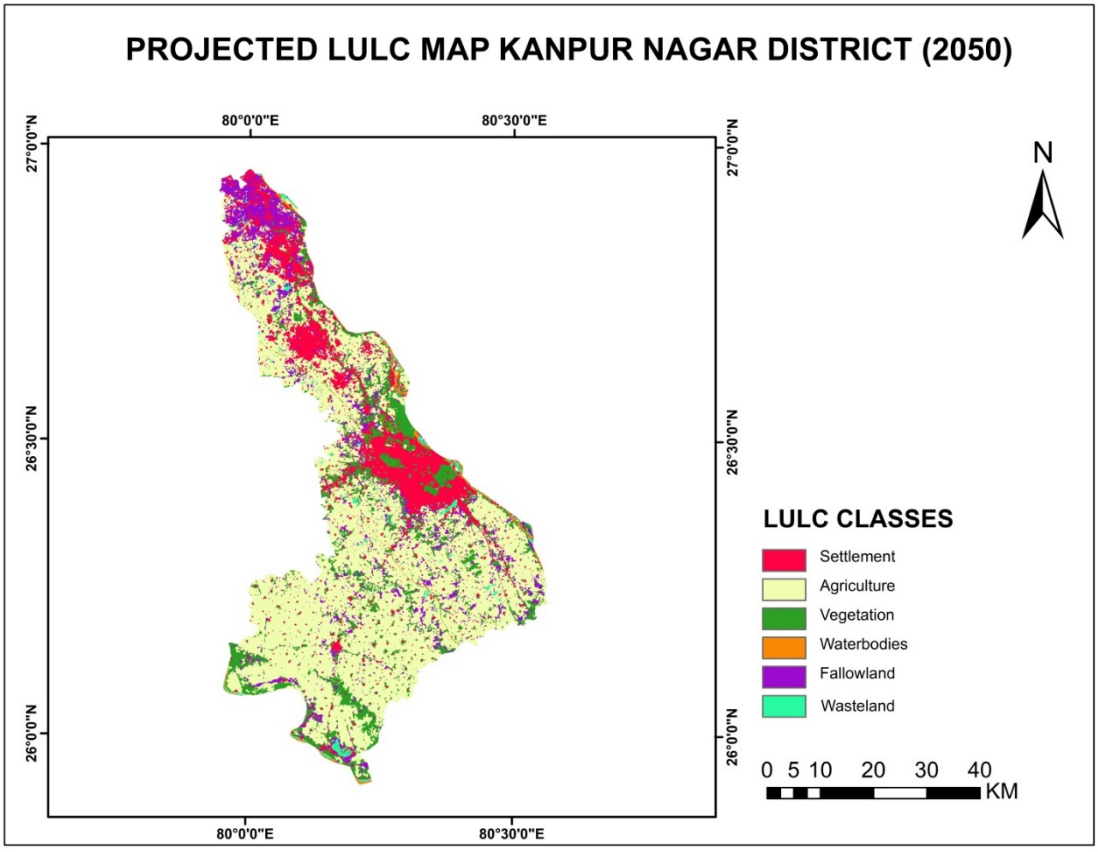

Figure 14. *Projected land use and land cover map for year 2030*

5. CONCLUSION

The research study demonstrates GIS and remote sensing's ability to retrieve and analyses patio-temporal data. In this study, an attempt was to create a spatial database of LULC in the Kanpur Nagar district. For this, a comprehensive LULC map was created. For a total of 40 years, four distinct years were spent studying urbanization in the Kanpur Nagar district.

The research has shown that urbanization and spatiotemporal growth can be quantified and compared across time. Landsat data proved to be an adequate data source for evaluating Kanpur's growing and increasingly changing urban growth. In this study using the combined cellular automata and Markov chain model future changes of LULC have been predicted for 2050. LCM landscape changes in Idrisi Elva edition 17.0 for more than 30 years was measured. A transition probability matrix that depicts the transition from one class to another overall time intervals was generated. Multi-temporal Landsat images were used to generate LULC maps, which helps in the CA- Markov process to predict the future spatial and temporal changes of LULC. According to the simulation results, an increase in the settlement area by 114 sq. km from 2020 to 2050 is expected. In the case of various social phenomena in Kanpur, the spreading out of land use in an urban area continues to expand along with transport nodes and roads or other patterns. With the establishment of industries, uncontrolled migration to Kanpur city from multiple directions in terms of better employment options has expanded. Kanpur is one of India's most industrialized cities, and the city's better employment, education, as well as other services act as a pull factor for newcomers. These demographic and economic factors encourage spatial growth and allow the city to spread out into fertile agricultural land. Growing population growth places strain on existing resource bases, and Kanpur should have a master plan in place for at least the next 20 to 50 years. Because there is less scope for horizontal expansion of the city, planners and city developers should consider vertical expansion of the city.

5. REFERENCES

Anderson J.R, Hardy, E.E., Roach, J.T., Witmer, R.E: A Land Use and Land Cover Classification System for Use with Remote Sensor Data, Geological survey professional paper, United States Government printing office, Washington, 1976

Moghal A. A. B., Dafalla M. A., Elkady T. Y., and Al-Shamrani M.A., Lime Leachability Studies on Stabilized Expansive Semi-Arid Soil. International Journal of GEOMATE, Vol. 9, Issue 18, 2015, pp.1467-1471.

Awal ASMA, Hosseini H. and Hossain M.Z., Strength, Modulus of Elasticity and Shrinkage Behaviour of Concrete Containing Waste Carpet Fiber, International Journal of GEOMATE, Vol. 9, Issue 17, 2015, pp. 1441-1446.

Hossain M.Z., For Chapter in a Book, Soil Mechanics, 4th ed. Vol. 2, Sakai, Ed. Sankeisha Publisher's Name, Year, pp. 11–60.

Annan B., Unpublished Work but Accepted, Vol., Issue, Year.

Kimura S., Journal Paper Title, J. of Computer Science, Vol. 1, Issue 2, 1987, pp. 23-49.

Islam M.R., Conference proceedings, in Proc. 2nd Int. Conf. on GEOMATE, 2011, pp. 8-13.

Hossain M.Z. and Awal ASMA, Experimental Validation of a Theoretical Model for Flexural Modulus of Elasticity of Thin Cement Composite, Const. Build. Mat., Vol.25, No.3, 2011, pp.1460-1465.

OIKON®
WITH US DEVELOPMENT IS NATURAL

OIKON Ltd. – Institute of Applied Ecology is a leading licensed and accredited consulting company / research institute in the field of applied ecology in Croatia and the region.

OIKON offers services in the areas of nature and environment protection, industrial ecology, renewable energy, natural resource management, ecological modeling, landscape analysis and design, geographic information systems (GIS), remote sensing and ICT, environmental law, policy and economics, feasibility studies, as well as program and project management.

Our **Department of Environmental Engineering** is a leader in the field of environmental engineering and a major provider of environmental impact assessments and strategic impact assessments, together with the accompanying mitigation measures and monitoring programs.

We are specialists in large infrastructural developments in many of which we have participated in the past 22 years:

- Environment Impact Assessments (EIAs) for over 1,000 km or about 80% of newly built motorways in Croatia and Bosnia and Herzegovina;
- Hundreds of km of highways – approx. 30% of newly built highways;
- Hundreds of km of railways – approximately 80% of newly built or planned railways;
- Almost 1,000 km of high pressure gas pipelines;
- Numerous other mayor infrastructural projects, such as transmission lines and wind farms.

22+
years of experience

1,400+
completed projects

300+
satisfied clients

4
departments

4
laboratories

50+
employees

Oikon Ltd. – Institute of Applied Ecology
Trg senjskih uskoka 1-2
HR-10020 Zagreb, Croatia
T +385 1 5507 100
E oikon@oikon.hr

Croatian Quality

Fore more, visit our web page: **OIKON.hr**

Follow us on social media

WINDOR® d.o.o.
A. Buk 54a, HR- 34310 Pleternica
T. +385.34.268.002
E. kontakt@windor.hr
W. www.windor.hr

ULTRA AD 77

Aluminij-drvo prozor

Vrhunac dugoročnog ulaganja u istraživanje i razvoj

Savršen spoj slavonskog masivnog hrasta iznutra, koji interijer čini ugodnim i toplim te aluminija izvana koji ščiti od vanjskih utjecaja i jednostavan je za održavanje.
Stolarija pruža izvrsnu toplinsku izolaciju; u profile se ubrizgavaju PUR profili što u konačnici poboljšava ukupni toplinski koeficijent prozora.

Prirodni materijali i moderan dizajn

- **jedinstveni profili na tržištu**
- **konkurentna cijena proizvoda**
- **visoka kvaliteta izrade i ugradnje**
- **profesionalni pristup**
- **garancija na ugrađene proizvode**

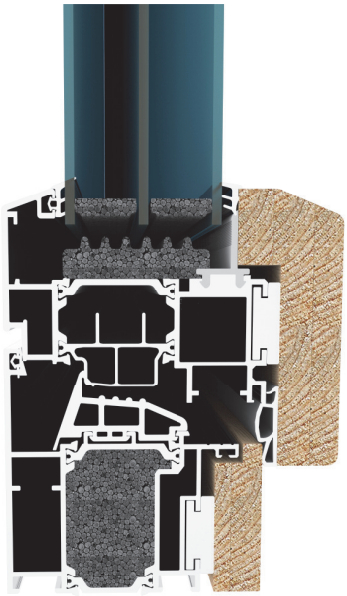

Toplinska provodljivost profila Uf

1,2

Toplinska provodljivost stakla Ug

0,5

Ukupna toplinska provodljivost Uw

0,8

Gumiimpex-GRP – the first company in Croatia which started in 2005. with used tires recycling.

Tire waste area in the Recycling plant collects all used tires - car, bus and truck used tires, agricultural and industrial used tires (tractors, dumpers, forklifts), used airplanes tires…

TIRE RECYCLING

Ecological procedure - with multiple mechanical chopping, used tires are completely exploatable - all extraced elements are ready for use again: rubber granulates, steel and textile fibers.

RUBBER GRANULATE PRODUCTS

- Sports fields
- Sports tracks
- Safety floor coverings
- Stable coverings
- Sound bumpers
- Wheels for containers, ...

Varaždin
Pavleka Miškine 64c
T: +385 42 404 500
www.gumiimpex.hr

Trnovec Bartolovečki
Gospodarska 9
T: +385 42 684 444
E: info@grp.hr

SIRRAH projekt d.o.o.
Ribarska 4
31000 Osijek
Tel: +385 31 250 000

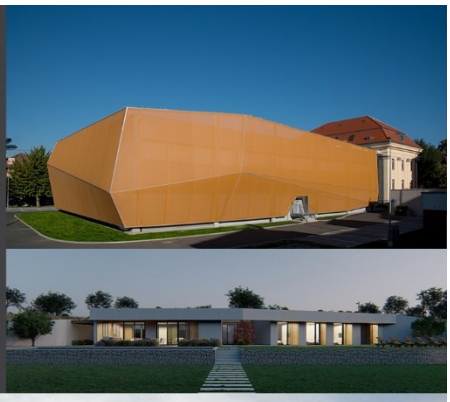

arhitektura

sport / rekreacija

industrija

trgovina

turizam

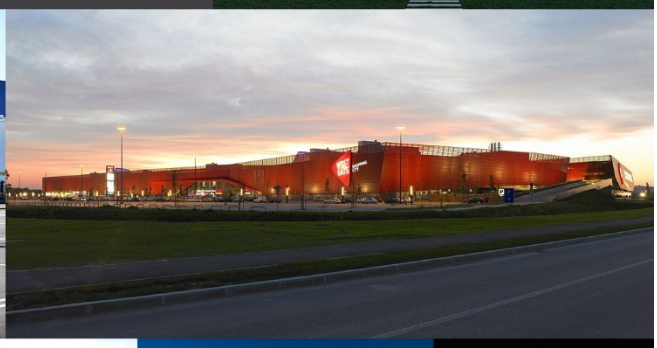

MEĐIMURSKE VODE d.o.o.

za javnu vodoopskrbu i javnu odvodnju

40000 ČAKOVEC, Matice hrvatske 10

Tel.: 040/373 700

Besplatni telefon za prijavu kvara:
0800 313 111

voda@medjimurske-vode.hr

www.medjimurske-vode.hr

QUALITY SYSTEM CERTIFICATION DNV ISO 9001

BUSINESS CONTINUITY MANAGEMENT DNV ISO 22301

Sveučilište u Zagrebu
GEOTEHNIČKI FAKULTET
Zavod za geotehniku

GEOTEHNIČKI LABORATORIJ
GEOTECHNICAL LABORATORY

od 1974
since 1974

ZAŠTO SURAĐIVATI S NAMA

Stručno osposobljeni djelatnici
Suvremena geomehanička oprema
Standardne i specijalne metode ispitivanja
Suradnja u nastavnom programu fakulteta
Suradnja u znanstvenim projektima fakulteta
Suradnja s gospodarstvom

KONTAKTIRAJTE NAS

Adresa
HALLEROVA ALEJA 7,
42000 VARAŽDIN

Telefon
042 408 938

Fax
042 313 587

Mobitel (Voditelj laboratorija)
091 408 9007

E-mail
geolab@gfv.unizg.hr
geolab.gfv@gmail.com

WHY COOPERATE WITH US

Professionally trained employees
Modern geomechanical equipment
Standard and special test methods
Collaboration in the faculty curriculum
Collaboration in faculty scientific projects
Cooperation with the economy

CONTACT US

Adress
HALLEROVA ALEJA 7,
Hr-42000 VARAŽDIN

Telephone
+385 42 408 938

Fax
+385 42 313 587

Mobile(Laboratory manager)
+385 91 408 9007

E-mail
geolab@gfv.unizg.hr
geolab.gfv@gmail.com

Sveučilište u Zagrebu
GEOTEHNIČKI FAKULTET

ZAVOD ZA GEOTEHNIKU

GEOFIZIČKO-GEOTEHNIČKI ISTRAŽNI RADOVI

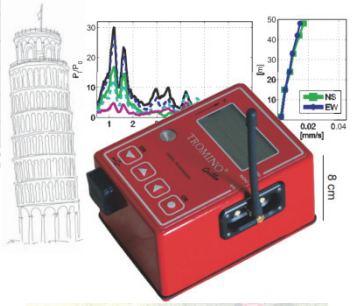

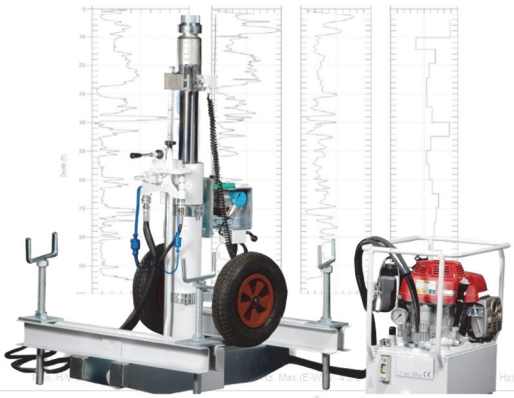

GEOFIZIČKI ISTRAŽNI RADOVI

- Geoelektrična istraživanja (sondiranje, profiliranje, tomografija)
- Seizmička refrakcija (P i S valovi)
- Višekanalna analiza površinskih valova (MASW)
- Seizmička karotaža
- Seizmički efekti miniranja
- Mikrotremor
- Georadar

GEOTEHNIČKI ISTRAŽNI RADOVI

- Istražno bušenje u svim vrstama tla i stijena
- Statički penetracijski test (CPT, CPTU, SCPT)
- Standardni penetracijski test (SPT)
- Bušenje, ugradnja i pokusno crpljenje zdenaca i piezometara
- Izrada geotehničke dokumentacije (izvješća, elaborati, projekti)
- Geotehnički nadzor i savjetovanje

Varaždin, Hallerova aleja 7, Tel: + 385 (0) 42 408 900, Faks: + 385 (0) 42 313 587
E-mail: ured.dekana@gfv.unizg.hr, www.gfv.unizg.hr

UNIVERSITY OF ZAGREB
FACULTY OF GEOTECHNICAL ENGINEERING
DEPARTMENT OF HYDROTECHNICS

Main research areas:
- Water management
- Groundwater protection
- Hydrology
- Hydrogeochemistry
- Advanced technologies for water treatment

Experience and knowledge transfer applications:
- Preparation of methodology for karstic groundwater bodies quality status and risk assessment
- Preparation of national methodology for status assessment of coastal karstic groundwater bodies
- Delineation of drinking water protection zones and protection measures
- Preparation of mathematical models of intergranular aquifers



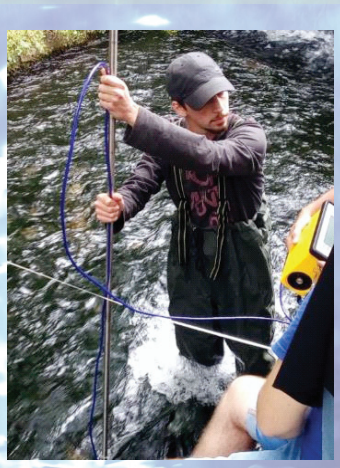


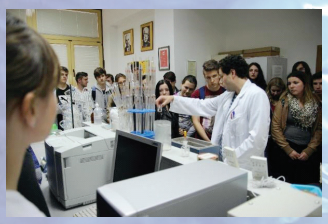






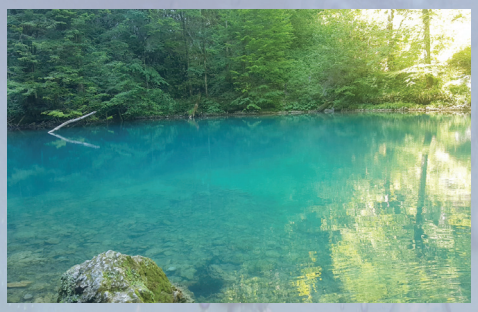


GRADUATE STUDY OF ENVIRONMENTAL ENGINEERING WATER MANAGMENT

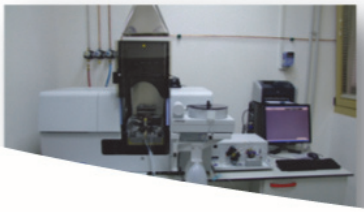

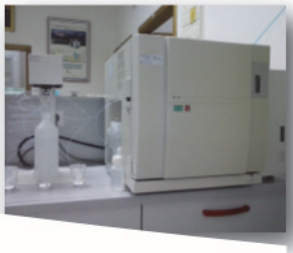

SVEUČILIŠTE U ZAGREBU
GEOTEHNIČKI FAKULTET
Hallerova aleja 7, 42 000 VARAŽDIN
tel.: 042 / 408 – 900
fax: 042 / 313 – 587
M.B. 03042316

GEOTEHNIČKI FAKULTET
Zavod za hidrotehniku
Laboratorij za geokemiju okoliša
tel.: 042 / 408 – 937
fax: 042 / 313 – 587

LABORATORIJ ZA GEOKEMIJU OKOLIŠA

- osnovan je 2006. godine sa znanstvenom, stručnom i obrazovnom svrhom
- opremljen instrumentima i pratećom opremom za prikupljanje uzoraka tala, sedimenata, prirodnih i otpadnih voda
- vrši terenske i laboratorijske analize prikupljenih uzoraka
- obavlja usluge agrokemijskih analiza tla za poljoprivrednike na temelju kojih se daje preporuka za gnojidbu

Zavod za hidrotehniku

LABORATORIJ ZA GEOKEMIJU OKOLIŠA

Tel.: 042 / 408 – 937
Fax: 042 / 313 – 587
E-mail: lgo@gfv.unizg.hr

LABORATORIJ ZA GEOKEMIJU OKOLIŠA

Laboratorij za geokemiju okoliša osnovan je u sklopu Zavoda za hidrotehniku Geotehničkog fakulteta u Varaždinu. Laboratorij sudjeluje u izvođenju praktične nastave iz kolegija preddiplomskog i diplomskog studija te Združenog međunarodnog doktorskog studija kao i u znanstvenim te stručnim projektima. Na taj način ispunjava svoju obrazovnu, znanstvenu i stručnu svrhu. Smješten je na 100 m² prostora i opremljen modernom opremom za provedbu geokemijskih terenskih i laboratorijskih ispitivanja, što uključuje prikupljanje uzoraka tla, sedimenata i vode. U laboratoriju se obavljaju i usluge agrokemijskih analiza tla.

Pokazatelji koje mjerimo u uzorcima voda, eluata tala i sedimenata:

~ atomskom apsorpcijskom spektrometrijom: Al, As, B, Ba, Ca, Cd, Co, Cr, Cu, Fe, Hg, K, Li, Mg, Mn, Mo, Na, Ni, Pb, Se, Si, Sr, Ti, V, Zn
~ amonijak, nitriti, nitrati, ukupni dušik
~ bromidi, fenoli, fluoridi, fosfati, jodidi, kloridi
~ silikati, sulfidi, sulfati, sulfiti
~ suspendirana tvar, mutnoća, KPK
~ alkalitet, ukupna tvrdoća, karbonatna tvrdoća, nekarbonatna tvrdoća, kalcijeva tvrdoća, magnezijeva tvrdoća
~ slobodni CO_2, koncentracija otopljenog kisika i zasićenost kisikom
~ pH, električna vodljivost, ukupna otopljena tvar – TDS
~ trasiranje podzemnih tokova (koncentracija natrijevog fluoresceina)
~ ukupni organski ugljik i ukupni dušik – TOC/DOC/TN
~ razaranje tla zlatotopkom
~ ekstrakcija izmjenjivih kationa iz tla amonijevim acetatom i kalijevim kloridom

Provođenje agrokemijskih analiza tla u svrhu modernizacije poljoprivredne proizvodnje, racionalizacije gnojidbe, povećanja prinosa i zaštite prirodnih resursa.

Ispitivanje fizikalnih i kemijskih svojstava prirodnih i otpadnih voda.

Određivanje pH, pKCl, ukupnog $CaCO_3$, NO_3^-, NO_2^-, NH_4^+, fosfora i kalija, humusa, teških metala i drugih kemijskih svojstava tla.

Ispitivanje sastava eluata otpada.

Kontakti: izv.prof.dr.sc. Anita Ptiček Siročić
voditeljica laboratorija
tel: 042 / 408 – 957
e-mail: anita.pticek.sirocic@gfv.unizg.hr

dr.sc. Dragana Dogančić
stručna suradnica
tel: 042 / 408 – 956 ili 042 / 408—937
e-mail: ddogan@gfv.unizg.hr

Saša Zavrtnik, dr.med.vet.
laborant
tel: 042 / 408—937
e-mail: lgo@gfv.unizg.hr

DEPARTMENT OF ENVIRONMENTAL ENGINEERING

MAIN RESEARCH AREAS:

- Waste management
- Solar photocatalysis
- Waste treatment technologies
- Chemical sensors
- Environmental monitoring
- Waste mechanics

Laboratory of Environmental Engineering

Special interest in wastewater management, air quality, waste management and disposal, energy efficiency and renewable energy sources, R&D of chemical sensors for environmental and industrial applications, microfluidics.

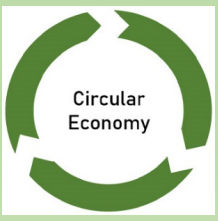

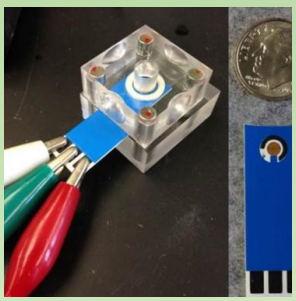

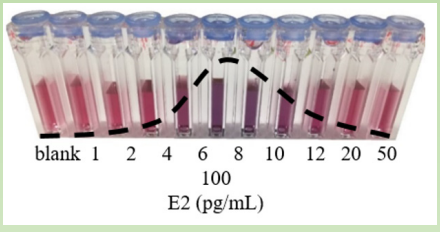

Sveučilište u Zagrebu • University of Zagreb

STUDENTSKI CENTAR VARAŽDIN

Student Centre Varaždin

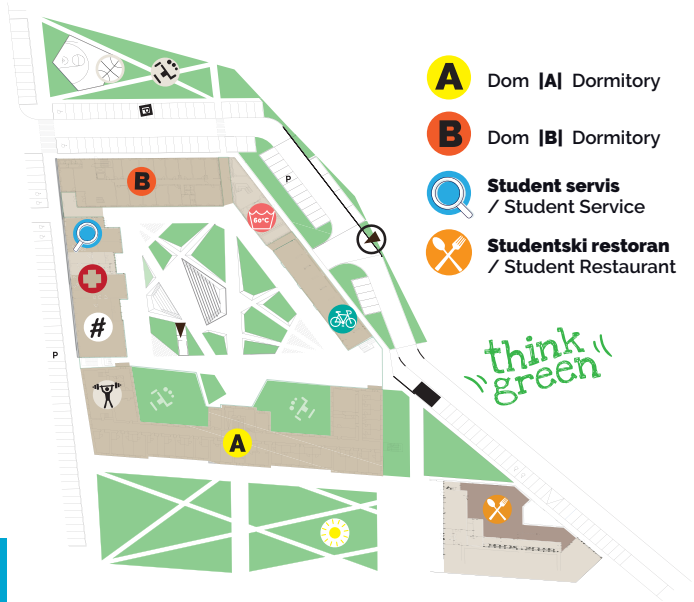

- **A** Dom |A| Dormitory
- **B** Dom |B| Dormitory
- **Student servis** / Student Service
- **Studentski restoran** / Student Restaurant
- **Studentski klub** / Student Club
- **Studentska ambulanta** / Student Infirmary
- **Gym**
- **Praonica rublja** / Student Laundry Room
- **Spremište za bicikle** / Bicycle Storage
- **Sportsko igralište** / Sports Playground
- **Fitness park** / Fitness Park
- **Solarni park** / Solar Park
- **Ulaz u podemnu garažu** / Underground Garage Enterence

www.scvz.unizg.hr

scvarazdin

Student Council
Faculty of Geotechnical Engineering

- ✓ As the student representatives we promote student interests and take care of the student standard at the Faculty council.
- ✓ We take care on student rights, encourage students to be involved in international mobility, advise students in their needs, etc.

- ✓ We are participating in many projects; form student promotions, study promotions, to scientific and professional project with our professors.
- ✓ We are working on the networking of current students with former students and potential employers.
- ✓ Through various activities our goal is to be the leader of the student standard promotion in Varaždin.

✓ **Every student is important to us.**

CONTACT:
Email: studentski.zbor@gfv.unizg.hr

Studentski zbor
Geotehničkog fakulteta

KRITERIJI ZA UPIS

Lista poretka prijavljenih kandidata za upis sastavlja se prema sljedećem sustavu bodovanja:

a) Na temelju uspjeha u srednjoj školi = do 500 bodova

b) Na temelju položenih ispita na državnoj maturi
- matematika (osnovna razina) = do 500 bodova

c) Na temelju provjere posebnih sposobnosti = nema bodova

d) Temeljem dodatnih postignuća učenika = IZRAVAN UPIS (1000 bodova)
- osvojeno jedno od prva tri mjesta na državnim natjecanjima u RH iz matematike, fizike, kemije, biologije, informatike, astronomije, statistike ili tehničkih znanosti za vrijeme srednjoškolskog obrazovanja.

AKADEMSKI NAZIVI

Završetkom preddiplomskog studija Inženjerstvo okoliša stječe se 180 ECTS bodova te akademski naziv sveučilišni prvostupnik/prvostupnica inženjer/inženjerka Inženjerstva okoliša (univ.bacc.ing.amb.).

Završetkom diplomskog studija Inženjerstvo okoliša stječe se 120 ECTS bodova te akademski naziv magistar/magistra inženjer/inženjerka Inženjerstva okoliša (mag.ing.amb.).

Završetkom doktorskog studija Inženjerstvo okoliša stječe se 180 ECTS bodova te akademski naziv doktora znanosti (dr.sc.).

DODATNE INFORMACIJE

TAJNIŠTVO: pon-pet: 07:00 - 15:00
tel: 042/408-901
ured.tajnika@gfv.unizg.hr

REFERADA: pon-pet: 09:00 - 12:00
tel: 042/408-904
studentska.referada@gfv.unizg.hr

Točne datume upisa i ostale relevantne informacije možete potražiti na web stranicama fakulteta: www.gfv.unizg.hr

ADRESA: Geotehnički fakultet Sveučilišta u Zagrebu, Hallerova aleja 7, 42000 Varaždin

Studij inženjerstva okoliša – Geotehnički fakultet

inzenjerstvo_okolisa

STUDIJ INŽENJERSTVA OKOLIŠA

FAKULTET
KOJIM ĆEŠ
MIJENJATI SVIJET
NA
BOLJE

STUDIJ INŽENJERSTVA OKOLIŠA

Geotehnički fakultet Sveučilišta u Zagrebu

Opis zvanja - kompetencije i osposobljenost

Završetkom sveučilišnoga **preddiplomskog studija** na Geotehničkom fakultetu steći ćeš osnovne kompetencije u identificiranju, definiranju i rješavanju inženjerskih zadaća u Inženjerstvu okoliša.

Od praktičnih znanja kao prvostupnik Inženjerstva okoliša posjedovat ćeš sposobnost korištenja laboratorijske i terenske opreme, promatranja, bilježenja i analize podataka dobivenih laboratorijskim i terenskim ispitivanjima. Znat ćeš izraditi tehničke nacrte ručno i pomoću računala, te pripremiti prezentaciju tehničkih izvješća.

Znanja i kompetencije koja stekneš završetkom sveučilišnoga preddiplomskog studija odgovarajuća su za praćenje diplomskoga sveučilišnog programa na Geotehničkom fakultetu, a omogućavaju ti i praćenje diplomskih studija iz srodnih područja na drugim tehničkim studijima te praćenje različitih programa cjeloživotnog obrazovanja.

Diplomski studij Inženjerstvo okoliša traje dvije godine, a uključuje smjerove Geoinženjerstvo okoliša, Upravljanje vodama i Upravljanje okolišem. Ovaj studij mogu upisati studenti koji su završili sveučilišni preddiplomski studij ili strani studij ekvivalentnog programa.

Završetkom diplomskoga studija bit ćeš osposobljen upravljati okolišem na održiv način i preuzeti osobnu i timsku odgovornost za strateško odlučivanje i uspješnu provedbu zadataka pri izradi elaborata, studija i projekata iz inženjerstva okoliša, kao i primijeniti legislativu iz područja zaštite okoliša te preuzeti društvenu i etičku odgovornost za posljedice.

Doktorski studij Inženjerstvo okoliša traje tri godine, a njegovim završetkom stječu se kompetencije za provođenje samostalnog istraživačkog rada.

Mogućnost zaposlenja

Znanstvenu karijeru možeš nastaviti razvijati upisom na poslijedoktorski studij Inženjerstvo okoliša na našem Fakultetu. A ako si bio vrlo uspješan student, možda započneš svoju akademsku karijeru kao asistent na našem Fakultetu.

Izvan akademske ili znanstvene sredine, popis mogućih poslodavaca kod kojih se možeš zaposliti doista je raznolik. To su sve institucije državne i lokalne uprave, kao i svi gospodarski subjekti koji zapošljavaju osobe za obavljanje stručnih poslova zaštite okoliša, kao što su na primjer komunalna poduzeća, centri za gospodarenje otpadom, pročišćivači otpadnih voda, eksploatacijska polja. Nadalje, to su i svi oni gospodarski subjekti koji se bave obnovljivim izvorima energije te oni koji svojim proizvodnim procesom mogu naštetiti okolišu.

Ako želiš možeš postati i inspektor za zaštitu okoliša, a s ovim stručnim nazivom ti ni vrata Europske unije neće biti zatvorena.

Pogodnosti studiranja

Tijekom studiranja na našem Fakultetu kao student Sveučilišta u Zagrebu na raspolganju imaš razne pogodnosti. Detaljnije o pogodnostima možeš saznati u našem vodiču za brucoše:
http://www.gfv.hr/modules/m_gfv/datoteke/vodic_za_brucose_a5_final_v1.pdf

Znanost i suradnja s gospodarstvom

Na Geotehničkom fakultetu provode se i znanstvena istraživanja. Fakultet raspolaže akreditiranim geotehničkim laboratorijem, kao i laboratorijem za inženjerstvo okoliša, laboratorijem za geokemiju okoliša, informatičkim centrom za GIS. Primjereno smo opremljeni i za terenske istraživačke radove. Budući da istraživači koji ih provode sudjeluju i u izvođenju nastave, studentima se prenose najnovije spoznaje i rezultati istraživanja.

Velik doprinos nastavi i znanstvenom radu daje znanstvena i stručna suradnja Geotehničkog fakulteta sa srodnim visokoškolskim institucijama u Republici Hrvatskoj i svijetu. Usporedno s nastavom i znanstveno-istraživačkim radom, Fakultet održava i razvija i suradnju s gospodarstvom kroz izradu mnogobrojnih studija i projekata iz područja Inženjerstva okoliša.

Sveučilište u Zagrebu
GEOTEHNIČKI FAKULTET

Sveučilišni doktorski studij Inženjerstva okoliša

odgovor je na zahtjeve naše svakodnevice gdje se susrećemo s problemima onečišćenja okoliša, klimatskim promjenama, potrošnjom resursa kao što su mineralne sirovine, tlo, vode, neadekvatnog upravljanja otpadom i niz drugih okolišnih problema.
https://www.gfv.unizg.hr/static/doktorski-studij

Nastavna struktura doktorskog studija koncipirana je u formi pet izbornih modula:

1. Održivo gospodarenje otpadom
2. Okoliš i priroda
3. Geoinženjerstvo okoliša
4. Upravljanje vodama
5. Energetika

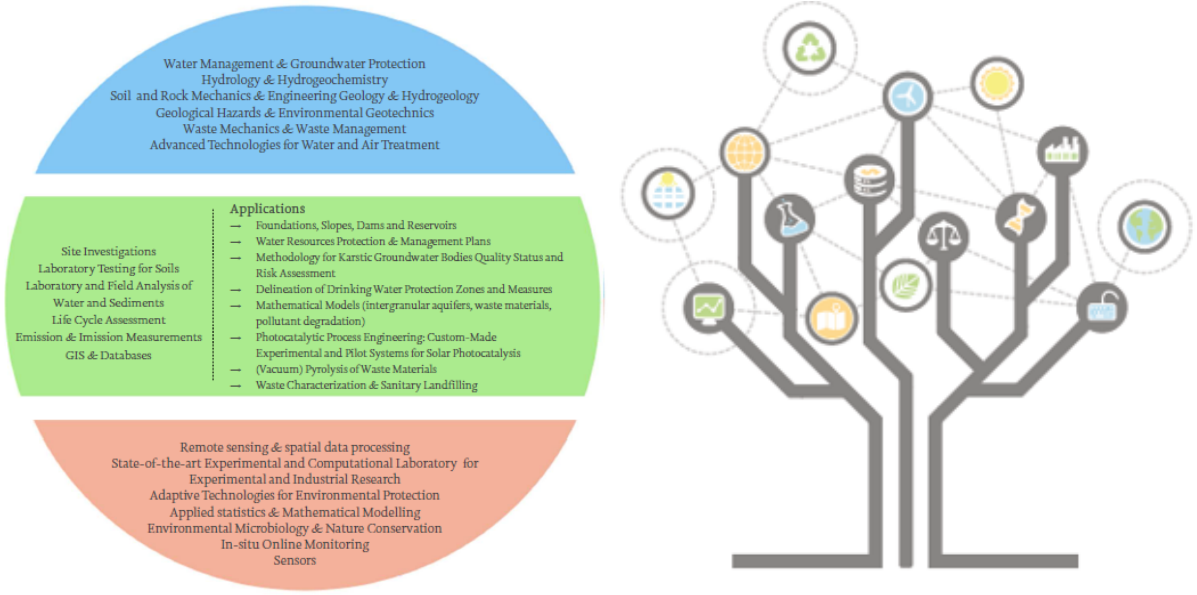

Postgraduate doctoral study of Environmental Engineering

Problems concerning the field of environmental engineering demand both professional and scientific research approach, which is the only way of finding specific solutions to them. The programme emphasizes current societal needs concerning circular economy, which should enable sustainable waste management, natural resources management and protection, introduction of renewable energy sources and contributes to the mitigation of climate changes.
https://www.gfv.unizg.hr/static/doktorski-studij

The curriculum of the doctoral study consists of five modules:

1. Sustainable waste management
2. Environment and nature
3. Environmental Geoengineering
4. Water management
5. Energetics